Physics Lib.

DO NOT TAKE FROM LIBRARY

Copy 2.

THE PHYSICAL REVIEW

VOLUME 48 | *Second Series* | NUMBER 12

DECEMBER 15, 1935

Published for the

AMERICAN PHYSICAL SOCIETY

by the

AMERICAN INSTITUTE OF PHYSICS
Incorporated

LANCASTER, PA., AND NEW YORK, N. Y.

THE
PHYSICAL REVIEW
A Journal of Experimental and Theoretical Physics
VOL. 48, NO. 12 DECEMBER 15, 1935 SECOND SERIES

Collisions of Alpha-Particles with Neon Nuclei*

WILLIAM W. EATON, *Sloane Physics Laboratory, Yale University*
(Received August 15, 1935)

The tracks of more than 700,000 alpha-particles from a source of thorium active deposit have been photographed in a Wilson chamber filled with a mixture of approximately 85 percent neon, 10 percent air, and 5 percent hydrogen. The collisions with nuclei have been studied by replacing the film in the camera and projecting; convenient methods for doing this are described. A range-velocity curve for neon recoil atoms has been constructed by plotting the measured ranges against the calculated velocities for 85 forks. No interactions have been observed which give any evidence of the disintegrations of nuclei, with the emission of protons or neutrons. From a particular study of six elastic, coplanar collisions in which high energies have been transferred to the recoil atoms, it is concluded that the probability of disintegrating Ne^{20} with alpha-particles of less than 6-cm range (in air) is small; from this a lower limit for the mass of Na^{23} is calculated. The methods of measurement and calculation have been thoroughly tested by applying them to collisions with other nuclei, three with hydrogen, five with "air," one with helium, and one with deuterium.

I. INTRODUCTION

THE observation of forked alpha-particle tracks in the Wilson cloud chamber has in the past led to knowledge along two general lines. Firstly, the study[1-7] of elastic collisions has provided a test of the inverse square law and of the nuclear theory of the atom, and has yielded range-velocity relations for the various recoil atoms concerned, and, secondly, the study[8, 9, 10] of the relatively few inelastic collisions observed has thrown light on the disintegration of nuclei by alpha-particles, giving an idea as to the mechanism and energy balance. It was the general idea of the present work to attempt to obtain information along both of these lines in the case of neon. In particular, the disintegration of a fluorine atom by an alpha-particle should give rise to a proton and a Ne^{22} recoil atom, as Chadwick and Constable[11] have shown, and in case such a process is ever observed in a cloud chamber—the chance is greater than for any other element besides nitrogen—the range velocity relations for neon recoil atoms may become useful. Furthermore, since a disintegration yield from neon under bombardment of alpha-particles has been observed by Rutherford and Chadwick,[12] using scintillation methods, there is a possibility, however small, that such disintegration might be observed in the cloud chamber. The recording of

* Part of a dissertation presented to the Faculty of the Graduate School of Yale University in candidacy for the degree of Doctor of Philosophy

[1] Blackett, Proc. Roy. Soc. **A102**, 294 (1922).
[2] Blackett, Proc. Roy. Soc. **A103**, 62 (1923).
[3] Akiyama, Jap. J. Phys. **2**, 279 (1923).
[4] Auger and Perrin, Comptes rendus **175**, 340 (1922).
[5] Harkins and Ryan, J. Am. Chem. Soc. **45**, 2095 (1923).
[6] Blackett and Lees, Proc. Roy. Soc. **A134**, 658 (1932).
[7] Feather, Proc. Roy. Soc. **A141**, 194 (1933).
[8] Blackett, Proc. Roy. Soc. **A107**, 349 (1925).
[9] Blackett and Lees, Proc. Roy. Soc. **A136**, 325 (1932).
[10] Harkins, Zeits. f. Physik **50**, 97 (1928); Harkins and Schuh, Phys. Rev. **35**, 809 (1930).
[11] Chadwick and Constable, Proc. Roy. Soc. **A135**, 48 (1932).
[12] Rutherford and Chadwick, Proc. Phys. Soc. London **36**, 417 (1924).

such an event would be of particular interest, since up to the present time alpha-particle disintegrations of nitrogen atoms only have been observed in the cloud chamber.

II. Experimental Arrangements and Analysis of the Tracks

The Wilson cloud chamber which was used in the work has been described by F. N. D. Kurie.[13] It is of the conventional piston type, the expansions being effected by periodically connecting the space underneath the piston to an evacuated flask by means of a synchronizing mechanism. The illumination was provided by a pair of ordinary carbon arcs, through which about 30–40 amperes were passed at the moment of expansion. An attempt was made to use photoflood lamps for illumination, but experiment showed that eight ordinary photofloods grouped very closely around the chamber were insufficient to give proper contrast on the film. The addition of a 2000-watt photoflood improved the situation only slightly, so that the arcs were finally resorted to. The camera was designed and constructed by Kurie[13] and is of a very convenient type. By a system of mirrors, two photographs were taken at right angles to one another on a single 35-mm moving picture film through a single lens. The image planes were slightly inclined so that practically all regions of the chamber were in focus. An automatic motor-drive device moved the film forward between expansions, and wound up the exposed film on a reel. The shutter was a Wollensak Betax (automatic) and was operated by an electromagnetic cable release.

The source of alpha-particles was a short length of copper wire which had been allowed to collect thorium active deposit by exposure to a quantity of mesothorium and its products. It was mounted outside the chamber and separated from it by a very thin sheet of mica waxed over a slit. The beam of alpha-particles was thus collimated so that the vertical spread was about 15° and the horizontal spread about 60°. The space between the mica and the wire was in all cases evacuated. The stopping power of the mica was first determined by weighing, and was afterwards checked by measurements of the actual ranges of the particles in the chamber. The value was about 0.9 cm air equivalent, so that with the arrangements described it was possible to bombard the gas in the chamber with alpha-particles of two residual ranges, 7.7 and 3.9 cm.

Photographs were taken on 100-foot reels of supersensitive panchromatic grayback film, the development being carried out with modified Eastman D–76 fine grain developer. The individual pictures were examined visually quite conveniently by projecting them on a screen with a Leica projector. A typical stereoscopic pair is shown in Fig. 1(d) with a neon collision almost in the plane of the chamber.

In order to study the collisions which were recorded, the film was replaced in the camera in exactly the same position it occupied when a given exposure was made. It was then illuminated by a 500-watt projection lamp and a condenser system, and the two images produced by the sets of mirrors received on a specially designed movable screen. In order to find the plane of any collision relative to the camera (within limits of inclination to the horizontal of 45°–90°) it was obviously necessary only to adjust the screen so that the two images of a given fork coincided. This was true provided the collision was coplanar, and thus the act of combining the two images in this way provided a fairly sensitive test upon this point. It was found that the actual process of combining simultaneously the images of the three tracks of a given fork could be simplified to a great extent by following a definite order in manipulations of the screen. The screen used was capable of horizontal motion in all directions, vertical motion, and rotation about three axes, and experiment showed that a great deal of time could be saved by having one axis of rotation lie in the plane of the screen itself. The most expeditious procedure was then in general to combine the two images of the alpha-particle track before collision so that they coincided with the axis lying in the screen, and then by rotating about this axis, the desired plane could easily be found, since the first adjustment was not disturbed by this process. The stand was designed so that a piece of photographic paper could be held flat in the position of the white screen, and when a given fork had been combined, the adjustment was secured by clamping, and prints taken of

[13] Kurie, Rev. Sci. Inst. **3**, 655 (1932).

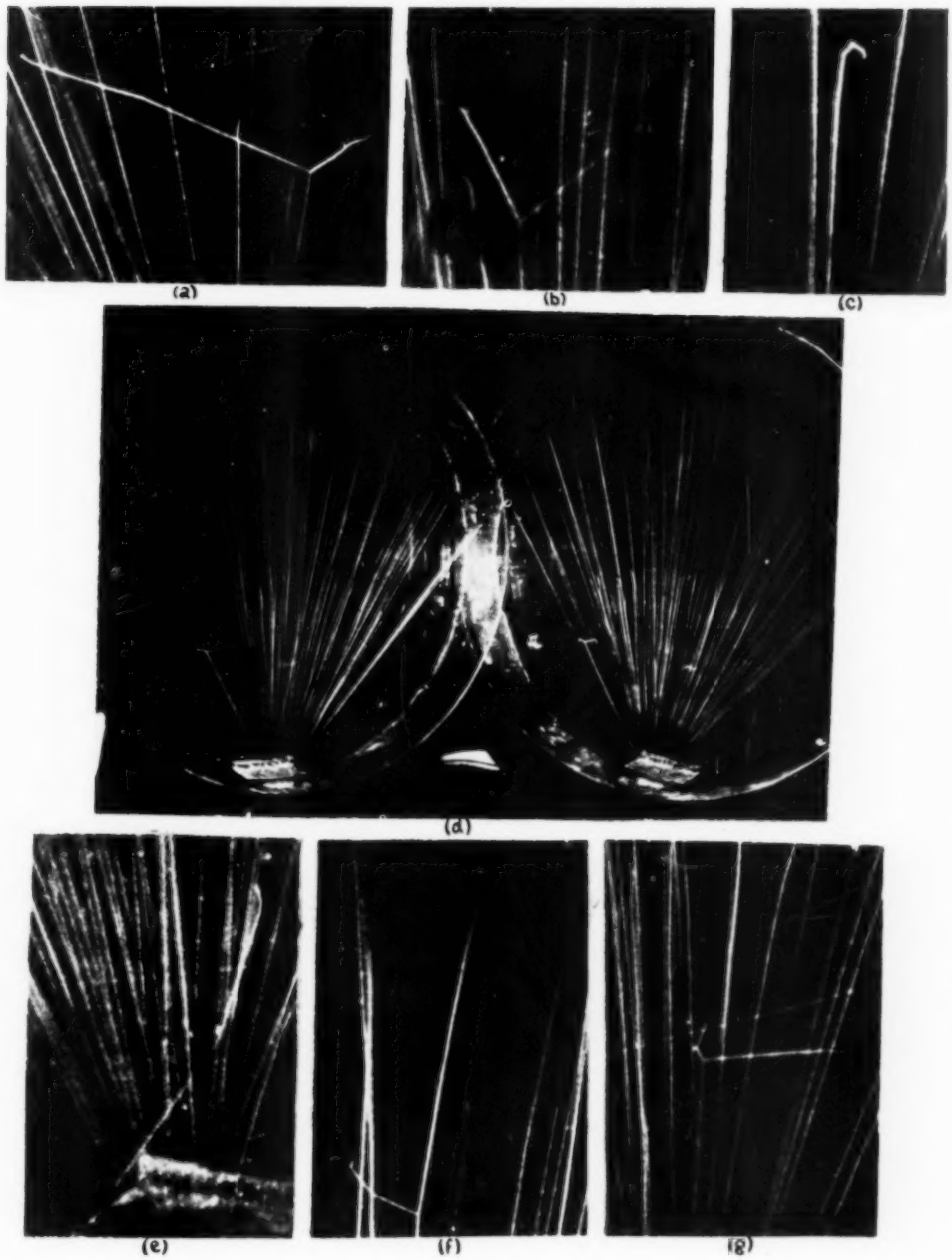

FIG. 1. (a) Alpha-particle-neon fork, with neon recoil atom making a second collision, producing a short spur: (b) Alpha-particle-deuterium fork: (c) Alpha-particle track showing approximate reversal of direction without any close collision. (No recoil track.) (d) Typical stereoscopic pair of photographs, showing collision of alpha-particle with neon atom: (e) Longest neon recoil track obtained. Reduced range of neon atom 8.4 mm (air), initial energy 1.1×10^6 electron volts: (f) Alpha-particle-hydrogen fork: (g) Alpha-particle-neon fork, with neon recoil atom making a second collision, producing a very short spur (compare (a)).

each image separately. By measuring each print independently it was thus possible to eliminate errors due to imperfect coincidence. The measurements of the two prints were usually weighted according to the orientation with respect to the camera, since at certain inclinations the errors were much larger than at others, because of the different angles at which the light struck the paper. In the case of events that took place in planes inclined at angles of from 45°–0° to the

vertical (45°–90° to the plane of the chamber) it was impossible to receive two images on a screen with an opaque backing, and so an attachment was added whereby a translucent screen could be supported by its edges alone, the images being combined by observing one through the screen and one directly. The screen was then replaced by small lantern slide plates and the two exposures taken. The method of course fails at 45° to the vertical.

In order to analyze a fork, it is necessary merely to measure lengths and angles on the prints, and this was done on a drawing board using a protractor and rules. Ordinarily the measurements on a given fork were confined to the angles ϕ and θ (angles which the directions of motion after collision of the alpha-particle and the recoil atom make, respectively, with the initial direction of motion of the alpha-particle), the lengths of the recoil track and the alpha-track after collision, or, if the latter is not obtainable, the distance of the point of collision from the source. In most cases the mass ratio of the struck particle to the alpha-particle was calculated from the angles alone, by using the formula $m/M = \sin\phi/\sin(2\theta+\phi)$, where m is the mass of the struck particle and M the mass of the alpha-particle. This is of very limited value in the case of atoms as heavy as neon, however, since the angle $(2\theta+\phi)$ approaches 180° nearly enough so that small errors in the angles cause large errors in the sine function. In the case of lighter atoms, it determines with fair accuracy the mass of the struck particle and gives an idea as to the elastic character of the collision, since, if energy is not conserved, the above formula will not hold. The velocity of recoil of the struck particle was calculated in all cases, either by the formula $u = (M \sin\phi/m \sin\theta)\, v$, where u is the velocity of recoil, v the velocity of the alpha-particle after collision as estimated from its range, or, in case v could not be so determined, by the formula $u = 2V\cos\theta/(1+m/M)$, where V is the velocity of the alpha-particle before collision estimated from the distance of the point of collision to the source. In case θ is not easily measured, and the alpha-particle track is not completely observed, we may calculate v directly from V using ϕ, and then calculate u from the energy equation.

The stopping power (for alpha-particles) of the gas relative to air was calculated from the known constants of the gases present in the chamber in case the composition was known, and checked by measurements of the ranges, or, when the mixture was unknown, by the latter method alone. All the ranges were reduced to standard air with the results of these measurements, and the stopping power of the gas mixture for the recoil atoms was arbitrarily taken as the same as that for fast alpha-particles.

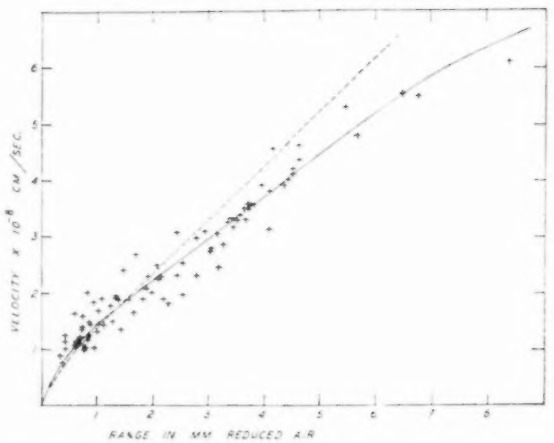

FIG. 2. Range-velocity curves for recoil atoms of neon and fluorine: Crosses and full line, present work on neon; broken line from Feather[7] on fluorine.

III. RESULTS

Over 10,000 stereoscopic pairs of photographs were taken of the alpha-particle tracks, a portion of them being in almost pure neon gas, and the remainder in a mixture of about 85 percent neon, 10 percent air, and 5 percent hydrogen. Estimates made of the number of tracks per photograph in the case of every run showed that the total number of tracks observed was roughly 700,000; of these about 450,000 were of the long range group and 250,000 were of the short range group.

Out of about 200 collisions which were measured, about 85 were selected as being suitable for the plot of recoil velocity against recoil range, and the result of this plot is shown in Fig. 2, a similar curve for fluorine atoms due to Feather being shown for comparison. It can be seen that the neon curve falls slightly below the fluorine curve, agreeing with the general rule that the ranges of recoil atoms of the same velocity are in proportion to their masses. The fact that there is

a certain amount of spread of the points on either side of the curve should not, for several reasons, appear unusual, for, added to the straggling of the recoil atoms themselves, which has been estimated by Blackett to be as much as 15 percent, there are always the inevitable errors in calculating the velocities of recoil due to the straggling of the alpha-particles, which comes into account when an alpha-particle range-velocity curve is used. Finally there are present the inherent errors of measurement, due to the method of reprojection and combination of the forks. Doubtless if stricter criteria had been used in selecting the collisions suitable for plotting the spread would have been less; on the other hand, considering the errors already present because of straggling, which probably account for most of the spread, this process could be carried to the extreme of not having enough points to determine a fairly accurate average curve.

The mass of neon was arbitrarily set at 20.2 in all the calculations. As Feather points out, a mistaken value of the mass in the case of two atoms having nearly the same weight, merely has the effect of moving a point from its position on its own range-velocity curve to a point very nearly on the range-velocity curve of the atom for which it is mistaken. Thus the curve shown may be considered correct for atoms of mass 20.2, and moreover the curves for Ne^{20} atoms or Ne^{22} atoms may easily be found merely by multiplying the velocity corresponding to any range by the ratios 20.2/20 and 20.2/22 respectively. This is a point which should not be overlooked in case the curve is ever used in the calculation of energies of Ne^{20} or Ne^{22} atoms.

It will be noticed that the two curves in Fig. 2 cross, which may seem rather odd. This, I believe, is due to a spurious effect which shows itself because of different methods of calculating stopping powers. In the present work account was taken[14] of the variation in the stopping power of neon (for alpha-particles) with velocity, whereas in Feather's calculations the relative stopping power of the gas was assumed to be constant, and was determined by measuring the ranges directly. This variation is important only for short range alpha-particles, and in the case of neon decreases with decreasing velocity. Thus for a given short range residual alpha-particle in a collision, a smaller velocity would be assigned to it than if the stopping power did not decrease in this region, therefore the calculated velocity of recoil would be low, which is what is observed. Of course, not all collisions with small recoils have small residual alpha-particle tracks, but a considerable number do, which may account for this effect.

According to the formula suggested by Blackett[2] $R \propto mZ^{-\frac{1}{2}}f(u)$, where R is the range, Z the atomic number, m the mass, and u the velocity of the recoil atom, the ratios of the ranges of recoil atoms of the same velocity should be proportional to the ratios of their masses and inversely proportional to the square roots of their atomic numbers. Comparing the present curve with that of Blackett and Lees[6] for nitrogen at a velocity of 5×10^8 cm/sec., the ratio of ranges is 1.52, whereas the formula predicts a value of 1.21. The comparison with Feather's fluorine curve shows a measured value of 1.20 as against a predicted value of 1.01. Thus whether the data are compared to nitrogen or fluorine, the range of the neon recoil atoms is greater than that predicted. This might possibly have an explanation in the electronic structure of the neon atom, or it might suggest a higher power of m in the above formula, although considering the complexity of the problem and the number of factors involved, it is probably unsafe to draw any conclusions. Besides, the above formula is known to be of rather restricted applicability.

Of particular interest are five collisions which are represented by the five highest velocity points on the curve as shown in Fig. 2, plus a sixth which was not plotted because of the fact that the recoil atom experienced a rather marked deflection which was difficult to measure accurately. Two of these collisions are shown in Fig. 1 (a) and (e). The salient features of these forks may be briefly catalogued as follows.

1. The reduced air ranges of the recoil atoms were greater than 5 mm and the distances of closest approach of the alpha-particle to the nucleus in the six cases, calculated on the inverse square law, ranged from 7.0 to 4.57×10^{-13} cm. These values, particularly the lowest, are very

[14] Gurney, Proc. Roy. Soc. **A107**, 340 (1925).

close to the value of the nuclear radius of neon, as estimated by Pollard.[15]

2. The collisions were in all cases apparently elastic, within the limits of experimental error. There was no indication of disintegration, and the appearance of the tracks was in no case such as to indicate the passage of any other type of particle except an alpha-particle or recoil atom. The mass ratios calculated from the angles were correct to within the experimental error, although this is by no means a sensitive test for heavy atoms, as has been pointed out earlier.

3. The collisions were, as nearly as could be determined, coplanar, and since the method described by which the photographs are projected and combined provides a fairly sensitive test upon this point, the evidence is good that no neutrons or high energy gamma-rays were given off in the processes involved.

4. The angle θ had, in the six cases, the values 45°, 26°, 26°, 25°, 24°, and 13°. If the internuclear force is Coulombian it may be shown that, for a given length of recoil, the ratios of the numbers of collisions for which θ lies within the ranges 90°–60°, 60°–30°, and 30°–0° are, respectively, 1, 2, and 1. The numbers in the present case are 0, 1, and 5. It is of course obvious that not too much reliance can be placed on the analysis of such a small number of collisions; on the other hand, it is of definite significance that in five out of the six cases, small angles of deflection were observed. For this means that these collisions were practically head-on, which is improbable from the point of view of the inverse square law. Thus the conclusion is that for distances of approach as close as those in the cases considered, an anomalous region has been reached, and the inverse square law in its simple form no longer applies.

While it is not true that in the case of nuclei which disintegrate because of alpha-particle penetration, every alpha-particle which gets into the nucleus will cause a disintegration, it is safe to summarize the above study of the six collisions in which the alpha-particle approached the nucleus very closely by saying that the disintegration of neon atoms with alpha-particles of 5 or 6 cm range or less is improbable. For example, if the atoms had been nitrogen, some of the collisions of the above type would certainly have caused breakdown of the nuclei.

To go further, it is interesting to consider the composition of the neon gas from the standpoint of isotopes. It is well known that ordinary neon is a mixture of about 90 percent Ne^{20} and 10 percent Ne^{22}. It is thus not only very improbable that all the six collisions referred to are with Ne^{22} atoms, but it is on the contrary quite reasonable to assume that they are all with Ne^{20} atoms. It is thus more in accord with the observations to confine the above conclusions to the Ne^{20}. It is worth noting that by analogy with the other nuclei containing an integral number of alpha-particles (C^{12} and O^{16}), this is what would be expected.

Providing we assume that Ne^{20} does not disintegrate for alpha-particle energies corresponding to ranges less than 6 cm, then a minimum value may be assigned to the mass of Na^{23}, which is formed in the hypothetical reaction,

$$_2He^4+{}_{10}Ne^{20}={}_{11}Na^{23}+{}_1H^1.$$

The result of such a calculation (using the latest values for the masses of alpha-particle and proton) shows that the Na^{23} nucleus must have a mass greater than 22.99945.

In view of the fact that some mention has been made in the past of collisions apparently not coplanar (Akiyama,[3] Auger and Perrin,[4] Feather[7]) it is worth mentioning the observations made during this work. It is true that there were a few forks observed, the three tines of which did not combine simultaneously on the screen. This type of collision was always rejected for measurement, and was considered of small importance on the following general reasoning:

1. Observations of a great many of the recoil tracks show that, in general, the recoil atom is peculiarly subject to deflections, particularly during the last few millimeters of its path. In some cases the recoil tracks are far from being straight, and a great many times they are curved so much towards the ends that accurate measurement of their lengths is impossible.

2. All of the collisions observed in which there was apparently lack of coplanarity were those in which the length of recoil was small. In the case of all the longer recoil forks, it was possible to combine the three tines simultaneously, referring of course to the parts of the tracks near the point of collision.

3. Only a relatively small percentage of even the shorter recoil forks, about 10 percent, exhibited this property.

[15] Pollard, Phys. Rev. **47**, 611 (1935).

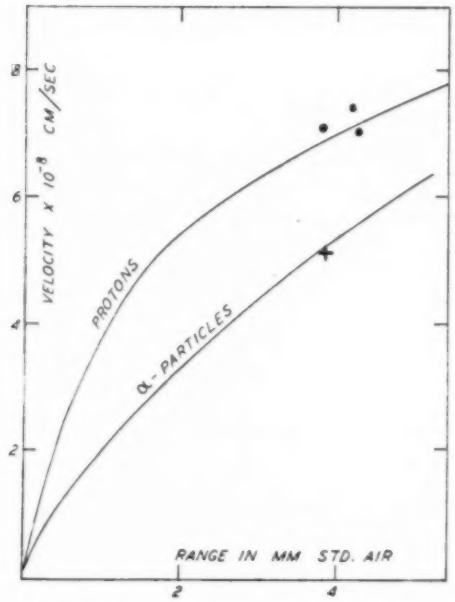

FIG. 3. Range-velocity curves for recoil atoms: of hydrogen (protons) and helium (alpha-particles). Full lines from Blackett and Lees,[6] dots and cross, collisions assigned to hydrogen and helium in present work.

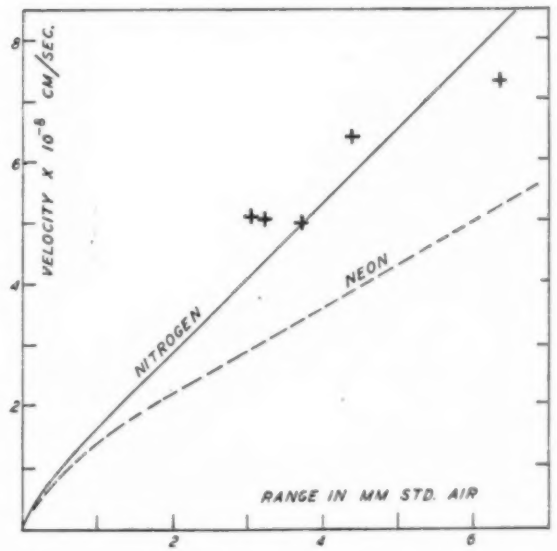

FIG. 4. Range-velocity curves for recoil atoms of nitrogen and neon. Full line from Blackett and Lees[6] on nitrogen; crosses, collisions assigned to air in present work; broken line, neon, from Fig. 2.

Thus a reasonable explanation of these apparently anomalous collisions seems to be that the recoil atom suffered a small deflection soon after collision. This would account for the facts in a very simple and direct way without injecting any hypotheses about gamma-rays or other losses of energy.[16] It may be that this explanation could be applied successfully to the collisions of this type reported by others.

During the greater part of the work, when there were present in the chamber other gases besides neon, there was of course a chance of striking these atoms. There were six collisions with hydrogen observed, of which three were suitable for measurement, and one with helium, which was doubtless present in the neon as an impurity. One of the hydrogen forks is shown in Fig. 1(f). The mass ratios in the three hydrogen forks were calculated to be 0.260, 0.238, and 0.242, in good agreement with 0.25, the correct value. In the case of the helium collision, the mass ratio came out to be 1.05, and the value of $\phi+\theta$ was measured as $90°\pm0.5°$. In Fig. 3 the calculated velocities have been plotted against the measured ranges in these cases, and the proton and alpha-particle range-velocity curves of Blackett and Lees have been drawn in for comparison. The fact that all three of the measurable hydrogen collisions had about the same velocity and range is unfortunate, but the agreement is excellent, as is that for helium.

The chance of colliding with an "air" atom was estimated from a rough knowledge of the composition of the gas in the chamber to be about one in fifteen. Since it was generally impossible to distinguish between a neon and an air collision, due to the inherent difficulties in applying the mass ratio formula which have already been discussed, the admittedly arbitrary criterion was decided upon that a mass value would be determined, above which all atoms would be classed as neon when calculated by the formula, and below which they would be classed as air, that value being chosen which would give the proper ratio of number of neon collisions to number of air collisions. No doubt a few points on the neon curve really represent air collisions, and *vice versa*, but this has a negligible effect on either curve as explained before. The ranges and velocities of those recoils, which were arbitrarily called air, have been plotted in Fig. 4, and the nitrogen curve of Blackett and Lees is drawn in for comparison, as is the present neon curve. The

[16] Smekal, Physik. Zeits. **27**, 383 (1926).

significance of this plot, considering the arbitrary way in which the points have been classed as air, is doubtful, and it would perhaps have been just as well to assign all of these doubtful collisions to neon, and plot them on the other curve.

In addition to the tracks photographed in neon, one run of about 600 pictures was taken with a mixture of about 30 percent deuterium and 70 percent air. In this series one collision with deuterium was observed, which is reproduced in Fig. 1(b). Unfortunately the complete track of the deuteron (right-hand tine of fork) after collision was not observed. It is interesting to note that this fork may be immediately recognized as a collision with a deuterium atom for the following reasons: The angle of deflection of the alpha-particle, ϕ, is about 25°, therefore it cannot have struck hydrogen since the maximum value of ϕ in hydrogen collisions is 14.5°; the value of ϕ is less than 30°, the maximum for deuterium collisions, so it is consistent with this explanation; the track of the struck particle is finer, showing less ionization, and has the appearance of a proton or deuteron track, and, finally, the value of m/M is calculated to be 0.57, in agreement with 0.5 for a deuteron collision.

In Fig. 1(g) is shown an unusual type of fork, the recoil atom of neon experiencing a marked deflection, producing a second small recoil. Fig. 1(c) shows a photograph of an unusual type of alpha-particle track. Because of a series of small deflections producing negligible recoil spurs, the atom has experienced a net deflection of about 180°, producing a curiously shaped track.

In conclusion, it is a pleasure to thank Professor A. F. Kovarik for constant advice and encouragement throughout the course of the work, Dr. Ernest Pollard for many helpful discussions, and Professor L. W. McKeehan for numerous suggestions regarding the composition.

DECEMBER 15, 1935 PHYSICAL REVIEW VOLUME 48

Anomalous Diffraction Gratings

R. W. Wood, *Johns Hopkins University*

(Received July 11, 1935)

Gratings similar to those described and studied by the author in 1907 and 1912 have been more fully investigated. They show narrow bright and dark bands in the continuous spectrum of a white source. Classical theory has never accounted for these anomalies, though tentative efforts were made at the time by Lord Rayleigh. The present work was done with a chromium plated echelette grating of 7200 lines to the inch ruled on copper, and one of 15,000 lines ruled by Dr. Babcock on an aluminum film on glass. The behavior of the bands as the incidence angle is altered has been very completely recorded by photography and the energy missing in the grating spectra has been found in excess in the spectrum of the central image. The dark bands appear to be due to the circumstance that diffracted wavelets from the lines are inhibited by the collective effects from neighboring lines, i.e., there is a sort of destructive interference along the plane of the grating. This obtains, however, only when the grating space is equal to an integral multiple of λ (for normal incidence) which means that the dark bands correspond to λ values which are passing off the grating on both sides at grazing emergence. The spectra formed by the Al grating are completely plane polarized, because of the circumstance that the width of the scratches is considerably less than the wave-length of the light. The dynamical action of the gratings is discussed, and the anomalous behavior is shown to be due to the presence of exceedingly narrow diffracting elements, which may be present even in the case of rather coarse rulings.

As is well known the distribution of intensity in the spectra formed by gratings varies in the different orders, some being bright in the red, others in the violet, and these variations are easily accounted for by elementary theory.

It is possible, however, to rule gratings showing bright and dark bands in very restricted spectral regions, and these anomalies have never been accounted for.

At the bottom of Fig. 1, Spectrogram 9, we have a photograph of the spectrum of a Mazda lamp filament taken with such a grating extending from the extreme red (at the right) to the violet. The black bands are very sharply

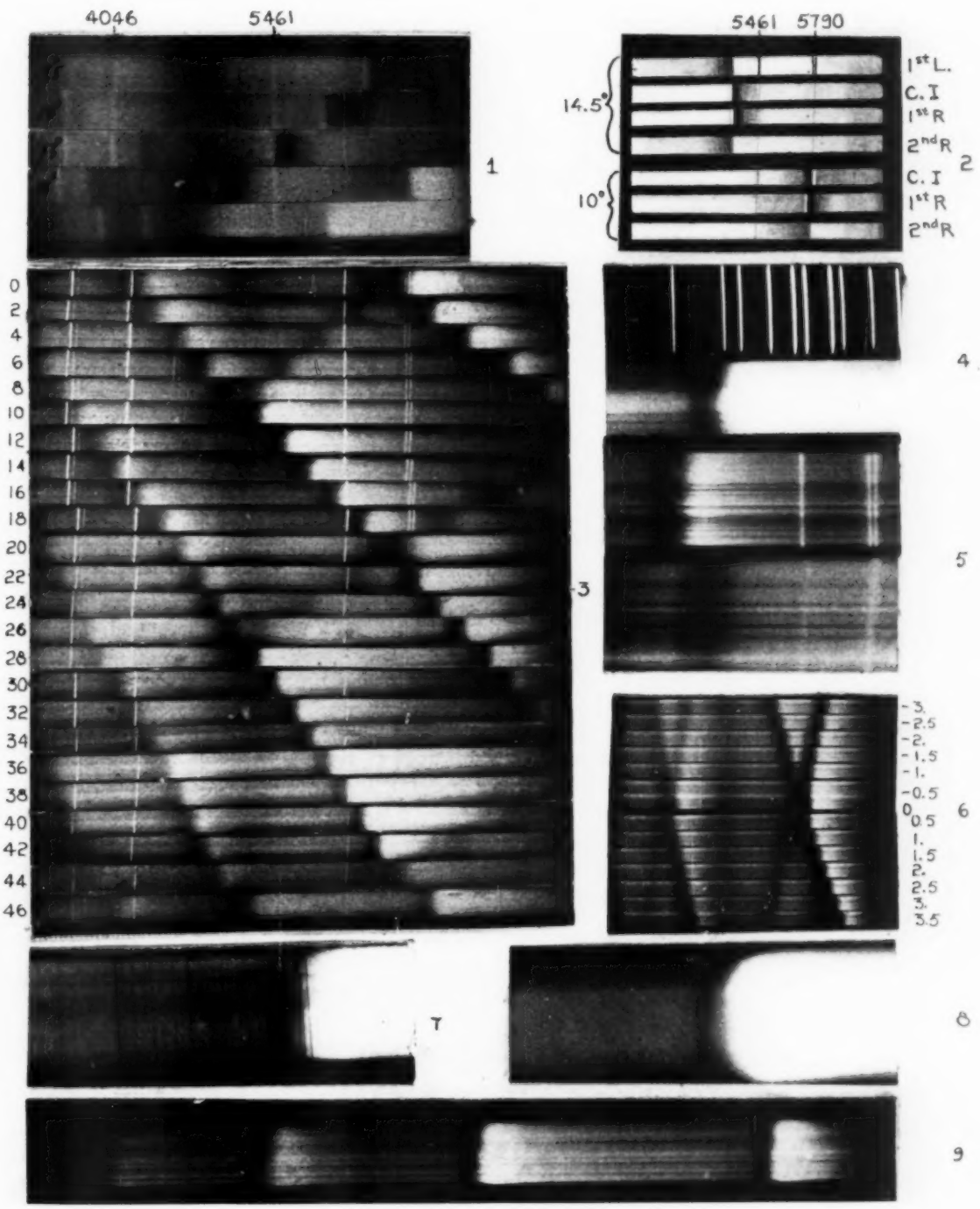

FIG. 1.

bounded on the short wave-length side, and the intensity increment in passing from the minimum to the maximum is from fifteen to twenty-fold. Until such maxima and minima can be accounted for by theory we must confess that our knowledge of the action of a grating is far from complete.

Gratings of this type were studied and described by the author in 1902[1] and again in 1912, and the late Lord Rayleigh became much interested in them and discussed them in several of his papers.[2] He pointed out that anomalies might be expected at regions in the spectrum corresponding to wave-lengths passing off the grating at grazing emergence in the spectra of higher orders, and this I verified in a number of cases, as reported in the second of the two earlier papers referred to above.

One of these gratings showed a narrow bright line in the red and a dark line in the green. These lines approached each other as the angle of incidence was decreased, meeting and canceling each other at 0° incidence. A further slight rotation of the grating developed a dark band at this point which split in two, one band moving up, the other down the spectrum as the incidence angle was increased. The motion of the bands in opposite directions is to be associated with the circumstance that, as the grating is turned, the wave-length passing off at grazing emergence increases on one side of the grating and decreases on the other. Though these effects were first noticed in a ruling on speculum metal the best results were obtained by ruling on a thin film of gold or silver deposited on a polished speculum flat. One of these showed a very bright first-order spectrum on one side and a faint one on the other, and it was in the latter that the bright and dark bands appeared. A very light rubbing with a "powder-puff" brightened the faint spectrum and caused the complete disappearance of the anomalies.

This led me to express the opinion that the faint spectrum came from the wavelets diffracted by the steep sides of an unsymmetrical groove and that the anomalies resulted from energy diffracted by very narrow and fragile ridges running along the edges of the groove, pressed up above the general level. This I have again verified by ruling on a copper flat. The effects shown by the old gratings were so complicated, however, that it was difficult to make any hypothesis as to the manner in which they operated. In one case, for example, a bright narrow line moved down the continuous spectrum towards a wider dark band which it finally entered without any loss of intensity! Lord Rayleigh[2] showed that, in the case of sound waves passing, at normal incidence, through very narrow parallel slits, the passage of energy through any slit might be prevented by the cooperative action of the other slits, *under the condition that the distance between the slits was an integral multiple of the wave-length*, which of course corresponds to the condition of the wave-length passing off of a grating at grazing emergence. He expressed the opinion that some such action operated in the case of the optical gratings. He developed this idea somewhat more fully in his subsequent paper *On the dynamical theory of the diffraction grating*, without however, arriving at any completely satisfactory explanation of the anomalies.

My interest in the subject, which has smoldered for more than a quarter of a century was rekindled by seeing a grating exhibited by Dr. John Strong at the Berkeley meeting of the Physical Society in 1934. The bands shown by this grating appeared to be of a simpler type and much easier to study. They were of the same wave-length in each spectrum, and were very black. As I have always pointed out, the first thing to do in any case where certain wave-lengths are absent as a result of an unknown process (i.e., a case of unexplained color) is to find out where the absent wave-lengths have gone. They did not appear to be present in excess in the central image, and Dr. Strong and I looked for an increased heating of a small sliver of the grating, illuminated by light from a monochromator, when the wave-length corresponded to that of the black band. The result was negative, but the experiment seemed worth trying as I have found that the total light reflected by a freshly ruled grating on speculum, (i.e., central image plus all of the spectra) may be much less than the light reflected from a corresponding area of unruled surface. This means absorption by the grating, and Lord Rayleigh stated in his paper that "the grooves were clearly acting as resonators" in the case where the anomalies were shown, though I have never been able to find out just what he had in mind or on what theoretical point he based this view. At one time I ran across a paper in which

[1] Wood, Phil. Mag. Sept. (1902); Feb. (1912).
[2] Rayleigh, Phil. Mag. July (1907).

the analogy of the reflection of sound waves by a series of parallel equidistant slats (Venetian blind) was cited as an illustration of resonance of this type, but I am unable to find the paper and have forgotten by whom it was written. I shall be grateful for the reference.

In the present paper very complete investigations with two gratings of this type will be discussed, one of 15,000 lines to the inch ruled on a surface of aluminum by Dr. Babcock of Mt. Wilson Observatory, the width of the diamond scratches being of the order of one-eighth of the grating space, or one-third of the wave-length of red light; the spectra formed by this grating are all completely plane polarized with the electric vector perpendicular to the groove, and are of low intensity, while the central image or directly reflected light is nearly as strong as from the unruled surface.

The other grating I ruled on a polished flat of copper, with a diamond edge ground to an angle of about 110 degrees, 7200 lines to the inch, the grooves symmetrical with respect to the normal, and meeting along their edges. The central image was extremely weak and there was a very strong concentration of energy in the spectra lying in the direction of reflection from the groove edges. The two gratings are therefore about as different in type as it is possible to make them. They have, however, this feature in common: At normal incidence the energy diffracted at nearly 90° is of considerable intensity. In the case of the aluminum grating this is due to the narrowness of the scratches, which also accounts for the polarization, for, as was shown by Lord Rayleigh, a very narrow scratch diffracts powerfully in the direction from which the incident light is coming, and the diffracted light is polarized perpendicular to the scratch, as in the case of light transmitted by a narrow slit. As we shall see, at oblique incidence with this grating the spectrum leaving at grazing emergence, which is the one which governs the appearance of the anomalous bands, is very bright on the side nearest the light source, i.e., in the direction from which the light is coming. In the case of the copper echelette, however, the strong spectrum at grazing emergence which controls the bands leaves the grating on the side farthest away from the source in the case of oblique incidence. The anomalous bands in this case appear to be due to fragile and very narrow ridges lying along the edges of the deep grooves, for the lightest rubbing with the rouged finger tip, abolishes completely the bright and dark bands and brightens up the entire spectrum. This makes it appear as if the ridges diffracted powerfully in the direction away from the source, instead of towards it. The importance of relative high intensity at grazing emergence appears to depend on the circumstance that the emission of a diffracted wavelet from a grating element can be abolished (or in certain cases augmented) by the cooperative effects exerted by neighboring elements.

One of the puzzling questions raised in my earlier paper was that regarding the manner in which such a great change in intensity could occur over a region only a few Angstrom units in width, which would appear to require the cooperation of a large number of lines. I do not now attach much significance to my observation that they could be seen when only a very narrow portion of the grating was illuminated, and I hope to be able to make some anomalous rulings of only 50, 100, 200, etc., lines, all made under the same condition, with the same point, to test this matter more fully. The circumstance is connected, I think, with the very high dispersion of a grating in the vicinity of grazing emergence, (becoming infinite at true grazing).

If we accept Lord Rayleigh's hypothesis, we may perhaps refer what we may term the high resolving power of the anomaly (i.e., great intensity change over a very narrow spectral region) to the circumstance that the annihilation of the diffracted wavelet at its source requires the combined cooperation of effects from a large number of neighboring lines.

This high resolving power is well shown in Spectrograms 7 and 8, Fig. 1, the former a small portion of the green region of the solar spectrum in which the little *b* triplet of magnesium lies at the right-hand edge of the dark band. The extremely sharp edge of the band on the short wave-length side is still better shown by Spectrogram 8, made with a Mazda lamp in the same region, as the edge is not masked by the Fraunhofer lines. As I have said before, until we can explain this photograph we cannot pretend that

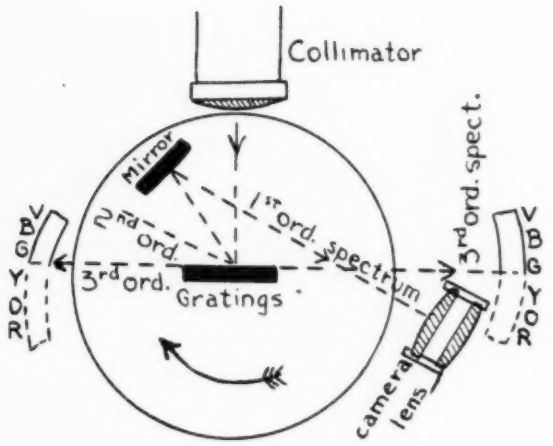

FIG. 2.

we have a completely satisfactory theory of the diffraction grating.

We will now take up the study of the behavior of a typical grating of this type, the one ruled on aluminum. Spectrogram 3, Fig. 1, gives a complete picture of the behavior of the grating at all angles of incidence from 0° to 46°. It is a composite of 23 spectrograms, mounted in coincidence. The source of light was a small Mazda lamp backed by a mercury arc, so that the strong mercury lines appear on the continuous spectrum and serve as reference marks. The lamp was focused on the slit of a collimator and the grating mounted on a graduated circle furnished with a vernier as shown in Fig. 2. The grating was at first set at normal incidence by holding a card perforated with a small hole in front of the collimator lens and turning the grating until the narrow beam was reflected back through the hole. The spectrum used was the first order to the *left* as shown in the figure, as it was desired to study the effects from zero to the largest possible angles of incidence, turning the grating clockwise as indicated. When working with the grating at angles which projected the spectrum in the direction of the collimator a mirror was used on which narrow horizontal strips of silver had been removed, the light passing through the clear spaces to the grating (tilted up very slightly) while the rays forming the spectrum were reflected from the silver strips. At large angles of incidence the mirror was dispensed with, though this reversed the spectra of course. The upper spectrum of Spectrogram 3, Fig. 1, was taken at normal incidence, and we find a dark band between the 5461 and 5790 mercury lines, and another nearly in coincidence with 4046. The grating space is 0.001667, and since the third-order green is passing off at grazing emergence on both sides we calculate the wave-lengths of these two bands as 0.001667 divided by 3 and 4, respectively, namely, 0.0005557 and 0.0004167. There should also be a band at 0.000833 corresponding to $0.00166 = 2\lambda$, and this was found by photographing the spectrum on an infrared plate.

Now at normal incidence it is clear that, since $\lambda = 0.000555$ is passing off at grazing in the third order, the red, orange, and yellow of the third order spectra are "below the horizon" (so to speak) of the grating, or more exactly this portion of the third-order spectra is absent, as indicated in Fig. 2. Turning the grating clockwise lifts the spectrum at the left above the horizon and depresses the one at the right. The grazing emergence λ is thus increased in the left-hand spectrum, causing the corresponding dark band to move towards the red, while in the right-hand spectrum it is diminished, causing the corresponding dark band to drift towards violet, in other words the single band at $\lambda = 0.000555$ at normal incidence is in reality two superposed bands, which divide as soon as the grating is rotated even through as small an angle 0.5°, one component moving *down*, and the other *up* the spectrum. So sensitive is the appearance of the band that a visual observation served better than the perforated card for setting the grating at normal incidence. We thus obtain a very clear picture of the relation between the two sets of dark bands, and the grazing λ's on each side. It is clear from the photograph that the bands which move towards the red are blacker and more distinctly defined than the other set, which have nearly disappeared at 40° incidence, and are invisible at all larger angles.

The successve spectra of Spectrogram 3, Fig. 1, were taken with 2° increments of the incidence angle. At 10° the violet band has moved up the spectrum and has met the green band which has moved down, and it is by this continuous meeting and crossing of the bands that the chess-board pattern is formed.

It will be noticed that at large angles of

incidence the dark band is narrower and more sharply defined on the short wave-length edge. Spectrograms 7 and 8, for example, were taken with an incidence angle of 60°, and are of course much more highly enlarged than the spectra of Spectrogram 3.

Another feature, of considerable importance for the discussion of the theory is that the bands become less conspicuous in the short wave-length region of the spectrum. For example in Spectrogram 9 the intensity ratio of the minimum to the maximum is about 1 : 15 in the red (at the right) and about 1 : 3 in the violet. There was only the barest suggestion of a band in the ultraviolet beyond the one shown at the left of Spectrogram 9. As we shall see presently, this feature may be explained when we come to the treatment of the dynamical action of the grating. Spectrogram 6 is similar to Spectrogram 3 except that the spectra were taken with half-degree angle increments on both sides of the normal or zero angle of incidence, the minus sign indicating counterclockwise rotation in Fig. 2.

The intensity in the region between the bands, which are receding from each other, is much greater in the case of counterclockwise rotation. This is to be expected since the upper left-hand branch of the X corresponds to the lower right-hand branch, which has the maximum on the long wave-length side.

Location of the Missing Energy

It is a matter of great importance to discover where the energy goes which is absent in the spectra.

As the dark and bright bands appear at the same wave-lengths in all of the spectra, one would expect the spectrum of the central image to show bright and dark bands at corresponding points unless the energy was lost by absorption. The central image was accordingly examined through a direct vision prism, and a faint dark band was seen at exactly the same wave-length as the bright maximum in the spectrum. As the spectra formed by this particular grating were completely plane polarized a properly oriented nicol prism was combined with the direct-vision prism, with the result that the dark band now became very distinct. There was, however, no trace of a *maximum* in the spectrum of the

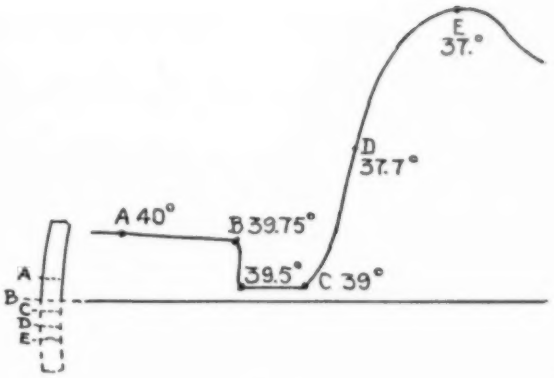

Fig. 3.

central image, to correspond to the dark minimum of the grating spectrum. It seemed probable, however, that this resulted from the circumstance that the intensity of the spectrum on the short wave-length side of the dark band was less than three times the intensity of the band (see Spectrogram 8) while the intensity of the central image was many times greater than that of the sum of all of the spectra. This would make it impossible to detect visually the very slight change of intensity at the point corresponding to the left-hand edge of the dark band. But this slight change might be augmented by multiple reflections as in the method of "reststrahlen." The grating was accordingly mounted in front of, and very close to, a silver on glass mirror and the light reflected to and fro between the mirror and grating. The spectrum of the multiply reflected light was then observed with the nicol and direct-vision prism and was seen to exhibit a fairly pronounced maximum bordering the minimum on the short wave-length side, as shown by Spectrogram 5, in which the upper spectrum is that formed by the grating in the vicinity of Hg 5461, and the lower that of the multiply reflected light, taken with the nicol and direct-vision prism. The poor resolution of the image obtained through the nicol and prism, and the smaller dispersion of the prism (requiring greater enlargement of the spectrogram) rendered the contrast less pronounced than when observed visually.

It thus appears that the energy, missing locally in the spectra, is found in the central image, which is faint in the regions corresponding to the bright bands of the spectra.

Form of Energy Curve and Its Relation to Grazing Emergence Angle

The very curious form of the curve of spectral intensity at the band should prove an important clue in developing a theory of the dynamical action of the grating. It is shown roughly by Fig. 3. The angle values given on the curve show the incidence angle necessary to bring the green mercury line to the corresponding part of the anomalous band, in other words they indicate the rate at which the band moves across a point of fixed λ value in the spectrum as the incidence angle is altered. The position of the fifth-order spectrum for this setting is shown at the left, the horizontal line which represents zero intensity being considered as the plane of the grating in this connection; the dotted portion of the spectrum (below the horizon) has no real existence of course. The letters indicate corresponding λ values on the curve and the grazing spectrum. It seemed very important to discover the exact point on this curve corresponding to the wave-length of grazing emergence from the grating. This was done in the following way: A very powerful end-on neon tube was placed in front of the collimator slit, and the grating set at an incidence angle of about 40°. The spectrum near grazing emergence was viewed by bringing the eye as close as possible to the edge of the grating, a good method when very faint lines are to be observed. By turning the grating the lines of the spectrum could be made to disappear in succession as they passed below what I have called "the horizon" of the grating. The camera was placed in position for photographing the spectra of the neon tube and the Mazda filament in coincidence in the spectrum of the first order, and the grating rotated until all of the red (as viewed directly in the grating) had passed below the horizon and disappeared. When the next to the last line (yellow) had just vanished (and this position could be determined with an accuracy of a small fraction of a degree) the photograph shown in Spectrogram 4 was made, showing that the grazing λ coincided with that of the sharp edge of the dark band on the short λ side. The bright bands in the spectra thus correspond to wave-lengths below the horizon in the spectra of higher order, the dark bands to wave-lengths very near and apparently a little below the horizon, while the portion of spectrum on the short wave-length side of the dark band corresponds to wave-lengths above the horizon, i.e., actually represented by a spectrum near grazing emergence.

In the case of the 7200 copper grating which was plated with chromium the anomalous bands were of a different type. With increasing angle of incidence they moved always towards the region of shorter wave-length, and were controlled by the grazing emergence spectrum on the side of the grating which was moving *away from* the light source. They thus corresponded to the bands of Fig. 1, Spectrogram 3, which slope down towards the left and disappear at large incidence angles. They were usually very black at the edge and shaded off gradually, sometimes towards the red and sometimes towards the violet, and were often bordered on the dark side by a rather narrow bright band. They were much more conspicuous when examined with a properly oriented nicol, as they were formed only when the electric vector was perpendicular to the groove. Another set of much fainter bands could be observed with opposite polarization, but their behavior has not yet been investigated.

It was found that if the central image was observed with a direct-vision prism and a nicol, bands of similar type and of equal intensity ratios were seen. These were usually similar in appearance and position to the bands in the first order spectrum on one side, and complementary to those of the other first order spectrum, i.e., the black edge occupied the same position but the band shaded off in the opposite direction. These effects are, however, so complicated that it seems doubtful whether they can be explained until a satisfactory theory of the simpler type of bands obtained with a grating formed of very fine scratches has been developed. In this case the spectra are formed by diffracted disturbances from the wide edges of the grooves and not from exceedingly narrow lines, and the anomalous bands, as I have said, appear to result from inhibiting or enhancing effects due to energy diffracted from narrow and fragile ridges bordering the grooves, which can be removed by very light rubbing.

Photographs of the spectra at incidence angles increasing from 7.5° to 23° are reproduced in

coincidence in Fig. 1, Spectrogram 1. Two sets of bands appear, one shaded off towards the right (red), the other towards the left, and both move down the spectrum as the incidence angle increases. The mercury lines 5461 and 4046 appear also on the continuous spectrum. The bright line on the edge of the dark band is fairly conspicuous.

Fig. 3 is a drawing representing the spectrum of the central image in coincidence with three spectra by the grating at the same incidence angles (10° and 14°). The positions of the yellow and green mercury lines are indicated.

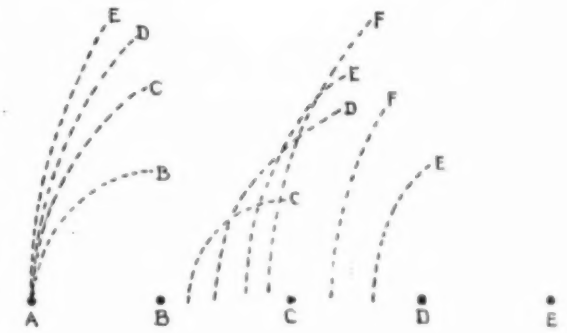

FIG. 4.

THEORY OF THE ANOMALIES

We will start with the simplest case possible and discuss in the most elementary manner the relation between the wave-length which leaves the grating at grazing emergence, and the distribution of intensity in the other spectra.

If, with normal incidence, the third-order spectrum can form for violet blue and green radiations (the yellow Hg lines being "on the horizon") it is obvious that for these wave-lengths there is less energy available for the formation of first and second-order spectra, than in the case of red and yellow radiations, which are not, in part, spent in the formation of a spectrum of third order. We should thus expect these spectra to be slightly brighter on the red side of the yellow lines than on the violet. This is roughly what we have, as shown in the upper spectrum of Fig. 1, Spectrogram 3. Rotation of the grating, however, raises one of the third-order spectra above the horizon, and depresses the other, and if we apply the previous reasoning to this case we find that the expected phenomenon in the other spectra would be high intensity in the red, a sudden decrease in the orange and another sudden and larger decrease in the green extending down to the violet, and not a doubling of a dark band, with a bright region between the two components, which is what we observe. We will now introduce another possible effect which we may perhaps term secondary diffraction.

HYPOTHESIS OF SECONDARY DIFFRACTION

Lord Rayleigh's analogy of the case of sound-waves passing through a system of very narrow parallel slits, in which case he showed theoretically that a decreased transmission might be expected when the distance between the slits was an integral number of λ is about the only foundation that I have been able to find on which to build an hypothesis. I have no physical picture of the process by which "the passage of the waves through a single slit is destroyed or lessened by the cooperative effect from the neighboring slits," but have been wondering whether it may not be termed "secondary diffraction," by which I mean that the emission of a diffracted wavelet from a single grating element is inhibited by the combined effects of diffracted wavelets from the other elements of the grating as they sweep across the surface at grazing emergence, in which direction they would all be in the same phase when arriving at the element in question. I have attempted to give in Fig. 4 a diagram of what I have in mind. It is of course only a very elementary and incomplete representation, and it is evident that only a very elaborate mathematical treatment of the whole subject will give a full explanation of all of the phenomena. For normal incidence, and with the grating space equal to 3λ, at the moment at which a secondary wavelet is about to start from grating element A secondary wavelets excited by previous waves in the incident train, arrive in phase at element A, wavelet B coming from element B, wavelet C from element C, etc. The envelope of these wavelets gives the diffracted wave front, which is extremely narrow and produces the ray leaving at grazing emergence. For slightly shorter waves the condition is as shown between elements B

and C, the wavelets from C, D and E arriving with a phase retardation. The envelope forms the wave front of the third-order spectrum leaving the grating "above the horizon," using the previous nomenclature. For waves longer than λ the condition is as shown between elements C and D—the secondary wavelets have an advance of phase, and since there is no envelope, no third-order spectrum is formed. If it can be shown that, in the last case the cooperative effects of adjacent rulings enhance, rather than suppress, the intensity of the diffracted disturbance from a single ruling a distinct advance will have been made in the development of the theory.

The conditions under which the effects of secondary diffraction might be expected to manifest themselves appear to be fulfilled in the case of all gratings of the following type. The spectra in which the anomalies occur must be weak and the spectra leaving at grazing emergence relatively strong. This condition is fulfilled if the grating is composed of exceedingly fine scratches or ridges, narrow in comparison to the grating space. In the case of the aluminum grating under consideration this was found to be the case, the width of the scratch appearing to be about one-eighth of the grating constant. Such fine ridges produce weak spectra, but diffract the light through a very wide angle, enabling the diffracted disturbance from one ridge to reach the neighboring ridge. The diffracted disturbances are polarized with the electric vector perpendicular to the ridge, in much the same way as the light transmitted by an exceedingly narrow slit. Though similar and equally marked bright and dark bands have been found with certain echelette gratings where the entire surface has been cut up by the rulings and only a very feeble central image appears, it has been found that the anomalies are caused by very narrow and fragile ridges of material along the edges of the groove, which are removed by the lightest possible rubbing with a rouged finger tip, causing the complete disappearance of the bands and a brightening of the entire spectrum.

It has been found that the anomalous bands are associated with the spectrum passing off at grazing emergence on the side of the grating which is nearest to the light source, in the case of large angles of incidence.

Assuming now that the dark bands in the spectrum result from the circumstance that the diffracted wavelets (which form the spectrum when united at the focus of a lens) are inhibited at the start by wavelets coming from the neighboring lines, we must account for the following experimentally observed phenomena.

1. That the dark minima are most pronounced in the long wave-length region of the spectrum and become less and less conspicuous as we descend towards violet. This can possibly be explained as a result of the circumstance that diffraction through a large angle, which is necessary if the secondary disturbance from one ridge is to reach the next adjacent ridge, will be more pronounced in the case of the longer waves.

2. That the set of bands which move towards the red with increasing angle of incidence become more pronounced (i.e., show a greater change of intensity in passing from maximum to minimum) as the incidence angle increases. This effect may perhaps be due to the fact that as the incidence angle increases, the grazing emergence spectrum passes off in a direction more and more nearly directed towards the source and Lord Rayleigh showed that in this direction the diffracted wave from a very narrow scratch had its maximum value. One might therefore expect a maximum effect, in this case, of the cooperative annihilating action of disturbances from neighboring grooves on the wavelet emitted by a single groove.

3. That the bands which move towards the violet become less pronounced with increasing incidence angle and disappear entirely at angles greater than 45°. This is shown on Fig. 1, Spectrogram 3 in which the dark lines which slope down towards the left are nearly invisible on the lower part of the figure. This results from the *decrease* in the intensity of wavelets diffracted in the direction away from the source which becomes more marked at large incidence angles, the grazing emergence spectrum eventually vanishing.

The above arguments apply only in the case of the grating composed of very fine scratches on a surface of aluminum. In the case of the echelette the governing spectrum is on the side away from the light source.

It seems probable that the optical constants of the metal will have to be taken into account (as was done by Voigt in his extension of Rayleigh's theory) especially since Strong's observation that the position of the bright bands varies with the nature of the metal composing the surface of the grating. This will affect the velocity of that portion of the diffracted wavelet which is traveling along the surface of the metal, as has been suggested by Langer.

Barium Hydride Spectra in the Infrared

PHILIP G. KOONTZ AND WILLIAM W. WATSON, *Yale University*

(Received September 23, 1935)

Quantum analyses of the (1,0), (1,1) and (2,1) bands of the infrared $^2\Sigma \rightarrow {}^2\Sigma$ system of BaH and some details of the $^2\Pi \rightarrow {}^2\Sigma$ band at 10,300A are presented. The spin doubling constant γ of the upper $^2\Sigma$ state is very large (-4.88) and decreases with increasing molecular rotation, $A \leqq 625$ cm^{-1} for the $^2\Pi$ state, and a perturbation occurs in the $^2\Pi_{1/2}$ levels at $J = 11\frac{1}{2}$.

OF the several band systems of the BaH molecule in the red and photographic infrared regions only the $^2\Pi \rightarrow {}^2\Sigma$ system whose $\Delta v = 0$ sequence lies between 6925A and 6380A has been thoroughly analyzed.[1-3] For the infrared systems discovered by one of the writers[4] the analysis of the (0,0) band of the $^2\Sigma \rightarrow {}^2\Sigma$ system with principal head at 8924A together with a necessarily incomplete analysis[5] of the (0,0) $^2\Pi_{1\frac{1}{2}} \rightarrow {}^2\Sigma$ sub-band at 10,000A have been reported. The present paper gives further details of these infrared bands.

The experimental arrangement for obtaining the spectrograms was similar to that used previously. Three hours' exposure, using Eastman I–P plates, was sufficient for good registration of the $\Delta v = 0$ and $+1$ sequences of the $^2\Sigma \rightarrow {}^2\Sigma$ system, the dispersion being about 4.9A/mm. With the new I–Z plates and an exposure time of six hours, the (0,0) $^2\Pi_{\frac{1}{2}} \rightarrow {}^2\Sigma$ sub-band between 10,603A and 10,853A could be photographed, but with low intensity. Although a complete quantum analysis of this band is therefore impossible, the measurements do yield some further information about this $^2\Pi$ state.

Table I contains the assignment of frequencies

[1] W. R. Fredrickson and W. W. Watson, Phys. Rev. **39**, 753 (1932).
[2] A. Schaafsma, Zeits. f. Physik **74**, 254 (1932).
[3] G. Funke, Zeits. f. Physik **84**, 610 (1933).
[4] W. W. Watson, Phys. Rev. **43**, 9 (1933).

TABLE I. *Assignment of frequencies for the infrared $^2\Sigma \rightarrow {}^2\Sigma$ bands of BaH (cm^{-1} units).*

$J''+\frac{1}{2}$	P_1	P_2	R_1	R_2	$J''+\frac{1}{2}$	P_1	P_2	R_1	R_2	$J''+\frac{1}{2}$	P_1	P_2	R_1	R_2
		(1,0) BAND					(1,1) BAND					(2,1) BAND		
1				12130.26	1			10975.37		1				12017.47
2				38.03	2		10963.05	78.97		2				25.40
3			12121.39	45.62	3	10954.41	58.26	82.40	11006.93	3			12009.14	32.69
4	12084.45	12091.38	24.13	52.86	4	46.08	53.41	85.54	14.85	4			11.69	39.59
5	74.36	85.63	26.56	59.68	5	36.25	48.25	88.56	22.30	5	11962.91		14.11	46.32
6	63.42	79.58	28.69	66.13	6	26.48	42.87	91.23	29.38	6	52.46		15.95	52.47
7	52.47	72.89	30.26	72.14	7	16.27	37.35	93.46	36.43	7	41.72	11961.30	17.47	58.16
8	41.41	66.47	31.54		8	06.04	31.49	95.79	43.09	8	30.55	54.39		63.42
9	29.89	58.91	32.41	82.92	9	895.44	25.57	97.73	49.49	9	19.07	47.30		68.36
10	17.96	51.39	32.79	87.68	10	84.52	19.30	99.42	55.58	10	07.27	39.58	19.39	72.89
11	05.62	43.44	32.79	92.07	11	73.52	12.78	11000.82	61.28	11	894.90	31.60	19.39	76.87
12	11992.91	35.07	32.41	96.03	12	62.36	06.02	01.98	66.94	12	82.21	23.30		80.46
13	79.88	26.46	31.54	99.54	13	50.88	899.18	02.68	72.14	13	69.41	14.71	17.96	83.71
14	66.45	17.47	30.47	202.54	14	39.44	91.91	03.28	77.06	14	56.17	05.54	16.67	86.41
15	52.46		29.02	05.19	15	27.30	84.51	03.54	81.51	15	42.63	896.16	14.11	88.78
16	38.75	11998.42	27.13	07.41	16	15.33	76.94	03.54	85.85	16	28.87	86.29	12.39	90.62
17	24.48	88.32	24.75	09.21	17	03.10	69.09	03.28	89.96	17	13.69	76.19	09.79	92.03
18	09.83	77.88	21.93	10.35	18	790.69	61.00	02.68	93.62	18	799.41	65.66	06.77	93.01
19	894.90	66.95	18.75	11.41	19	78.04	52.73	01.98	97.00	19	84.50	54.79	03.31	93.39
20	79.49	56.05	15.13	11.71	20	65.24	44.19	00.82	100.02	20	69.21	43.51	11999.42	93.39
21	63.83	44.39	11.10	11.71	21	52.14	35.43	10999.42	02.70	21	53.55	31.78	95.10	93.01
22	47.87	32.66	06.59	11.41	22	38.82	26.53	97.73	05.02	22	37.54	19.90	90.32	92.03
23	31.78	20.44	01.71	10.35	23	25.79	17.36	95.79	07.00	23	21.25	07.59	85.05	90.62
24	14.94	07.78	096.45	08.70	24		07.98	93.46	08.59	24	04.65	794.87	79.52	88.78
25	798.08	894.90	90.62	06.67	25		798.30	90.80	09.90	25	687.67	81.68	73.31	86.41
26	80.83	81.78	84.45	04.19	26		88.40	87.79	10.48	26	70.39	68.36	66.45	83.41
27	63.25	68.03	77.76	01.27	27		78.02	84.58	11.49	27	52.67	54.50	59.75	79.74
28	45.54	54.19	70.63	197.78	28		67.99	80.98		28	34.73	40.30	52.46	75.84
29	27.28	39.79	63.42	93.79	29		57.41	77.10		29	16.49	25.68	44.39	71.46
30	08.76	24.86	55.19	89.35	30			73.09		30	597.85	10.82	35.73	66.47
31	689.99	09.83	46.56	84.43	31			68.29		31	79.03	695.40	26.87	60.83
32		794.44	37.64	78.66	32			63.41		32	59.61		17.49	55.19
33	51.35	78.71	28.23							33	40.22	63.44	07.78	48.62
34	31.75	62.38	17.96							34	20.12	47.38	897.76	41.41
35	11.67	45.54	08.23							35	499.89	30.77		33.97
36	591.32	28.45	11997.23							36	79.20	13.37		
37	70.69	10.82	85.76							37	58.29			
38	49.68	693.02	73.79							38	36.83			
39	28.27	74.23	61.30											
40	06.48		48.80											
41	484.57													
42	62.55													

for the branches of the (1,0), (1,1) and (2,1) bands of the $^2\Sigma \rightarrow {}^2\Sigma$ system. These assignments have been made with the aid of the usual combination differences between the several bands of this and the $^2\Pi \rightarrow {}^2\Sigma$ system in the visible red, the lower $^2\Sigma$ state being common to both. The constants of the rotational energy terms are evaluated from the averages of the $\Delta_2 T_1$ and $\Delta_2 T_2$ differences by the semigraphical method in every case. We list these constants for the two $^2\Sigma$ states in Table II. Our values $B_0 = 3.3496$ and

TABLE II. *Constants from the quantum analysis of the infrared $^2\Sigma \rightarrow {}^2\Sigma$ system of BaH (cm^{-1} units).*

NORMAL $^2\Sigma$ STATE	UPPER $^2\Sigma$ STATE	
$B_0 = 3.3496$	$B_0 = 3.232$	$\gamma_0 = -4.88$ for $K < 12$
$B_1 = 3.2839$	$B_1 = 3.1609$	$\gamma_1 = -4.78$ "
$D = -1.10 \times 10^{-4}$	$B_2 = 3.0915$	$\gamma_2 = -4.66$ "
$\alpha = 0.066$	$D = -1.11 \times 10^{-4}$	
$\gamma = +0.186$	$\alpha = 0.070$	

$B_1 = 3.2839$ for the normal state agree exactly with the values $B_0 = 3.3495$ and $B_1 = 3.284$ given by Funke.[3]

The most interesting feature of these bands is the large size of the spin doubling in the upper $^2\Sigma$ state. This, the largest doubling recorded for any $^2\Sigma$ state, is due to the strong "pure precession" interaction with the $^2\Pi$ state but 1460 cm^{-1} below it. The magnitude of the Λ-doubling in the $\Pi_{1\frac{1}{2}}$ component of this $^2\Pi$ state is also evidence for this interaction.[5] With increasing rotational energy the constant γ of the spin doubling relation $\Delta\nu_{12}(K) = \gamma(K + \frac{1}{2})$ decreases for all vibrational states, the values for the highest K levels being -4.61, -4.52 and -4.39 for $v = 0$, 1 and 2, respectively. Similar change of the rate of variation of $\Delta\nu_{12}$ with K has been noted in the corresponding $^2\Sigma$ states of CaH and SrH. Probably the perturbing influence of neighboring energy levels is responsible for this departure from the usual linear relation.

Our partial analysis of the $^2\Pi_{\frac{1}{2}} \rightarrow {}^2\Sigma$ sub-band at 10,600A reveals the following facts. The R_1 and Q_1 branch heads occur at 10,603.33A and 10,746.37A, respectively. In the R_1 branch a perturbation centering at $R_1(10\frac{1}{2})$ is evident. In the discussion of another perturbation in the $^2\Pi_{1\frac{1}{2}c}$ levels at $J = 20\frac{1}{2}$ the nature of the possible perturbing levels has been considered.[5] Upper state combination differences between the R_1 lines and the few P_1 lines observed for low K levels yield the value 3.12 for $B_0{}^*, {}_{-\frac{1}{2}}$. The position of the Q_1 branch head would locate the $^2\Pi_{\frac{1}{2}}$ origin at about 9285 cm^{-1}. Since the $^2\Pi_{1\frac{1}{2}}$ origin comes at about 9910 cm^{-1}, the coupling constant A for this state must be then about 625 cm^{-1}. This agrees fairly well with the value $A = 640$ assumed in our previous discussion of this $^2\Pi$ state.

[5] W. W. Watson, Phys. Rev. **47**, 213 (1935).

DECEMBER 15, 1935 PHYSICAL REVIEW VOLUME 48

Analysis of the Spectrum of Se II

D. C. MARTIN, *Department of Physics, Cornell University*

(Received August 19, 1935)

An analysis of the spectrum of Se II is given with additions and corrections to that by Krishnamurty and Rao. The spectrum of selenium in this investigation was excited in a hollow cathode discharge with a helium atmosphere. Wave-length measurements were made in the region 500 to 2600A with a 1.5-meter grating vacuum spectrograph. New terms belonging to the $4s^24p^25p$ configuration have been found and identified. Several other terms, probably associated with the $4s^24p^24d$ and $4s^24p^25d$ configurations, have been found and J values assigned, but it has been found impossible at present to assign L and S values to them. Tables of all term values and line classifications known at present are listed.

INTRODUCTION

THE first extensive investigation of Se II was made by Bloch and Bloch[1] who published quite an accurate and complete list of wavelengths in the visible and ultraviolet regions of the spectrum from 6679–2197A. Lacroute[2] extended their earlier measurements into the vacuum region to 1235A. Recently two articles

[1] Leon and Eugene Bloch, Comptes rendus **185**, 761 (1927); Ann. de physique **13**, 233 (1930).

[2] M. P. Lacroute, J. de phys. et rad. **9**, 180 (1928).

TABLE I. *Term values of Se II.*

CONFIGURATION	TERM SYMBOL	J VALUE	RELATIVE TERM VALUE
$4s^24p^3$	^4S	$1\frac{1}{2}$	0
	^2D	$1\frac{1}{2}$	13168.2 (K & R)
	^2D	$2\frac{1}{2}$	13784.4 (K & R)
	^2P	$\frac{1}{2}$	23038.3 (K & R)
	^2P	$1\frac{1}{2}$	23894.8 (K & R)
$4s4p^4$	^4P	$2\frac{1}{2}$	83876.7 (K & R)
	^4P	$1\frac{1}{2}$	85579.5 (K & R)
	^4P	$\frac{1}{2}$	86437.7 (K & R)
$4s^24p^2(^3P)5s$	^4P	$\frac{1}{2}$	95270.0 (K & R)
—	1	$\frac{1}{2}$	96517.4
—	2	$2\frac{1}{2}$	96655.3
$4s^24p^2(^3P)5s$	^4P	$1\frac{1}{2}$	96753.3 (K & R)
—	3	$\frac{1}{2}$	98118.2
$4s^24p^2(^3P)5s$	^4P	$2\frac{1}{2}$	98674.4 (K & R)
	^2P	$\frac{1}{2}$	98896.1 (K & R)
—	4	$1\frac{1}{2}$	99368.5
$4s4p^4$	^2P	$1\frac{1}{2}$	100295.1 (K & R)
$4s^24p^2(^3P)5s$	^2P	$1\frac{1}{2}$	101356.0 (K & R)
—	5	$2\frac{1}{2}$	101631.5
—	6	$1\frac{1}{2}$	104694.4
—	7	$1\frac{1}{2}$	104873.7
—	8	$\frac{1}{2}$	105258.0
—	9	$\frac{1}{2}$	105973.8
$4s^24p^2(^1D)5s$	^2D	$2\frac{1}{2}$	108355.7 (K & R)
	^2D	$1\frac{1}{2}$	108449.8 (K & R)
—	10	$2\frac{1}{2}$	108833.9
—	11	$2\frac{1}{2}$	110297.4
—	12	$1\frac{1}{2}$	112403.4
$4s^24p^2(^3P)5p$	^4P	$\frac{1}{2}$	113048.7 (K & R)
	^4D	$\frac{1}{2}$	114299.0 (K & R)
	^4D	$1\frac{1}{2}$	114711.7 (K & R)
	^4D	$2\frac{1}{2}$	116068.1 (K & R)
	^4P	$1\frac{1}{2}$	116776.6 (K & R)
	^2S	$\frac{1}{2}$	117406.0
	^2D	$1\frac{1}{2}$	117739.6 (K & R)
	^4D	$3\frac{1}{2}$	117798.7 (K & R)
	^4P	$2\frac{1}{2}$	118398.0 (K & R)
	^4S	$1\frac{1}{2}$	119308.5 (K & R)
—	13	$\frac{1}{2}$	119343
$4s^24p^2(^3P)5p$	^2D	$2\frac{1}{2}$	120387.1 (K & R)
—	14°	$1\frac{1}{2}$	121051.5
$4s^24p^2(^3P)5p$	^2P	$\frac{1}{2}$	121273.2
	^2P	$1\frac{1}{2}$	121381.9
—	15	$2\frac{1}{2}$	121730
—	16	$2\frac{1}{2}$	122720
—	17	$1\frac{1}{2}$	123323
—	18°	$2\frac{1}{2}$	126329.7
—	19	$1\frac{1}{2}$	126464.7
$4s^24p^2(^1D)5p$	^2D	$2\frac{1}{2}$	127415.7
—	20	$\frac{1}{2}$	127867.5
$4s^24p^2(^1D)5p$	^2D	$1\frac{1}{2}$	127921.4
—	21°	$2\frac{1}{2}$	127984.3
—	22	$1\frac{1}{2}$	129010.4
$4s^24p^2(^1D)5p$	$2.3°.\ ^2F(?)$	$2\frac{1}{2}$	131165.4
	^2P	$1\frac{1}{2}$	132189.6
—	24	$2\frac{1}{2}$	133867.1
$4s^24p^2(^3P)6s$	^4P	$\frac{1}{2}$	134042.9 (K & R)
	^4P	$1\frac{1}{2}$	135635.6 (K & R)
—	25	$1\frac{1}{2}$	136188.2
$4s^24p^2(^3P)6s$	^4P	$2\frac{1}{2}$	137669.1 (K & R)
$5d$	^4F	$1\frac{1}{2}$	138365.7 (K & R)
$6s$	^2P	$\frac{1}{2}$	138525.7
—	26	$2\frac{1}{2}$	138535.9
—	27	$1\frac{1}{2}$	138711.0
$4s^24p^2(^3P)5d$	^4F	$2\frac{1}{2}$	138923.1 (K & R)
	^4F	$3\frac{1}{2}$	140011.8 (K & R)
—	28	$1\frac{1}{2}$	140131.3
—	29	$1\frac{1}{2}$	140745.8
—	30	$2\frac{1}{2}$	140930.1
$4s^24p^2(^3P)6s$	^2P	$1\frac{1}{2}$	140939 9
—	31	$2\frac{1}{2}$	140946.0
$4s^24p^2(^3P)5d$	^4F	$4\frac{1}{2}$	141710.1 (K & R)
—	32	$2\frac{1}{2}$	142171.0
—	33	$1\frac{1}{2}$	142302.2
—	34	$1\frac{1}{2}$	142374.1
—	35	$2\frac{1}{2}$	143341 7
—	36	$2\frac{1}{2}$	143919.5

have been published giving an analysis of Se II, one by Bartelt[3] and the other by Krishnamurty and Rao.[4] Bartelt[3] has identified several of the same terms as Krishnamurty and Rao[4] although his assignment of L and S values differs somewhat from theirs. He also has given term values for several higher terms, but it is doubtful whether his values are correct as he has used several lines of Se II which have been preferably otherwise assigned in the present investigation, and some of the other lines used by him have been identified as belonging to Se I and Se III. Many of the errors in Bartelt's work arose from his lack of ultraviolet data to correlate the values of the terms assigned from visible data. The analysis by Krishnamurty and Rao[4] seems to be the more accurate. In this paper, some corrections and additions are made to their analysis.

EXPERIMENTAL

A hollow cathode discharge tube with a water-cooled aluminum cathode, and with helium gas to maintain the discharge, was used to produce the spectrum of Se II in the ultraviolet region. The discharge tube was connected to a 1.5-meter grating vacuum spectrograph, the grating of which was ruled with 15,000 lines to the inch, giving a dispersion of 11.2A per mm. The region photographed was from 500 to 2600A. Helium and aluminum lines were used as standards of measurement.

In the visible region, Bloch and Bloch's[1] wave-length measurements were found to be very accurate and were used chiefly in calculating term values. Their method of excitation was the electrodeless discharge. Dr. J. E. Ruedy had taken some electrodeless discharge photographs of selenium in this laboratory, and measurements from his plates were used to check the measurements by Bloch and Bloch. Several important lines were also found on his plates which were not given at all by Bloch and Bloch.

DISCUSSION OF THE ANALYSIS

In this analysis, it was found that the assignments of a majority of term values agreed with the classification of Krishnamurty and

[3] O. Bartelt, Zeits. f. Physik **91**, 444 (1934).
[4] S. G. Krishnamurty and K. R. Rao, Proc. Roy. Soc. **A149**, 56 (1935).

TABLE II. *Classified lines of Se II.*

INT.	λ(air)	ν(vac)	CLASSIFICATION
2	9816.63	10184.0	$4s^24p^2(^1D)5p\ ^2P_{1\frac{1}{2}}$ – 34
1	9265.41	10789.9	27 – $4s^24p^2(^1D)5p\ ^2D_{1\frac{1}{2}}$
0	9127.76	10952.6	$4s^24p^2(^1D)5s\ ^2D_{2\frac{1}{2}}$ – $(^3P)5p\ ^4S_{1\frac{1}{2}}$
2	8679.13	11518.7	8 – $^4P_{1\frac{1}{2}}$
1	8309.52	12031.1	$4s^24p^2(^1D)5s\ ^2D_{2\frac{1}{2}}$ – $^2D_{2\frac{1}{2}}$
1	8274.55	12081.9	6 – $^4P_{1\frac{1}{2}}$
1	8217.53	12165.7	$4s^24p^2(^3P)5p\ ^4D_{\frac{1}{2}}$ – 19
0	8172.00	12233.5	$^4P_{1\frac{1}{2}}$ – 22
1	7838.81	12753.5	$4s4p^4\ \ ^2P_{1\frac{1}{2}}$ – $4s^24p^2(^3P)5p\ ^4P_{\frac{1}{2}}$
1	7796.15	12823.3	$4s^24p^2(^1D)5s\ ^2D_{1\frac{1}{2}}$ – $^2P_{\frac{1}{2}}$
0	7772.42	12866.0	7 – $^2D_{1\frac{1}{2}}$
0	7724.04	12943.0	$4s^24p^2(^3P)5s\ ^2P_{\frac{1}{2}}$ – $^4D_{\frac{1}{2}}$
0	7674.82	13026.0	$(^1D)5s\ ^2D_{2\frac{1}{2}}$ – $^2P_{1\frac{1}{2}}$
3	7391.99	13524.4	7 – $^4P_{2\frac{1}{2}}$ $4s^24p^2(^1D)5p\ ^2D_{2\frac{1}{2}}$ – $4s^24p^2(^3P)6s\ ^2P_{1\frac{1}{2}}$
2	7138.91	14003.9	$4s4p^4\ \ ^2P_{1\frac{1}{2}}$ – $5p\ ^4D_{\frac{1}{2}}$
1	6925.63	14435.1	7 – $^4S_{1\frac{1}{2}}$
00*d*	6715.51	14886.8	$4s^24p^2(^1D)5p\ ^2D_{2\frac{1}{2}}$ – 33
1	6695.78	14930.7	3 – $4s^24p^2(^3P)5p\ ^4P_{\frac{1}{2}}$
8	6534.95	15299.3	9 – $^2P_{\frac{1}{2}}$
8	6490.48	15402.9	$4s^24p^2(^3P)5s\ ^2P_{\frac{1}{2}}$ – $^4D_{\frac{1}{2}}$
6	6488.34	15408.0	9 – $^2P_{1\frac{1}{2}}$
6	6483.06	15420.6	$4s^24p^2(^3P)5s\ ^2P_{1\frac{1}{2}}$ – $^4P_{1\frac{1}{2}}$ $(^1D)5p\ ^2D_{1\frac{1}{2}}$ – 35
9	6444.25	15513.4	7 – $4s^24p^2(^3P)5p\ ^2D_{2\frac{1}{2}}$
1	6416.33	15580.9	12 – 21°
3	6370.62	15692.7	6 – $4s^24p^2(^3P)5p\ ^2D_{2\frac{1}{2}}$
3	6338.14	15773.2	$4s4p^4\ \ ^2P_{1\frac{1}{2}}$ – $^4D_{2\frac{1}{2}}$
2	6326.87	15801.2	$4s^24p^2(^3P)5p\ ^2D_{2\frac{1}{2}}$ – 25
0	6263.32	15961.6	$^4P_{\frac{1}{2}}$ – 22
00	6242.35	16015.2	8 – $4s^24p^2(^3P)5p\ ^2P_{\frac{1}{2}}$
4	6233.73	16037.3	$4s^24p^2(^3P)5s\ ^4P_{2\frac{1}{2}}$ – $^4D_{1\frac{1}{2}}$
2	6228.69	16050.3	$^2P_{1\frac{1}{2}}$ – $^2S_{\frac{1}{2}}$
2	6206.29	16108.2	5 – $^2D_{1\frac{1}{2}}$
2	6183.74	16167.0	5 – $^4D_{\frac{1}{2}}$
5	6135.04	16295.3	$4s^24p^2(^3P)5s\ ^4P_{1\frac{1}{2}}$ – $^4P_{\frac{1}{2}}$
0*d*	6131.99	16303.4	$5p\ ^2D_{1\frac{1}{2}}$ – $4s^24p^2(^3P)6s\ ^4P_{\frac{1}{2}}$
6	6123.49	16326.1	$^4S_{1\frac{1}{2}}$ – $^4P_{1\frac{1}{2}}$
6	6101.96	16383.7	$4s^24p^2(^3P)5s\ ^2P_{1\frac{1}{2}}$ – $4s^24p^2(^3P)5p\ ^2D_{1\frac{1}{2}}$
5	6096.12	16399.4	7 – $^2P_{\frac{1}{2}}$
5	6065.83	16481.3	$4s4p^4\ \ ^2P_{1\frac{1}{2}}$ – $^4P_{1\frac{1}{2}}$
10	6055.96	16508.1	7 – $^2P_{1\frac{1}{2}}$
1	6047.43	16531.4	1 – $^4P_{\frac{1}{2}}$
3	6030.12	16578.8	6 – $^2P_{\frac{1}{2}}$
1	6025.10	16592.7	3 – $^4D_{1\frac{1}{2}}$
1	6009.06	16636.9	$4s^24p^2(^3P)5p\ ^2S_{\frac{1}{2}}$ – $4s^24p^2(^3P)6s\ ^4P_{\frac{1}{2}}$
5	5990.92	16687.3	6 – $5p\ ^2P_{1\frac{1}{2}}$
2	5962.67	16766.4	5 – $^4P_{2\frac{1}{2}}$
00*d*	5922.66	16879.6	$4s^24p^2(^3P)5p\ ^4S_{1\frac{1}{2}}$ – 25
5	5886.34	16983.8	$^2P_{1\frac{1}{2}}$ – $4s^24p^2(^3P)5d\ ^4F_{1\frac{1}{2}}$
8	5866.27	17041.9	$5s\ ^2P_{1\frac{1}{2}}$ – $5p\ ^4P_{2\frac{1}{2}}$
1	5849.84	17089.8	$5p\ ^4P_{1\frac{1}{2}}$ – 24
5	5842.68	17110.7	$4s4p^4\ \ ^2P_{1\frac{1}{2}}$ – $4s^24p^2(^3P)5p\ ^2S_{\frac{1}{2}}$
2	5831.47	17143.6	$4s^24p^2(^3P)5p\ ^2P_{1\frac{1}{2}}$ – $6s\ ^2P_{\frac{1}{2}}$
3	5799.72	17237.5	$^4P_{2\frac{1}{2}}$ – $^4P_{1\frac{1}{2}}$
4	5790.03	17266.3	$^4P_{1\frac{1}{2}}$ – $^4P_{\frac{1}{2}}$
4	5784.76	17282.0	$^2D_{2\frac{1}{2}}$ – $^4P_{2\frac{1}{2}}$
3	5769.06	17329.0	27 – $5p\ ^2P_{1\frac{1}{2}}$
6	5747.62	17393.7	$4s^24p^2(^3P)5s\ ^4P_{2\frac{1}{2}}$ – $^4D_{2\frac{1}{2}}$
4	5733.05	17437.9	27 – $^2P_{\frac{1}{2}}$
4	5730.84	17444.6	$4s4p^4\ \ ^2P_{1\frac{1}{2}}$ – $^2D_{1\frac{1}{2}}$
6	5697.88	17545.5	$4s^24p^2(^3P)5s\ ^4P_{1\frac{1}{2}}$ – $^4D_{\frac{1}{2}}$
1	5672.52	17624.0	11 – $(^1D)5p\ ^2D_{1\frac{1}{2}}$
2	5655.49	17677.0	5 – $(^3P)5p\ ^2D_{1\frac{1}{2}}$
3	5652.37	17686.8	11 – 21°
6	5623.13	17778.8	$4s^24p^2(^3P)5s\ ^4P_{\frac{1}{2}}$ – $4s^24p^2(^3P)5p\ ^4P_{\frac{1}{2}}$
00	5616.65	17799.3	$5p\ ^4D_{2\frac{1}{2}}$ – 24
6	5591.16	17880.4	$(^3P)5s\ ^2P_{\frac{1}{2}}$ – $4s^24p^2(^3P)5p\ ^4P_{1\frac{1}{2}}$ $(^1D)5s\ ^2D_{1\frac{1}{2}}$ – 18°
4	5586.37	17895.7	$(^3P)5p\ ^4P_{1\frac{1}{2}}$ – $4s^24p^2(^3P)6s\ ^4P_{1\frac{1}{2}}$
8	5566.93	17958.3	$5s\ ^4P_{1\frac{1}{2}}$ – $5p\ ^4D_{1\frac{1}{2}}$
3	5560.54	17978.9	$5p\ ^2D_{2\frac{1}{2}}$ – $5d\ ^4F_{1\frac{1}{2}}$
8	5522.42	18103.0	$4s^24p^2(^3P)5s\ ^4P_{2\frac{1}{2}}$ – $4s^24p^2(^3P)5p\ ^4P_{1\frac{1}{2}}$ $4s4p^4\ \ ^2P_{1\frac{1}{2}}$ – $^4P_{2\frac{1}{2}}$
2	5484.08	18229.5	$4s^24p^2(^3P)5p\ ^4P_{\frac{1}{2}}$ – $6s\ ^4P_{1\frac{1}{2}}$
2	5455.58	18324.1	27 – 14°
3	5444.95	18360.5	$4s^24p^2(^3P)5p\ ^2D_{1\frac{1}{2}}$ – $4s^24p^2(^3P)6s\ ^4P_{2\frac{1}{2}}$
3	5401.01	18509.9	$5s\ ^2P_{\frac{1}{2}}$ – $5p\ ^2S_{\frac{1}{2}}$
2	5380.21	18581.5	10 – $(^1D)5p\ ^2D_{2\frac{1}{2}}$
9	5305.35	18843.7	$4s^24p^2(^3P)5s\ ^2P_{\frac{1}{2}}$ – $(^3P)5p\ ^2D_{1\frac{1}{2}}$
3	5301.03	18859.0	$5p\ ^4S_{1\frac{1}{2}}$ – $6s\ ^4P_{1\frac{1}{2}}$
4	5271.22	18965.7	$(^1D)5s\ ^2D_{1\frac{1}{2}}$ – $(^1D)5p\ ^2D_{2\frac{1}{2}}$
00	5257 96	19013.5	$4s4p^4\ \ ^2P_{1\frac{1}{2}}$ – $(^3P)5p\ ^4S_{1\frac{1}{2}}$
4	5253.63	19029.2	$4s^24p^2(^3P)5s\ ^4P_{\frac{1}{2}}$ – $^4D_{\frac{1}{2}}$ 4 – $^4P_{2\frac{1}{2}}$
4	5253.07	19031.2	$4s^24p^2(^3P)5s\ ^2P_{1\frac{1}{2}}$ – $^2D_{2\frac{1}{2}}$
3	5245.17	19059.9	$(^1D)5s\ ^2D_{2\frac{1}{2}}$ – $(^1D)5p\ ^2D_{2\frac{1}{2}}$
0	5243.75	19065.0	$(^3P)5s\ ^4P_{2\frac{1}{2}}$ – $(^3P)5p\ ^2D_{1\frac{1}{2}}$
1	5237.62	19087.4	10 – $(^1D)5p\ ^2D_{1\frac{1}{2}}$
10	5227.51	19124.3	$4s^24p^2(^3P)5s\ ^4P_{2\frac{1}{2}}$ – $(^3P)5p\ ^4D_{2\frac{1}{2}}$
3	5187.68	19271.1	$5p\ ^4P_{2\frac{1}{2}}$ – $6s\ ^4P_{2\frac{1}{2}}$
3	5183.01	19288.4	3 – $5p\ ^2S_{\frac{1}{2}}$
7	5175.98	19314.6	$4s^24p^2(^3P)5s\ ^4P_{1\frac{1}{2}}$ – $^4D_{2\frac{1}{2}}$
3	5171.54	19331.2	$5p\ ^4D_{1\frac{1}{2}}$ – $6s\ ^4P_{\frac{1}{2}}$
0	5150.12	19411.6	$^4P_{1\frac{1}{2}}$ – 25
5	5142.14	19441.7	$5s\ ^4P_{\frac{1}{2}}$ – $4s^24p^2(^3P)5p\ ^4D_{1\frac{1}{2}}$
3	5134.31	19471.4	$4s^24p^2(^1D)5s\ ^2D_{1\frac{1}{2}}$ – $4s^24p^2(^1D)5p\ ^2D_{1\frac{1}{2}}$
3	5109.59	19565.6	$^2D_{2\frac{1}{2}}$ – $^2D_{1\frac{1}{2}}$
1	5109.11	19567.4	$(^3P)5p\ ^4D_{2\frac{1}{2}}$ – $(^3P)6s\ ^4P_{1\frac{1}{2}}$
4	5093.26	19628.3	$(^1D)5s\ ^2D_{1\frac{1}{2}}$ – 21°

TABLE II.—*Continued.*

INT.	λ(air)	ν(vac)	CLASSIFICATION
6	5068.65	19723.6	$(^3P)5s\ ^4P_{2\frac{1}{2}} - 4s^24p^2(^3P)5p\ ^4P_{2\frac{1}{2}}$
0*d*	5063.42	19744.0	$5p\ ^4D_{3\frac{1}{2}} - 6s\ ^4P_{2\frac{1}{2}}$
			$^2D_{2\frac{1}{2}} - 28$
0*d*	5061.83	19750.2	$5 - 4s^24p^2(^3P)5p\ ^2P_{1\frac{1}{2}}$
4	5031.26	19870.2	$4s^24p^2(^3P)5p\ ^4D_{3\frac{1}{2}} - 6s\ ^4P_{2\frac{1}{2}}$
3	5019.32	19917.0	$5s\ ^2P_{1\frac{1}{2}} - 5p\ ^2P_{\frac{1}{2}}$
3	4992.75	20023.5	$^4P_{1\frac{1}{2}} - ^4P_{1\frac{1}{2}}$
1	4992.03	20026.4	$^2P_{1\frac{1}{2}} - ^2P_{1\frac{1}{2}}$
5	4975.66	20092.3	$4s4p^4\ ^2P_{1\frac{1}{2}} - ^2D_{2\frac{1}{2}}$
0	4897.56	20412.7	$4s^24p^2(^3P)5s\ ^2P_{\frac{1}{2}} - ^4S_{1\frac{1}{2}}$
0	4846.90	20626.0	$5p\ ^2D_{1\frac{1}{2}} - 5d\ ^4F_{1\frac{1}{2}}$
9	4844.96	20634.3	$5s\ ^4P_{2\frac{1}{2}} - 5p\ ^4S_{1\frac{1}{2}}$
8	4840.63	20652.7	$^4P_{1\frac{1}{2}} - ^2S_{\frac{1}{2}}$
1	4809.61	20785.9	$5p\ ^2D_{1\frac{1}{2}} - 6s\ ^2P_{\frac{1}{2}}$
1	4801.01	20823.1	$^4S_{1\frac{1}{2}} - 28$
00	4785.10	20892.4	$^4P_{1\frac{1}{2}} - 4s^24p^2(^3P)6s\ ^4P_{2\frac{1}{2}}$
2	4777.85	20924.1	$^4D_{1\frac{1}{2}} - ^4P_{1\frac{1}{2}}$
3	4765.52	20978.2	$4s4p^4\ ^2P_{1\frac{1}{2}} - 5p\ ^2P_{\frac{1}{2}}$
7	4763.65	20986.4	$4s^24p^2(^3P)5s\ ^4P_{1\frac{1}{2}} - ^2D_{1\frac{1}{2}}$
2	4761.85	20994.3	$5p\ ^4P_{\frac{1}{2}} - 6s\ ^4P_{\frac{1}{2}}$
6	4740.97	21086.9	$4s4p^4\ ^2P_{1\frac{1}{2}} - 4s^24p^2(^3P)5p\ ^2P_{1\frac{1}{2}}$
2	4733.57	21119.8	$4s^24p^2(^3P)5p\ ^2S_{\frac{1}{2}} - 6s\ ^2P_{\frac{1}{2}}$
0	4732.46	21124.8	$^4D_{2\frac{1}{2}} - 5d\ ^4F_{2\frac{1}{2}}$
0	4719.32	21183.6	$^2D_{1\frac{1}{2}} - ^4F_{2\frac{1}{2}}$
2	4718.23	21188.5	$1 - 5p\ ^2S_{\frac{1}{2}}$
2	4685.45	21336.7	$4s^24p^2(^3P)5p\ ^4D_{\frac{1}{2}} - 6s\ ^4P_{1\frac{1}{2}}$
0	4663.47	21437.3	$^4S_{1\frac{1}{2}} - 29$
6	4648.44	21506.6	$5s\ ^4P_{\frac{1}{2}} - 4s^24p^2(^3P)5p\ ^4P_{1\frac{1}{2}}$
2	4630.56	21589.6	$5p\ ^4P_{1\frac{1}{2}} - 5d\ ^4F_{1\frac{1}{2}}$
3	4628.12	21601.0	$^4D_{2\frac{1}{2}} - 6s\ ^4P_{2\frac{1}{2}}$
2	4625.37	21613.9	$^4P_{2\frac{1}{2}} - 5d\ ^4F_{\frac{1}{2}}$
1	4623.74	21621.5	$^4S_{1\frac{1}{2}} - 30$
2	4621.58	21631.6	$^4S_{1\frac{1}{2}} - 4s^24p^2(^3P)6s\ ^2P_{1\frac{1}{2}}$
0	4620.86	21635.0	$6 - 18°$
2	4620.32	21637.5	$4s^24p^2(^3P)5p\ ^4S_{1\frac{1}{2}} - 31$
5	4618.77	21644.7	$5s\ ^4P_{1\frac{1}{2}} - 4s^24p^2(^3P)5p\ ^4P_{2\frac{1}{2}}$
0	4610.67	21682.8	$4 - 14°$
7	4604.34	21712.6	$4s^24p^2(^3P)5s\ ^4P_{2\frac{1}{2}} - 4s^24p^2(^3P)5p\ ^2D_{2\frac{1}{2}}$
3	4599.96	21733.3	$5p\ ^4P_{2\frac{1}{2}} - 28$
2	4597.93	21742.9	$2 - 4s^24p^2(^3P)5p\ ^4P_{2\frac{1}{2}}$
2	4596.59	21749.2	$4s^24p^2(^3P)5p\ ^4P_{1\frac{1}{2}} - 6s\ ^2P_{\frac{1}{2}}$
0	4594.51	21759.0	$^4P_{1\frac{1}{2}} - 26$
00	4589.07	21784.8	$^2D_{2\frac{1}{2}} - 32$
2	4567.19	21889.2	$^4D_{\frac{1}{2}} - 25$
6	4563.95	21904.7	$4 - 4s^24p^2(^3P)5p\ ^2P_{\frac{1}{2}}$
3	4561.75	21915.3	$4s^24p^2(^3P)5p\ ^2D_{2\frac{1}{2}} - 33$
1	4552.64	21959.2	$^2P_{1\frac{1}{2}} - 35$
2	4541.40	22013.5	$4 - 4s^24p^2(^3P)5p\ ^2P_{1\frac{1}{2}}$
4	4516.25	22136.0	$4s^24p^2(^3P)5s\ ^4P_{\frac{1}{2}} - ^2S_{\frac{1}{2}}$
1	4514.11	22146.5	$5p\ ^4P_{1\frac{1}{2}} - 5d\ ^4F_{2\frac{1}{2}}$
1	4483.48	22297.9	$^4D_{2\frac{1}{2}} - ^4F_{1\frac{1}{2}}$
2	4476.70	22331.6	$10 - 23°$
8	4467.60	22377.1	$4s^24p^2(^3P)5s\ ^4P_{2\frac{1}{2}} - 14°$
			$^2P_{\frac{1}{2}} - 4s^24p^2(^3P)5p\ ^2P_{\frac{1}{2}}$
0	4449.56	22467.8	$5p\ ^4D_{2\frac{1}{2}} - 26$
7	4449.15	22469.9	$5s\ ^4P_{\frac{1}{2}} - 4s^24p^2(^3P)5p\ ^2D_{1\frac{1}{2}}$
8	4446.02	22485.8	$^2P_{\frac{1}{2}} - ^2P_{1\frac{1}{2}}$
1	4436.96	22531.7	$5p\ ^4P_{2\frac{1}{2}} - 30$
4	4434.92	22542.0	$7 - 4s^24p^2(^1D)5p\ ^2D_{2\frac{1}{2}}$
			$4s^24p^2(^3P)5p\ ^4P_{2\frac{1}{2}} - (^3P)6s\ ^2P_{1\frac{1}{2}}$
3	4433.74	22548.0	$^4P_{2\frac{1}{2}} - 31$
5	4432.33	22555.2	$5s\ ^4P_{1\frac{1}{2}} - 4s^24p^2(^3P)5p\ ^4S_{1\frac{1}{2}}$
3	4426.12	22586.8	$5p\ ^4P_{\frac{1}{2}} - 6s\ ^4P_{1\frac{1}{2}}$
1	4415.14	22643.0	$27 - 5p\ ^4D_{2\frac{1}{2}}$
3	4413.16	22653.1	$2 - ^4S_{1\frac{1}{2}}$
0	4411.17	22663.4	$8 - (^1D)5p\ ^2D_{1\frac{1}{2}}$
0	4402.51	22708.0	$4s^24p^2(^3P)5s\ ^4P_{2\frac{1}{2}} - (^3P)5p\ ^2P_{1\frac{1}{2}}$
6	4401.02	22715.7	$(^1D)5s\ ^2D_{1\frac{1}{2}} - 23°$
2	4399.94	22721.2	$6 - 4s^24p^2(^1D)5p\ ^2D_{2\frac{1}{2}}$
2	4399.17	22725.2	$4s^24p^2(^3P)5p\ ^2S_{\frac{1}{2}} - 28$
8	4382.87	22809.7	$(^1D)5s\ ^2D_{2\frac{1}{2}} - 23°$
00	4372.69	22862.8	$(^3P)5p\ ^4S_{1\frac{1}{2}} - 32$
4	4355.15	22954.9	$^2D_{2\frac{1}{2}} - 35$
2	4354.64	22957.6	$^4D_{1\frac{1}{2}} - 4s^24p^2(^3P)6s\ ^4P_{2\frac{1}{2}}$
2	4347.79	22993.7	$^4S_{1\frac{1}{2}} - 33$
3	4345.41	23006.3	$^2D_{1\frac{1}{2}} - 29$
4	4337.60	23047.7	$7 - 4s^24p^2(^1D)5p\ ^2D_{1\frac{1}{2}}$
7	4320.39	23139.6	$4s^24p^2(^3P)5p\ ^4P_{\frac{1}{2}} - 25$
2	4318.91	23147.5	$^4D_{3\frac{1}{2}} - 31$
4	4309.09	23200.2	$^2D_{1\frac{1}{2}} - 4s^24p^2(^3P)6s\ ^2P_{1\frac{1}{2}}$
3	4307.95	23206.4	$^2D_{1\frac{1}{2}} - 31$
2	4304.13	23227.0	$6 - 4s^24p^2(^1D)5p\ ^2D_{1\frac{1}{2}}$
4	4297.31	23263.9	$3 - (^3P)5p\ ^2P_{1\frac{1}{2}}$
5	4280.36	23356.0	$10 - (^1D)5p\ ^2P_{1\frac{1}{2}}$
7	4248.00	23533.9	$4s^24p^2(^3P)5p\ ^2S_{\frac{1}{2}} - (^3P)6s\ ^2P_{1\frac{1}{2}}$
3	4230.05	23633.7	$5s\ ^4P_{1\frac{1}{2}} - 5p\ ^2D_{2\frac{1}{2}}$
3	4226.37	23654.3	$5p\ ^4D_{1\frac{1}{2}} - 5d\ ^4F_{1\frac{1}{2}}$
6	4212.58	23731.8	$2 - 5p\ ^2D_{2\frac{1}{2}}$
0	4205.32	23772.7	$4s^24p^2(^3P)5p\ ^4P_{2\frac{1}{2}} - 32$
4	4198.05	23813.9	$^4D_{1\frac{1}{2}} - 4s^24p^2(^3P)6s\ ^2P_{\frac{1}{2}}$
3	4196.24	23824.2	$^4D_{1\frac{1}{2}} - 26$
4	4194.55	23833.8	$(^1D)5s\ ^2D_{2\frac{1}{2}} - 4s^24p^2(^1D)5p\ ^2P_{1\frac{1}{2}}$
1	4182.20	23904.2	$(^3P)5p\ ^4P_{2\frac{1}{2}} - 33$
10	4180.94	23911.4	$4s^24p^2(^3P)5p\ ^4D_{3\frac{1}{2}} - 4s^24p^2(^3P)5d\ ^4F_{1\frac{1}{2}}$
9	4175.32	23943.6	$^4D_{2\frac{1}{2}} - ^4F_{2\frac{1}{2}}$
2	4169.65	23976.1	$^4P_{2\frac{1}{2}} - 34$
00	4167.86	23986.4	$^4D_{1\frac{1}{2}} - 27$
3	4165.66	23999.1	$27 - 4s^24p^2(^3P)5p\ ^4D_{1\frac{1}{2}}$
5	4159.75	24033.1	$4s^24p^2(^3P)5p\ ^4S_{1\frac{1}{2}} - 35$
	4154.64	24062.7	$^4D_{2\frac{1}{2}} - 28$

TABLE II.—*Continued.*

INT.	λ(air)	ν(vac)	CLASSIFICATION
4	4153.93	24066.8	$^4D_{\frac{1}{2}}$ – $4s^24p^2(^3P)5d\ ^4F_{\frac{1}{2}}$
2	4138.99	24153.7	$^4P_{\frac{1}{2}}$ – 30
4	4137.31	24163.5	$^4P_{\frac{1}{2}}$ – $4s^24p^2(^3P)6s\ ^2P_{\frac{1}{2}}$
6	4136.28	24169.5	$^4P_{\frac{1}{2}}$ – 31
6	4126.57	24226.4	$^4D_{\frac{1}{2}}$ – $4s^24p^2(^3P)6s\ ^2P_{\frac{1}{2}}$
3	4114.35	24298.3	$5s\ ^4P_{\frac{1}{2}}$ – 14°
2	4097.91	24396.3	2 – 14°
6	4091.95	24431.4	$4s^24p^2(^3P)\ 5p\ ^2D_{\frac{1}{2}}$ – 32
8	4070.16	24562.1	$^2D_{\frac{1}{2}}$ – 33
6	4062.06	24611.1	$^4S_{\frac{1}{2}}$ – 36
2	4058.20	24634.5	$^2D_{\frac{1}{2}}$ – 34
1	4047.77	24698.0	5 – 18°
3	4038.31	24755.8	1 – $4s^24p^2(^3P)5p\ ^2P_{\frac{1}{2}}$
2	4019.50	24871.7	$4s^24p^2(^3P)5p\ ^4D_{\frac{3}{2}}$ – $6s\ ^2P_{\frac{1}{2}}$
6	4018.52	24877.8	$^4D_{\frac{3}{2}}$ – 31
6	4007.90	24943.7	$^2D_{\frac{1}{2}}$ – 35
5	4003.08	24973.7	$5s\ ^2P_{\frac{1}{2}}$ – 18°
3	3948.80	25317.0	$5p\ ^4P_{\frac{1}{2}}$ – $4s^24p^2(^3P)5d\ ^4F_{\frac{1}{2}}$
1	3924.02	25476.9	$4s^24p^2(^3P)5p\ ^4P_{\frac{1}{2}}$ – $4s^24p^2(^3P)6s\ ^2P_{\frac{1}{2}}$
2	3917.06	25522.2	$^4P_{\frac{3}{2}}$ – 36
1	3916.49	25525.9	$^4P_{\frac{1}{2}}$ – 33
1	3913.81	25543.4	$^4D_{\frac{3}{2}}$ – 35
5	3877.28	25784.0	5 – $4s^24p^2(^1D)5p\ ^2D_{\frac{3}{2}}$
0	3839.91	26034.9	$4s4p^4\ \ ^2P_{\frac{1}{2}}$ – 18°
3	3836.25	26059.8	$4s^24p^2(^3P)5s\ ^2P_{\frac{1}{2}}$ – $4s^24p^2(^1D)5p\ ^2D_{\frac{1}{2}}$
2	3818.75	26179.2	$5p\ ^2D_{\frac{1}{2}}$ – 36
1	3811.62	26228.1	$^4D_{\frac{1}{2}}$ – $4s^24p^2(^3P)6s\ ^2P_{\frac{1}{2}}$
4	3793.63	26352.5	5 – 21°
3	3763.24	26565.3	$4s^24p^2(^3P)5s\ ^2P_{\frac{1}{2}}$ – $4s^24p^2(^1D)5p\ ^2D_{\frac{1}{2}}$ $5p\ ^4P_{\frac{1}{2}}$ – 35
3	3754.31	26628.5	$5s\ ^2P_{\frac{1}{2}}$ – 21°
4	3686.21	27120.4	$4s4p^4\ \ ^2P_{\frac{1}{2}}$ – $4s^24p^2(^1D)5p\ ^2D_{\frac{1}{2}}$
2	3639.40	27469.3	$^4P_{\frac{1}{2}}$ – $(^3P)5p\ ^4P_{\frac{1}{2}}$
1	3623.30	27591.3	$4s^24p^2(^3P)5p\ ^4D_{\frac{1}{2}}$ – 33
4	3618.73	27626.1	$4s4p^4\ \ ^2P_{\frac{1}{2}}$ – $4s^24p^2(^1D)5p\ ^2D_{\frac{1}{2}}$
4	3610.50	27689.1	$^2P_{\frac{1}{2}}$ – 21°
00	3589.41	27851.8	$4s^24p^2(^3P)5p\ ^4D_{\frac{3}{2}}$ – 36
2	3588.16	27861.5	$4s4p^4\ \ ^4P_{\frac{1}{2}}$ – $4s^24p^2(^3P)5p\ ^4D_{\frac{1}{2}}$
0	3584.32	27891.4	$4s^24p^2(^3P)5p\ ^4P_{\frac{1}{2}}$ – $6s\ ^2P_{\frac{1}{2}}$
1	3535.76	28274.4	$4s4p^4\ \ ^4P_{\frac{1}{2}}$ – $5p\ ^4D_{\frac{1}{2}}$
4	3444.27	29025.5	$4s^24p^2(^3P)5s\ ^2P_{\frac{1}{2}}$ – $(^1D)5p\ ^2D_{\frac{1}{2}}$
4	3384.98	29533.8	5 – 23°
3	3353.67	29809.5	$4s^24p^2(^3P)5s\ ^2P_{\frac{1}{2}}$ – 23°
4	3242.19	30834.5	$4s4p^4\ \ ^4P_{\frac{3}{2}}$ – $4s^24p^2(^3P)5p\ ^4D_{\frac{1}{2}}$
3	3238.43	30870.3	$^2P_{\frac{1}{2}}$ – 23°
2	3228.17	30968.4	$^4P_{\frac{1}{2}}$ – $4s^24p^2(^3P)5p\ ^2S_{\frac{1}{2}}$
5	3204.58	31196.4	$^4P_{\frac{1}{2}}$ – $^4P_{\frac{1}{2}}$
2	3200.93	31231.9	$4s^24p^2(^3P)5s\ ^4P_{\frac{1}{2}}$ – 21°
7	3141.13	31826.5	$4s4p^4\ \ ^4P_{\frac{1}{2}}$ – $4s^24p^2(^3P)5p\ ^2S_{\frac{1}{2}}$
6	3134.42	31894.6	$^2P_{\frac{1}{2}}$ – $(^1D)5p\ ^2P_{\frac{1}{2}}$
3	3108.54	32160.1	$^4P_{\frac{1}{2}}$ – $(^3P)5p\ ^2D_{\frac{1}{2}}$
3	3105.50	32191.6	$^4P_{\frac{3}{2}}$ – $^4D_{\frac{3}{2}}$
4	3046.24	32817.9	$^4P_{\frac{1}{2}}$ – $^4P_{\frac{3}{2}}$
7	3041.31	32871.1	$^4P_{\frac{3}{2}}$ – $^4S_{\frac{3}{2}}$
7	3038.66	32899.7	$^4P_{\frac{5}{2}}$ – $^4P_{\frac{1}{2}}$
6	2963.91	33729.4	$^4P_{\frac{1}{2}}$ – $^4S_{\frac{3}{2}}$
6	2952.28	33863.0	$^4P_{\frac{3}{2}}$ – $^2D_{\frac{3}{2}}$
2	2947.13	33922.2	$^4P_{\frac{5}{2}}$ – $^4P_{\frac{3}{2}}$
1	2934.18	34071.1	3 – $4s^24p^2(^1D)5p\ ^2P_{\frac{1}{2}}$
2	2905.07	34412.5	$4s^24p^2(^3P)5s\ ^4P_{\frac{1}{2}}$ – 23°
6	2895.88	34521.7	$4s4p^4\ \ ^4P_{\frac{5}{2}}$ – $4s^24p^2(^3P)5p\ ^4P_{\frac{3}{2}}$
0	2888.14	34614.3	$^4P_{\frac{1}{2}}$ – 14°
2	2872.08	34807.8	$^4P_{\frac{1}{2}}$ – $4s^24p^2(^3P)5p\ ^2D_{\frac{3}{2}}$
5	2821.52	35431.5	$^4P_{\frac{3}{2}}$ – $^4S_{\frac{3}{2}}$
4	2738.16	36510.1	$^4P_{\frac{5}{2}}$ – $^2D_{\frac{3}{2}}$
1	2357.48	42405.2	$^4P_{\frac{1}{2}}$ – 21°
2	2113.95	47289.8	$^4P_{\frac{3}{2}}$ – 14°

INT.	λ(vac)	ν(vac)	CLASSIFICATION
2	1667.15	59982.6	$4s^24p^2\ \ ^2P_{\frac{1}{2}}$ – $4s4p^4\ \ ^4P_{\frac{3}{2}}$
4	1621.23	61681.6	$^2P_{\frac{1}{2}}$ – $^4P_{\frac{1}{2}}$
1	1598.95	62541.1	$^2P_{\frac{1}{2}}$ – $^4P_{\frac{1}{2}}$
			$^2P_{\frac{1}{2}}$ – $^4P_{\frac{3}{2}}$
5	1426.65	70094.2	$^2D_{\frac{3}{2}}$ – $^4P_{\frac{3}{2}}$
2	1414.25	70708.7	$^2D_{\frac{3}{2}}$ – $^4P_{\frac{5}{2}}$
0	1401.01	71377.0	$^2P_{\frac{1}{2}}$ – $4s^24p^2(^3P)5s\ ^4P_{\frac{1}{2}}$
0	1392.81	71797.3	$^2P_{\frac{3}{2}}$ – $4s4p^4\ \ ^4P_{\frac{1}{2}}$
1	1380.96	72413.2	$^2D_{\frac{5}{2}}$ – $^4P_{\frac{3}{2}}$
1	1372.51	72859.2	$^2P_{\frac{1}{2}}$ – $4s^24p^2(^3P)5s\ ^4P_{\frac{3}{2}}$
2	1364.83	73269.2	$^2D_{\frac{3}{2}}$ – $4s4p^4\ \ ^4P_{\frac{1}{2}}$
0	1360.86	73482.9	$^2P_{\frac{1}{2}}$ – 1
0	1356.57	73715.3	$^2P_{\frac{3}{2}}$ – $4s^24p^2(^3P)5s\ ^4P_{\frac{1}{2}}$
1	1347.31	74222.0	$^2P_{\frac{3}{2}}$ – 3
0	1337.13	74787.0	$^2P_{\frac{1}{2}}$ – $4s^24p^2(^3P)5s\ ^4P_{\frac{3}{2}}$
3	1333.32	75001.0	$^2P_{\frac{1}{2}}$ – $^2P_{\frac{1}{2}}$
7	1318.25	75858.1	$^2P_{\frac{3}{2}}$ – $^2P_{\frac{3}{2}}$
8	1308.89	76400.8	$^2P_{\frac{1}{2}}$ – $4s4p^4\ \ ^2P_{\frac{1}{2}}$
3	1294.41	77255.1	$^2P_{\frac{3}{2}}$ – $^2P_{\frac{1}{2}}$
8	1290.97	77461.3	$^2P_{\frac{1}{2}}$ – $4s^24p^2(^3P)5s\ ^2P_{\frac{1}{2}}$
3	1286.41	77735.9	$^2P_{\frac{1}{2}}$ – 5
2	1276.84	78318.5	$^2P_{\frac{3}{2}}$ – $4s^24p^2(^3P)5s\ ^2P_{\frac{1}{2}}$
3	1237.61	80800.6	$^2P_{\frac{1}{2}}$ – 11
7	1234.88	80979.7	$^2P_{\frac{1}{2}}$ – 12
2	1229.04	81364.4	$4s^24p\ \ ^2P_{\frac{1}{2}}$ – 13
3	1224.63	81657.2	$^2P_{\frac{3}{2}}$ – 6
2	1221.94	81837.1	$^2P_{\frac{3}{2}}$ – 7
2	1218.27	82083.6	$^2P_{\frac{1}{2}}$ – 8
4	1218.01	82101.1	$^2D_{\frac{3}{2}}$ – $4s^24p^2(^3P)5s\ ^4P_{\frac{3}{2}}$
7	1205.69	82940.0	$^2P_{\frac{3}{2}}$ –
3	1205.25	82970.5	$^2D_{\frac{5}{2}}$ – $4s^24p^2(^3P)5s\ ^4P_{\frac{1}{2}}$
0	1199.72	83352.7	$^2D_{\frac{3}{2}}$ – 1
2	1196.40	83584.4	$^2D_{\frac{3}{2}}$ – $4s^24p^2(^3P)5s\ ^4P_{\frac{1}{2}}$

TABLE II.—*Continued.*

INT.	λ(vac)	ν(vac)		CLASSIFICATION			
10	1192.29	83872.4		$^4S_{1\frac{1}{2}}$	–	$4s4p^4$	$^4P_{2\frac{1}{2}}$
2	1183.99	84460.0		$^2P_{1\frac{1}{2}}$	–	$4s^24p^2(^1D)5s$	$^2D_{2\frac{1}{2}}$
3	1182.65	84556.1		$^2P_{1\frac{1}{2}}$	–		$^2D_{1\frac{1}{2}}$
4	1178.05	84886.2		$^2D_{2\frac{1}{2}}$	–	$(^3P)5s$	$^4P_{2\frac{1}{2}}$
1	1177.31	84939.6		$^2P_{1\frac{1}{2}}$	–	10	
2	1170.76	85414.6		$^2P_{\frac{1}{2}}$	–	$4s^24p^2(^1D)5s$	$^2D_{1\frac{1}{2}}$
8	1168.53	85577.4		$^4S_{1\frac{1}{2}}$	–	$4s4p^4$	$^4P_{1\frac{1}{2}}$
5	1166.53	85724.4		$^2D_{1\frac{1}{2}}$	–	$4s^24p^2(^3P)5s$	$^2P_{\frac{1}{2}}$
4	1157.31	86407.2		$^2P_{1\frac{1}{2}}$	–	11	
8	1156.91	86437.1		$^4S_{1\frac{1}{2}}$	–	$4s4p^4$	$^4P_{\frac{1}{2}}$
7	1155.99	86508.4		$^2D_{2\frac{1}{2}}$	–		$^2P_{1\frac{1}{2}}$
9	1141.94	87569.9		$^2D_{2\frac{1}{2}}$	–	$4s^24p^2(^3P)5s$	$^2P_{1\frac{1}{2}}$
0	1138.36	87845.3		$^2D_{2\frac{1}{2}}$	–	5	
1	1133.89	88191.9		$^2D_{1\frac{1}{2}}$	–	$4s^24p^2(^3P)5s$	$^2P_{1\frac{1}{2}}$
1	1130.48	88458.0		$^2D_{1\frac{1}{2}}$	–	5	
0	1129.79	88512.0	$4s^24p^3$	$^2P_{1\frac{1}{2}}$	–	12	
1	1119.04	89362.7		$^2P_{\frac{1}{2}}$	–	12	
3	1099.97	90911.4		$^2D_{2\frac{1}{2}}$	–	6	
8	1097.82	91089.2		$^2D_{2\frac{1}{2}}$	–	7	
1	1090.43	91707.1		$^2D_{1\frac{1}{2}}$	–	7	
5	1085.88	92090.8		$^2D_{1\frac{1}{2}}$	–	8	
4	1077.54	92804.3		$^2D_{1\frac{1}{2}}$	–	9	
9	1057.41	94570.3		$^2D_{2\frac{1}{2}}$	–	$4s^24p^2(^1D)5s$	$^2D_{2\frac{1}{2}}$
3	1052.09	95048.5		$^2D_{2\frac{1}{2}}$	–	10	
2	1050.57	95186.1		$^2D_{1\frac{1}{2}}$	–	$4s^24p^2(^1D)5s$	$^2D_{2\frac{1}{2}}$
10	1049.65	95270.0		$^4S_{1\frac{1}{2}}$	–	$(^3P)5s$	$^4P_{\frac{1}{2}}$
1	1047.67	95450.0		$^2P_{1\frac{1}{2}}$	–	13	
4	1045.31	95665.0		$^2D_{1\frac{1}{2}}$	–	10	
3	1038.36	96306.0		$^2P_{\frac{1}{2}}$	–	13	
3	1036.16	96509.8		$^2D_{2\frac{1}{2}}$	–	11	
10	1033.60	96749.1		$^4S_{1\frac{1}{2}}$	–	$4s^24p^2(^3P)5s$	$^4P_{1\frac{1}{2}}$
6	1029.56	97128.6		$^2D_{1\frac{1}{2}}$	–	11	
1	1022.11	97836.4		$^2P_{1\frac{1}{2}}$	–	15	
9	1014.01	98618.6		$^2D_{2\frac{1}{2}}$	–	12	
9	1013.40	98677.7		$^4S_{1\frac{1}{2}}$	–	$4s^24p^2(^3P)5s$	$^4P_{2\frac{1}{2}}$
3	1011.84	98830.3		$^2P_{1\frac{1}{2}}$	–	16	
2	1011.15	98897.5		$^4S_{1\frac{1}{2}}$	–	$4s^24p^2(^3P)5s$	$^2P_{\frac{1}{2}}$
1	997.14	100286.8		$^2P_{\frac{1}{2}}$	–	17	
2	997.06	100295.2		$^4S_{1\frac{1}{2}}$	–	$4s4p^4$	$^2P_{1\frac{1}{2}}$
0	986.71	101347.0	$4s^24p^3$	$^4S_{1\frac{1}{2}}$	–	$4s^24p^2(^3P)5s$	$^2P_{1\frac{1}{2}}$
6	983.94	101632.4		$^4S_{1\frac{1}{2}}$	–	5	
3	974.94	102570.4		$^2P_{1\frac{1}{2}}$	–	19	
2	961.77	103974.5		$^2P_{1\frac{1}{2}}$	–	20	
4	953.88	104835.4		$^2P_{\frac{1}{2}}$	–	20	
3	951.26	105123.4		$^2P_{1\frac{1}{2}}$	–	22	
2	950.02	105260.9		$^4S_{1\frac{1}{2}}$	–	8	
2	943.61	105976.0		$^4S_{1\frac{1}{2}}$	–	9	
				$^2P_{\frac{1}{2}}$	–	22	

INT.	λ(vac)	ν(vac)		CLASSIFICATION			
1	926.38	107947.1		$^2D_{2\frac{1}{2}}$	–	15	
0	922.90	108353.6		$^4S_{1\frac{1}{2}}$	–	$4s^24p^2(^1D)5s$	$^2D_{2\frac{1}{2}}$
5	921.12	108563.5		$^2D_{1\frac{1}{2}}$	–	15	
4	918.84	108833.5		$^4S_{\frac{1}{2}}$	–	10	
2	917.94	108940.0		$^2D_{2\frac{1}{2}}$	–	16	
9	912.89	109542.2		$^2D_{2\frac{1}{2}}$	–	17	
2	907.81	110154.7		$^2D_{1\frac{1}{2}}$	–	17	
				$^2P_{1\frac{1}{2}}$	–	$4s^24p^2(^3P)6s$	$^4P_{\frac{1}{2}}$
8	906.63	110298.1		$^4S_{1\frac{1}{2}}$	–	11	
0	894.99	111732.7		$^2P_{1\frac{1}{2}}$	–	$4s^24p^2(^3P)6s$	$^4P_{1\frac{1}{2}}$
6	890.59	112285.4		$^2P_{1\frac{1}{2}}$	–	25	
5	887.48	112678.6		$^2D_{2\frac{1}{2}}$	–	19	
0	883.77	113151.6		$^2P_{\frac{1}{2}}$	–	25	
6	882.61	113300.8		$^2D_{1\frac{1}{2}}$	–	19	
0	872.27	114643.5		$^2P_{\frac{1}{2}}$	–	26	
4	871.83	114701.0	$4s^24p^3$	$^2D_{1\frac{1}{2}}$	–	20	
2	871.02	114808.1		$^2P_{1\frac{1}{2}}$	–	27	
3	867.83	115229.5		$^2D_{2\frac{1}{2}}$	–	22	
0	865.90	115486.9		$^2P_{\frac{1}{2}}$	–	$4s^24p^2(^3P)6s$	$^2P_{\frac{1}{2}}$
00	864.59	115661.8		$^2P_{\frac{1}{2}}$	–	27	
1	855.81	116848.0		$^2P_{1\frac{1}{2}}$	–	29	
0	854.46	117033.0		$^2P_{1\frac{1}{2}}$	–	30	
0	854.35	117048.7		$^2P_{1\frac{1}{2}}$	–	$4s^24p^2(^3P)6s$	$^2P_{1\frac{1}{2}}$
4	849.60	117703.0		$^2P_{\frac{1}{2}}$	–	29	
4	844.00	118483.4		$^2P_{1\frac{1}{2}}$	–	34	
0	838.43	119271.3		$^2P_{\frac{1}{2}}$	–	33	
9	832.74	120085.4		$^2D_{2\frac{1}{2}}$	–	24	
8	828.48	120702.8		$^2D_{1\frac{1}{2}}$	–	24	
3	820.68	121850.6		$^2D_{2\frac{1}{2}}$	–	$4s^24p^2(^3P)6s$	$^4P_{1\frac{1}{2}}$
3	816.99	122401.1		$^2D_{2\frac{1}{2}}$	–	25	
00	814.86	122720.4		$^4S_{1\frac{1}{2}}$	–	16	
3	801.59	124742.5		$^2D_{2\frac{1}{2}}$	–	26	
1	800.54	124915.3		$^2D_{2\frac{1}{2}}$	–	27	
3	797.69	125362.3		$^2D_{1\frac{1}{2}}$	–	$4s^24p^2(^3P)6s$	$^2P_{\frac{1}{2}}$
4	786.49	127146.7		$^2D_{2\frac{1}{2}}$	–	30	
1	783.84	127577.1		$^2D_{1\frac{1}{2}}$	–	29	
0	782.66	127769.2		$^2D_{1\frac{1}{2}}$	–	$4s^24p^2(^3P)6s$	$^2P_{1\frac{1}{2}}$
00	782.09	127862.5		$^4S_{1\frac{1}{2}}$	–	20	
0	775.09	129016.5		$^4S_{1\frac{1}{2}}$	–	22	
2	774.43	129127.2	$4s^24p^3$	$^2D_{1\frac{1}{2}}$	–	33	
0	746.02	134045.5		$^4S_{1\frac{1}{2}}$	–	$4s^24p^2(^3P)6s$	$^4P_{\frac{1}{2}}$
0	737.30	135630.5		$^4S_{1\frac{1}{2}}$	–		$^4P_{1\frac{1}{2}}$
0	726.41	137663.3		$^4S_{1\frac{1}{2}}$	–		$^4P_{2\frac{1}{2}}$
00	721.88	138527.2		$^4S_{1\frac{1}{2}}$	–		$^2P_{\frac{1}{2}}$
0	710.47	140751.9		$^4S_{1\frac{1}{2}}$	–	29	
7	709.57	140930.4		$^4S_{1\frac{1}{2}}$	–	30	
3	697.65	143338.3		$^4S_{1\frac{1}{2}}$	–	35	
1	694.83	143920.0		$^4S_{1\frac{1}{2}}$	–	36	

Rao.[4] In addition, the $4s^24p^2(^3P)5p\ ^2S_{\frac{1}{2}}$ and $4s^24p^2(^1D)5p\ ^2D_{2\frac{1}{2}}$ and $^2P_{1\frac{1}{2}}$ terms have been found and identified. Also the terms *a* and *c* in the notation of Krishnamurty and Rao have been identified as $4s^24p^2(^3P)5p\ ^2P_{\frac{1}{2}}$ and $4s^24p^2(^1D)5p\ ^2D_{1\frac{1}{2}}$, respectively, and their $4s^24p^2(^3P)5p\ ^2P_{\frac{1}{2}}$ term has been changed to $4s^24p^2(^3P)5p\ ^2P_{1\frac{1}{2}}$.

A few changes have also been made in the assignment of higher term values. The $4s^24p^2(^3P)5d\ ^4P_{1\frac{1}{2}}$ and $^4F_{1\frac{1}{2}}$ terms have been reclassified as $4s^24p^2(^3P)6s\ ^2P_{1\frac{1}{2}}$ and $^2P_{\frac{1}{2}}$, respectively. This change has been made because certain transitions indicate that the latter term has a *J* value of $\frac{1}{2}$ and because this assignment gives the expected value for the doublet interval mentioned. The other assignments of Krishnamurty and Rao with respect to the $4s^24p^25d$ terms are questionable although the assignments of the ^4F terms with the above correction noted seem to be justified. However it is thought that their assignment of the $4s^24p^24d\ ^4F$ terms is incorrect as most of the lines used by them in determining those terms have been found both reasonable and necessary for other important transitions. It is also doubtful whether the *α*, *b*, and $4s^24p^25d\ ^4D_{3\frac{1}{2}}$ terms given by Krishnamurty and Rao are real as some of the lines used in their assignment are regarded as representing essentially other transitions as here reported, and at least one line, λ1259.5, probably belongs to sulphur instead of selenium.

Several new terms have been found in the course of this research which probably are associated with the $4s^24p^24d$, $4s^24p^25d$, and $4s^24p^25p$ configurations. These terms have only been assigned *J* values and numbers for notation purposes as it is impossible at present, and of somewhat questionable significance, to assign definite *L* and *S* values to them.

The analysis of Se II is rendered very difficult, because for the higher states, the multiplets from different configurations overlap considerably. The multiplets as a whole come closer together and the intervals within each multiplet become larger than those for the corresponding spectra of O II and S II. This is due to a breakdown in the Russell-Saunders coupling. As Bacher and Goudsmit[5] point out, when the Russell-Saunders coupling breaks down, it becomes impossible to distinguish between the different multiplets of the same configuration without ambiguity, and the use of symbols, except for the *J* value, is meaningless and oftentimes misleading.

The series limits were approximately determined by the Rydberg formula from the various members of the multiplets $4s^24p^25s\ ^4P$ and ^2P and $4s^24p^26s\ ^4P$ and ^2P. From these limits, an average value of 173,557 cm^{-1} was calculated as the interval between the ground states, $4s^24p^3\ ^4S_{1\frac{1}{2}}$, of Se II and, $4s^24p^2\ ^3P_0$, of Se III, which corresponds to an ionization potential of 21.3 volts. This is slightly lower than the value given by Krishnamurty and Rao[4] which is evidently based on an average of series limits calculated from the $4s^24p^25s$ and $4s^24p^26s\ ^4P$ terms and the $4s^24p^24d$ and $4s^24p^25d\ ^4F$ terms. Their value would be expected to be somewhat in error due to the fact that the assignment of the $4s^24p^24d\ ^4F$ term is probably incorrect.

Terms and Classified Lines

All of the terms thus far established are listed in Table I with the notations indicated as determined by the author. As the series limits are not very accurately known, all values are given relative to the ground state $4s^24p^3\ ^4S_{1\frac{1}{2}}$. The electron configuration, where known, is given in the first column, the term symbol, or a number, in the second column, the *J* value in column 3, and the relative term value in the last column. *A* (K & R) is placed after the terms which are here found to be in complete agreement with those given by Krishnamurty and Rao.[4]

All of the classified lines are collected in Table II. Relative intensities, based on a scale of 10 for a maximum, are given in column 1. Column 2 contains the wave-length measurements, and the wave numbers, all corrected to vacuum, are given in column 3. The last column contains the line classifications.

The author wishes to express his appreciation to Professor R. C. Gibbs for his helpful advice and criticism during the course of this investigation. He also wishes to thank Dr. J. E. Ruedy for his many useful suggestions and for the use of some of his spectral plates and data.

[5] Bacher and Goudsmit, *Atomic Energy States* (1933), p. 11.

Overtone Absorption Bands of Gaseous HF

D. E. KIRKPATRICK AND E. O. SALANT, *Department of Physics, Washington Square College, New York University*

(Received August 19, 1935)

With a 21-foot grating, the structure of the 3←0 and 4←0 vibration-rotation absorption bands of gaseous HF was observed and the lines measured. The vibrational constants of the molecules are, using also Imes' measurements of the 1←0 band: $\omega_e=4141.305$, $x_e\omega_e=90.866$, $y_e\omega_e=0.921$. These constants do not permit evaluation of the energy of dissociation, but the simple Birge formula gives rough agreement. Rotational constants are compared with those obtained from the fundamental band and agree, in general, satisfactorily. No evidence of associated molecules is observed in the overtone bands.

IN the present communication, measurements of the 3←0 and 4←0 vibration-rotation absorption bands of gaseous HF are described and discussed in some detail; the results of these measurements have been already announced briefly.[1]

The fundamental band of HF was measured by Imes[2] with a plane grating and thermopile and the rotational constants B_e and α_e (in Mulliken's notation[3]) were determined therefrom. The center of this band, at 2.52μ, and the unresolved 2←0 band barely detected at 1.27μ by Schaefer and Thomas[4] were used to obtain the vibrational constants ω_e and $x_e\omega_e$. The resulting value for the anharmonic term seemed to be inconsistent with its value for the other hydrogen halides. It was, therefore, deemed worth while to measure the higher overtone bands of HF in the region where photographic spectroscopy could be employed.

The most satisfactory of various absorption cells was a copper tube 225 cm long, with fluorite windows fastened securely by clamps and high melting point paraffin wax, and with side tubes attached with silver solder.

Hydrogen fluoride was generated[5] by heating KHF_2 in a copper retort which had a sealed-in copper-constantan thermocouple to facilitate control of the rate of heating. This was necessary in order to prevent sputtering of the KHF_2 melt into the retort outlet and to reject the moist gas evolved before the constant boiling mixture is attained (at 504°C).

The spectrograph was a 21-foot, 15,000-line concave grating in a Paschen mount, having a dispersion of 2.64A/mm in the first order region of 8790A and 1.33A/mm in the second order of 6744A. The slit width was 0.04 mm. Eastman infrared sensitive plates, types IP and IN, sensitized in NH_4OH, were used in the region of the 3←0 and 4←0 bands, respectively. A Schott-Jena RG1 filter was used to eliminate higher order radiation below 6000A. Neon lines, as suggested by Meggers and Humphreys,[6] were used for calibration at 8790A and international iron standards at 6744A. Conversion to vacuum wave numbers was made from Kayser[7] and the spectrograms were microphotometered with a Moll, type A instrument.

A 500-watt compact filament projection bulb served as a source of continuous radiation and made possible satisfactory exposures on IP plates in thirty minutes when the cell was empty. Because of clouding and etching of the windows by the HF, exposures of four hours were required with gas at a pressure of *one* atmosphere in the cell. As the time of exposure could not be predetermined, it was found convenient to place several small pieces of plate as test strips next to the whole plate, and to develop a test strip every hour until the correct density was indicated.

A spectrogram of the 3←0 band is shown in Fig. 1 and a microphotometer trace of the same band is given in Fig. 2. No spectrogram or tracing of the 4←0 band satisfactory for reproduction could be obtained.

Nine rotational lines in the positive branch and six in the negative branch of the 3←0

[1] E. O. Salant and D. E. Kirkpatrick, Phys. Rev. **46**, 318 (1934).
[2] E. S. Imes, Astrophys. J. **50**, 251 (1919).
[3] R. S. Mulliken, Phys. Rev. **36**, 611 (1930).
[4] Schaefer and Thomas, Zeits. f. Physik **12**, 330 (1923).
[5] J. W. Mellor, *Comprehensive Treatise on Inorganic and Theoretical Chemistry* (Longmans, Green & Co., 1922), Vol. II, p. 128.
[6] Meggers and Humphreys, Bur. Standards J. Research **10**, 427 (1933).
[7] H. Kayser, *Tabelle der Schwingungszahlen.*

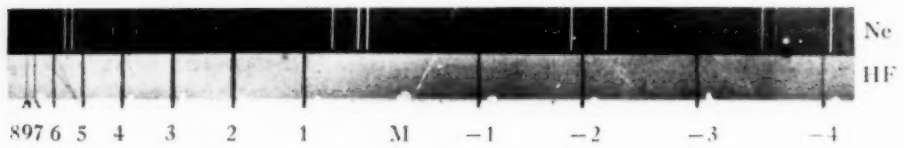

FIG. 1. A portion of the (3←0) band.

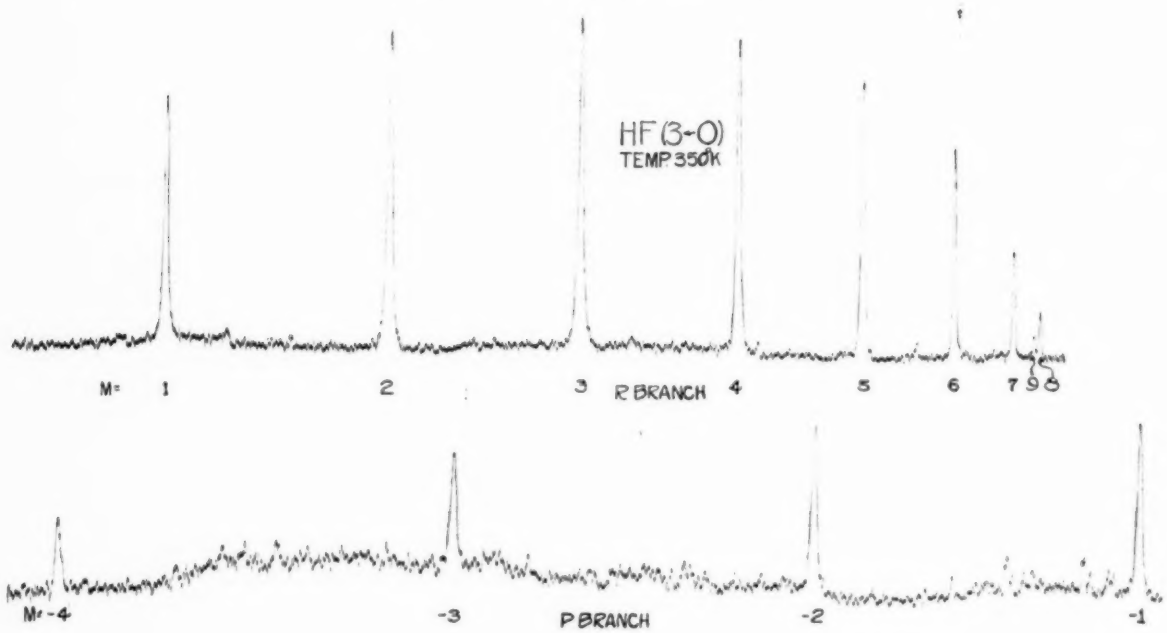

FIG. 2.

band appear. The ninth line of the positive branch appears as a weak line between the seventh and eighth lines, as far as we are aware the only case of reversal of a branch in a non-electronic band. (This is shown more clearly in the microphotometer trace than in the reproduction of the spectrogram.)

Six lines of the positive and five lines of the negative branch of the 4←0 band were observed.

Wave-length and wave number values of the lines of the two bands appear in Table I, together with the values calculated by equations fitted to the measurements by the method of Birge and Shea.[8]

The equations for the band lines are, for the 3←0 band:

$$\nu = 11{,}372.88 + 38.83M - 2.257M^2 - 0.00655M^3, \quad (1)$$

and for the 4←0 band:

$$\nu = 14{,}831.68 + 38.101M - 2.980M^2 - 0.00546M^3, \quad (2)$$

where M is the ordinal number of the line, ± 1, ± 2, etc.

The values of the molecular constants, calculated from Eqs. (1) and (2), by neglecting the third power terms in $(v+\frac{1}{2})$ and the sixth power terms in $(J+\frac{1}{2})$, are given in Table II, in the notation of Mulliken,[3] Eqs. (2c) to (4c). All values indicated as depending on the 1←0 band have been evaluated with the coefficients of the ordinal numbers calculated by Czerny[9] from Imes' measurements of that band.

The agreement of our values with those found from the 1←0 band is satisfactory, with the exception of β_e, which for the latter band is opposite in sign and several times larger than the values found in the present work.

[8] Birge and Shea, *A Rapid Method of Calculating the Least Squares Solution of a Polynomial of any Degree* (Univ. of California Press, Berkeley, 1927), p. 93.

[9] M. Czerny, Zeits. f. Physik **45**, 476 (1927).

TABLE I. *Lines in the two bands in the HF spectrum.*

M	λ_{air} ±0.03A	ν_{vac} ±0.04 cm^{-1}	$\nu_{calc.}$	$\Delta\nu$
(3←0) HF, 8790.42A = 11,372.88 cm^{-1} vac.				
		R BRANCH		
9	8667.08	11534.75	11534.76	−0.01
8	8666.35	11535.72	11535.72	.00
7	8669.29	11531.81	11531.85	− .04
6	8675.80	11523.15	11523.19	− .04
5	8685.88	11509.78	11509.79	− .01
4	8699.55	11491.70	11491.67	+ .03
3	8716.80	11468.95	11468.88	+ .07
2	8737.70	11441.52	11441.46	+ .06
1	8762.26	11409.45	11409.45	.00
		P BRANCH		
−1	8822.32	11331.78	11331.80	− .02
−2	8857.92	11286.24	11286.24	.00
−3	8897.31	11236.27	11236.25	+ .02
−4	8940.49*	11182.00	11181.87	+ .13
−5	8987.57*	11123.43	11123.12	+ .31
−6	9038.94*	11060.21	11060.06	+ .15
(4←0) HF, 6744.67A = 14,831.68 cm^{-1} vac.				
M	λ_{air} ±0.02A	$\nu_{vac.}$ ±0.05 cm^{-1}	$\nu_{calc.}$	$\Delta\nu$
		R BRANCH		
6	6686.36	14951.70	14951.83	−0.13
5	6688.44	14947.05	14947.00	+ .05
4	6693.38	14936.02	14936.05	− .03
3	6701.02	14918.99	14919.02	− .03
2	6711.39	14895.94	14895.92	+ .02
1	6724.55	14866.79	14866.80	− .01
		P BRANCH		
−1	6759.18	14790.62	14790.60	+ .02
−2	6780.74	14743.59	14743.60	− .01
−3	6805.15	14690.70	14690.70	.00
−4	6832.44*	14632.03	14631.95	+ .08
−5	6862.61*	14567.70	14567.36	+ .34

* These lines are very weak and in the case of the (3←0) band occur in a region where there is a paucity of good calibration lines.

The value of 50 cm^{-1} previously listed in the literature for $x_e\omega_e$ obtained by the use of the 1←0 and 2←0 bands, is seen to be very different from any of the values obtained by using any pair of the 1←0, 3←0, and 4←0 bands. This discrepancy is due, presumably, to the insufficient accuracy of the prism-thermopile instrument available to the observers of the 2←0 band.

Calculation of the center of the 1←0 band with the values of ω_e and $x_e\omega_e$ obtained from the 3←0 and 4←0 bands results in a discrepancy of 5 cm^{-1}. It appears to be necessary, therefore, to use a third power term in $(v+\frac{1}{2})$ to account for the centers of these three bands with the accuracy implied by the measurements. The vibrational constants obtained by using all three bands are, then, $\omega_e = 4141.305$ cm^{-1}, $x_e\omega_e = 90.866$ cm^{-1}, $y_e\omega_e = 0.921$ cm^{-1}. The center of the 2←0 band should be, according to these values, at 7752 cm^{-1}, 1.29μ instead of at 1.27μ as found hitherto. A difficulty arises, however, in the calculation of the energy of dissociation. The quantum number at dissociation which one finds with the above values of the vibrational constants appears to have an imaginary value. Whether this is due to an inaccuracy in the determination of the coefficient of the $(v+\frac{1}{2})^3$ term or to the necessity for still higher powers of the vibrational quantum number for a valid description of the upper vibrational levels, cannot be settled definitely although the latter contingency is thought to be the more likely. Attempts, so far, to detect still higher harmonics have failed. The heat of dissociation calculated with the ω_e and $x_e\omega$ obtained from the 3←0 and 4←0 bands, 140 kcal./mole, is seen to agree approximately with

TABLE II. *Molecular constants of HF.*

	ω_e	4134.16 {1←0, 3←0}	4132.32 {1←0, 4←0}	4123.12 {3←0, 4←0} cm^{-1} vac.
	$x_e\omega_e$	85.80 "	84.88 "	83.04 " cm^{-1} vac.
		(1←0)	(2←0)	(3←0) (4←0)
Band center, λ		2.52μ	1.29μ calc.	8790.42A 6755.67A air
Band center, ν		3962.56	7751.69 "	11372.88 14831.68 cm^{-1} vac.
B_e		20.925		20.920 20.913 cm^{-1} vac.
B_0		20.543		20.544 20.540 cm^{-1} vac.
α_e		0.7632		0.7523 0.745 cm^{-1} vac.
D_e		−0.00214		−0.00215 −0.00215 cm^{-1} vac.
β_e		−0.000830		+0.000256 0.000314 cm^{-1} vac.
I_e		1.321×10^{-40}		1.322×10^{-40} 1.323×10^{-40} gm cm^2
r_e		0.901×10^{-8}		0.901×10^{-8} 0.901×10^{-8} cm

$$\text{Energy of dissociation} = \frac{(\omega_e - x_e\omega_e)^2}{4x_e\omega_e} = 140 \text{ kcal./mole}$$

the 120 kcal./mole obtained from the data in F_2,[10] H_2,[11] and HF.[12]

An interesting distinction between the anharmonicity factor x_e of HF and that of the other hydrogen halides can be drawn. For HCl[13] this factor is 0.0174, for HBr[14] 0.0171, for HI[15] 0.0172, whereas for HF it is 0.0219. This larger value is reflected, of course, in the greater intensity of the overtone bands of this gas,—very much longer columns of the other hydrogen halides than the 225 cm employed here have yet to reveal a 4←0 band.[16] It would be interesting if this unusually large anharmonicity should be related, too, to the exceptional readiness of HF molecules to associate. In connection with this matter of association, a spectrogram was taken with the gas at 85°C as well as at 30°C, but no variation in intensity of the lines was observed, contrary to what might be expected from the vapor densities at those temperatures.

We take great pleasure in acknowledging our indebtedness to Dr. R. L. Garman of the Department of Chemistry for the microphotometric tracings.

[10] Wartenberg, Springer and Taylor, Zeits. f. physik. Chemie, Erganzungsband Bodenstein Festband, 61 (1931).
[11] Jevons, *Report on Band Spectra of Diatomic Molecules* (The Physical Society, London, 1932).
[12] Landolt-Börnstein, *Phys-Chem. Tabellen*, p. 1489.
[13] Meyer and Levin, Phys. Rev. **34**, 44 (1929).
[14] Plyler and Barker, Phys. Rev. **44**, 373 (1931).
[15] Nielsen and Nielsen, Phys. Rev. **47**, 585 (1935).

[16] Mr. F. A. Valente of this laboratory reports that examination of the region of the 4←0 band of HCl, with the 21-foot grating and 50 meters of the gas, showed no trace of absorption.

DECEMBER 15, 1935 PHYSICAL REVIEW VOLUME 48

Tables for Determining Atomic Wave Functions and Energies

PHILIP M. MORSE, L. A. YOUNG* AND EVA S. HAURWITZ, *George Eastman Research Laboratory of Physics, Massachusetts Institute of Technology*

(Received July 26, 1935)

Tables have been constructed so that wave functions and energies, for any atomic state having $1s$, $2s$ and $2p$ electrons, can be computed by variational means. Exchange terms are included, so that singlet and triplet states can be minimized separately. By using the tables a state can be calculated in a few hours. A few of the possible states have been worked out. The best parameters, the total energies and the term values are given for the states $(1s^2)\,{}^1S$, $(1s, 2s)\,{}^1S$, ${}^3S$; $(1s, 2p)\,{}^1P$, ${}^3P$; $(1s^2, 2s)\,{}^2S$; $(1s^2, 2p)\,{}^2P$; $(1s^2, 2s^2)\,{}^1S$; $(1s^2, 2s, 2p)\,{}^1P$, ${}^3P$; $(1s^2, 2p^2)\,{}^1S$, ${}^1D$, ${}^3P$; $(1s^2, 2s^2, 2p)\,{}^2P$; $(1s^2, 2s^2, 2p^6)\,{}^1S$; of the atoms He, Li, Be, B, C, N, O, F, Ne, Na and Mg. The intramultiplet separations have been computed, including the spin-spin interaction when necessary: the check with experiment being fairly satisfactory. By the use of an empirical correction rule, term values can be predicted to within a few hundred wave numbers.

THE CONSTRUCTION OF THE TABLES

THERE is a general need for relatively simple wave functions for use in the calculation of atomic properties. In many cases it is more important to have functions expressible in a simple analytic form than it is to have functions as accurate as those of Hartree, for instance. In the hope of partially satisfying this need, the writers have developed a set of tables from which wave functions and energies for a large number of atomic states can be obtained. The variational method is used, and the tables are arranged so that any atomic state containing $1s$, $2s$ and $2p$ electrons can be computed.

Practical considerations governed the choice of the number of parameters used in the trial functions. Four were used in all, one for the $1s$ function, two for the $2s$ and one for the $2p$ functions. While it was realized that an extra parameter in the $2p$ function would give somewhat better results, it was decided that any more than four parameters would greatly increase the complexity of the computations. The tables as finally constructed are easy to use, and the best parameters for any atomic state can be computed in a few hours.

* Now at the Research Laboratory of Molecular Physics, Carnegie Institute of Technology.

The form of the wave functions used is as follows:

$$
\begin{aligned}
1s \quad & u_1(r) = (\mu^3 a^2/\pi)^{\frac{1}{2}} e^{-\mu a r}, \\
2s \quad & u_2(r) = (\mu^5/3\pi N)^{\frac{1}{2}}[re^{-\mu r} - (3A/\mu)e^{-\mu b r}], \\
2p \quad & u_3(r) = (\mu^5 c^5/\pi)^{\frac{1}{2}} r\cos\theta e^{-\mu c r}, \\
& u_4(r) = (\mu^5 c^5/2\pi)^{\frac{1}{2}} r\sin\theta e^{i\varphi-\mu c r}, \\
& u_5(r) = (\mu^5 c^5/2\pi)^{\frac{1}{2}} r\sin\theta e^{-i\varphi-\mu c r}.
\end{aligned} \tag{1}
$$

The constant A is fixed so that u_2 is orthogonal to u_1, a proceeding which very materially simplifies the results. Its value is given by:

$$A = (a+b)^3/(1+a)^4.$$

The constant N is a normalizing factor,

$$N = 1 - 48A/(1+b)^4 + 3A^2/b^3.$$

The parameter μ is a scale factor, whose best value can be determined analytically, leaving but three parameters to be determined numerically.[1]

The wave functions are arranged in determinantal form, and the energy integral computed in atomic units (one atomic unit equals 13.537 electron volts, equals 109,737 wave numbers). Since the functions are mutually orthogonal, this integral turns out to be a simple sum of individual electron energy integrals, each of which is given as a function of the parameters in the tables.[2] The integrals involved are defined as follows:

$$
\begin{aligned}
& -\int \bar{u}_n \nabla^2 u_n dv = \mu^2 T_n, \quad 2\int (u_n^2/r) dv = \mu V_n, \\
& 2\int [u_n^2(r_1) u_m^2(r_2)/r_{12}] dv_1 dv_2 = \mu V_{nm},
\end{aligned} \tag{2}
$$

$$2\int [\bar{u}_n(r_1)\bar{u}_n(r_2)u_m(r_1)u_m(r_2)/r_{12}] dv_1 dv_2 = \mu X_{nm}.$$

(2, continued)

The energy W for any given atomic state is the sum of $\mu^2 T$, where T is a linear combination of the T's, and μV, where V is a linear combination of the V's and X's. Since neither V nor T depends on μ, we can minimize for μ immediately, obtaining

$$\mu = -(V/2T), \quad W = -(V^2/4T). \tag{3}$$

The minimization for the other three parameters, a, b and c, can be done graphically.

Some examples of the constitution of T and V are given here: for the state $(1s^2, 2s)$ for an atom of nuclear charge Ze,

$$
\begin{aligned}
T &= 2T_1 + T_2, \\
V &= -Z(2V_1 + V_2) + V_{11} + 2V_{12} - X_{12};
\end{aligned}
$$

for the state $(1s^2, 2s^2, 2p)$

$$
\begin{aligned}
T &= 2T_1 + 2T_2 + T_3, \\
V &= -Z(2V_1 + 2V_2 + V_3) + V_{11} + V_{22} + 4V_{12} \\
&\quad + 2V_{13} + 2V_{23} - 2X_{12} - X_{13} - X_{23}.
\end{aligned}
$$

For configurations giving rise to more than one multiplet different linear combinations of determinants can be formed of the type discussed by Slater and Johnson.[3] For instance, for helium-like states $(1s, 2p)$, the two combinations are:

$$
\begin{aligned}
&{}^1P, \quad T = T_1 + T_2, \quad V = -Z(V_1 + V_3) + V_{13} + X_{13}, \\
&{}^3P, \quad T = T_1 + T_3, \quad V = -Z(V_1 + V_3) + V_{13} - X_{13}.
\end{aligned}
$$

For the states $(1s^2, 2p^2)$ the combinations are:

$$
\begin{aligned}
&{}^3P, \quad T = 2T_1 + 2T_3, \quad V = -2Z(V_1 + V_3) + V_{11} + 4V_{14} + V_{34} - 2X_{13} - X_{34}, \\
&{}^1D, \quad T = 2T_1 + 2T_3, \quad V = -2Z(V_1 + V_3) + V_{11} + 4V_{14} + V_{44} - 2X_{13}, \\
&{}^1S, \quad T = 2T_1 + 2T_3, \quad V = -2Z(V_1 + V_3) + V_{11} + 4V_{14} + V_{33} - V_{34} + V_{44} - 2X_{13} + X_{34}.
\end{aligned}
$$

The energies can then be minimized separately, obtaining somewhat different parameters for the different states, and thus giving better answers than can be obtained by means of perturbation methods. In this way the functions are arranged to include exchange in the amount required by LS coupling, so that they are better, in this respect, than the Hartree wave functions.

[1] Trial functions similar to these have been used by a number of workers to determine wave functions for a few of the states dealt with here. In particular, see: Zener, Phys. Rev. **36**, 51 (1930); Eckart, Phys. Rev. **36**, 878 (1930); Ochiai, Proc. Phys.-Chem. Soc. Japan **14**, 388 (1932); Wilson, J. Chem. Phys. **1**, 210 (1933); Fock and Petrashen, Physik. Zeits. Sowjetunion **6**, 368 (1934).

[2] A limited number of these energy tables have been mimeographed, and are available for interested workers. Those wishing copies please write Physics Department, Massachusetts Institute of Technology, Cambridge, Mass.

[3] Slater, Phys. Rev. **34**, 1293 (1929); Johnson, Phys. Rev. **39**, 197 (1932); Condon, Phys. Rev. **36**, 1121 (1930).

TABLE I. *Wave function parameters and energies.*

TWO-ELECTRON STATES

Atom	He	Li	Be	B	C	N	O	F	Ne
					$(1s^2)\ ^1S$ *State*				
$a\mu$	1.69	2.69	3.69	4.69	5.69	6.69	7.69	8.69	9.69
Wcal	5.695	14.445	27.195	43.945	64.695	89.445	118.195	150.945	187.695
Wexp	5.807	14.560	27.313	44.065	64.813	89.562	118.311	151.061	187.811
Termcal	186100	597500	1228300	2078300	3147300	4435100	5941500	7666300	9609200
Termcor	199100	610500	1241300	2091300	3160300	4448100	5954500	7679300	9622200
Termexp	198300	610100	1241300	2091400	3160200				
					$(1s\ 2s)\ ^3S$ *State*				
a	3.28	2.75	2.50	2.42	2.34	2.29	2.26	2.23	2.21
$a\mu$	2.00	3.00	4.00	5.00	6.00	7.00	8.00	9.00	10.00
b	2.57	1.98	1.74	1.61	1.53	1.47	1.42	1.39	1.36
$b\mu$	1.57	2.17	2.76	3.34	3.92	4.49	5.06	5.63	6.20
2μ	1.22	2.19	3.17	4.15	5.13	6.11	7.10	8.10	9.10
Wcal	4.348	10.217	18.589	29.467	42.846	58.726	77.106	97.986	121.366
Wexp	4.350	10.221							
Termcal	38200	133500	283900	489400	749500	1064000	1432500	1854700	2330400
Termcor	38200	133600	284100	489700	749900	1064500	1433100	1855400	2331200
Termexp	38500	134000							
					$(1s\ 2s)\ ^1S$ *State*				
a	3.28	2.75	2.50	2.42	2.34	2.29	2.26	2.23	2.21
$a\mu$	2.00	3.00	4.00	5.00	6.00	7.00	8.00	9.00	10.00
b	2.57	1.98	1.74	1.61	1.53	1.47	1.42	1.39	1.36
$b\mu$	1.57	2.17	2.76	3.34	3.92	4.49	5.06	5.63	6.20
2μ	1.22	2.19	3.17	4.15	5.13	6.11	7.10	8.10	9.10
Wcal	4.295	10.085	18.372	29.160	42.448	58.236	76.524	97.312	120.600
Wexp	4.292								
Termcal	32400	119100	260100	455700	705800	1010200	1368600	1780700	2246300
Termcor	32400	119200	260300	456000	706200	1010700	1369200	1781400	2247100
Termexp	32000								
					$(1s\ 2p)\ ^3P$ *State*				
a	3.63	2.77	2.49	2.35	2.27	2.23	2.20	2.17	2.15
$a\mu$	1.99	2.98	3.97	4.97	5.96	6.96	7.96	8.96	9.96
$2c\mu$	1.10	2.15	3.19	4.23	5.24	6.24	7.25	8.26	9.26
Wcal	4.261	10.047	18.339	29.133	42.428	58.225	76.523	97.322	120.627
Wexp	4.266	10.055							
Termcal	28600	114900	256500	452800	704000	1009000	1368500	1781800	2249300
Termcor	28600	115200	257100	453700	705200	1024000	1370300	1783900	2251700
Termexp	29200	115800							
$^3P_0-{}^3P_1$ cal	−.983	−5.58	−12.7	−18.2	−10.6	+5.9	+55.0	+164	+328
$^3P_0-{}^3P_1$ exp	−.991	−5.15							
$^3P_1-{}^3P_2$ cal	+.119	+3.64	+20.4	+65.6	+165	+332	+611	+1050	+1672
$^3P_1-{}^3P_2$ exp	−.065	+2.10							
					$(1s\ 2p)\ ^1P$ *State*				
a	4.13	3.06	2.70	2.53	2.42	2.35	2.30	2.26	2.23
$a\mu$	2.00	3.00	4.00	5.00	6.00	7.00	8.00	9.00	10.00
$2c\mu$	0.97	1.96	2.96	3.96	4.96	5.96	6.96	7.96	8.96
Wcal	4.245	9.980	18.212	28.942	42.172	57.902	76.133	96.864	120.095
Wexp	4.248	9.987	18.219	28.949	42.185				
Termcal	26900	107500	242500	431800	675800	973600	1325700	1731500	2190900
Termcor	26900	107800	243100	432400	677000	975100	1327500	1733600	2193300
Termexp	27200	108300	243300	433300	677000				

THREE-ELECTRON STATES

Atom	Li	Be	B	C	N	O	F	Ne	Na
					$(1s^2\ 2s)\ ^2S$ *State*				
a	4.03	3.24	2.90	2.70	2.58	2.50	2.43	2.40	2.37
$a\mu$	2.69	3.69	4.68	5.68	6.68	7.68	8.68	9.68	10.68
b	3.19	2.59	2.29	2.11	1.99	1.90	1.84	1.79	1.74
$b\mu$	2.13	2.95	3.70	4.43	5.15	5.85	6.54	7.22	7.89
2μ	1.34	2.28	3.23	4.20	5.17	6.14	7.11	8.08	9.06
Wcal	14.838	28.526	46.723	69.423	96.627	128.334	164.544	205.257	250.474
Wexp	14.956	28.648	46.847	69.550	96.755	128.463	164.672		250.603
Termcal	43100	146100	304800	518800	788100	1112600	1492300	1927200	2417300
Termcor	43100	146300	305200	519400	788900	1113600	1493500	1928600	2418900
Termexp	43500	146900	305900	520200	789600	1114000	1493700		2418800
					$(1s^2\ 2p)\ ^2P$ *State*				
a	5.15	3.44	2.92	2.68	2.53	2.45	2.38	2.33	2.29
$a\mu$	2.69	3.68	4.68	5.67	6.67	7.67	8.67	9.67	10.67
$2c\mu$	1.05	2.14	3.19	4.23	5.25	6.27	7.29	8.30	9.31
Wcal	14.701	28.228	46.272	68.822	95.876	127.431	163.488	204.048	249.108
Wexp	14.820	28.357	46.407	68.961	96.020	127.582	163.645		249.259
Termcal	28100	113400	255400	452900	705700	1013500	1376400	1794500	2267500
Termcor	28100	114000	256600	454700	708100	1016500	1380000	1798700	2272300
Termexp	28600	114900	257500	455600	708900	1017400	1380800		2272300
$^2P_{1/2}-{}^2P_{3/2}$ cal	0.42	7.1	35.8	111	265	541	982	1664	2633
$^2P_{1/2}-{}^2P_{3/2}$ exp		6.6	34.1	107	259	532	985		2296

FOUR-ELECTRON STATES

Atom	Be	B	C	N	O	F	Ne	Na	Mg
					$(1s^2\ 2s^2)\ ^1S$ *State*				
a	3.85	3.40	3.14	2.97	2.82	2.76	2.68	2.63	2.58
$a\mu$	3.70	4.72	5.74	6.74	7.74	8.74	9.74	10.74	11.74
b	3.28	2.91	2.59	2.50	2.41	2.34	2.29	2.26	2.22
$b\mu$	3.15	3.98	4.82	5.67	6.54	7.43	8.33	9.24	10.16
2μ	1.92	2.77	3.65	4.54	5.44	6.35	7.27	8.20	9.14
Wcal	29.095	48.378	72.643	101.902	136.161	175.423	219.690	268.963	323.243
Wexp	29.333	48.694	73.069	102.446	136.832	176.223		270.029	324.448
Termcal	62400	181600	353400	578900	858900	1193800	1583800	2018000	2529200
Termcor	75400	205600	388400	624900	915900	1261800	1662800	2098000	2620200
Termexp	75200	202600	386200	624300	918400	1267600		2131700	2646900
					$(1s^2\ 2s\ 2p)\ ^3P$ *State*				
a	3.60	3.12	2.87	2.71	2.60	2.51	2.45	2.40	2.36
$a\mu$	3.69	4.68	5.68	6.68	7.68	8.68	9.68	10.68	11.68
b	3.00	2.51	2.25	2.07	1.94	1.84	1.77	1.71	1.65
$b\mu$	3.07	3.77	4.45	5.10	5.74	6.37	6.99	7.59	8.17
$2c\mu$	1.84	2.86	3.89	4.90	5.90	6.90	7.90	8.90	9.90
2μ	2.05	3.00	3.96	4.93	5.91	6.91	7.90	8.90	9.90
Wcal	28.995	48.201	72.428	101.666	135.915	175.175	219.445	268.725	323.015
Wexp	29.137	48.361	72.595	101.838	136.088	175.341		268.895	323.186
Termcal	51500	162200	329800	553000	831900	1166600	1556900	2002800	2504200
Termcor	52700	164000	332200	556000	834900	1170300	1561700	2008200	2510200
Termexp	53200	165500	333800	557600	836600	1170800		2007500	2508000
$^3P_0-{}^3P_1$ cal	0.423	4.91	20.7	58.5	127	243	425	693	1071
$^3P_0-{}^3P_1$ exp	0.68	6.4	23.0	63.2	137	260			
$^3P_1-{}^3P_2$ cal	2.59	15.6	53.6	137	290	544	935	1509	2312
$^3P_1-{}^3P_2$ exp	2.35	16.4	56.1	144	306	572		1604	2472

TABLE I.—*Continued.*

FOUR-ELECTRON STATES (*Continued*)

Atom	Be	B	C	N	O	F	Ne	Na	Mg
					($1s^2\ 2s\ 2p$) ^1P *State*				
a	4.12	3.33	2.97	2.77	2.64	2.54	2.48	2.42	2.38
$a\mu$	3.69	4.68	5.68	6.68	7.68	8.68	9.68	10.68	11.68
b	4.27	3.04	2.50	2.20	2.00	1.88	1.79	1.72	1.66
$b\mu$	3.82	4.27	4.77	5.29	5.84	6.41	6.99	7.59	8.17
$2c\mu$	1.55	2.67	3.75	4.80	5.82	6.82	7.82	8.82	9.82
2μ	1.79	2.81	3.82	4.82	5.82	6.82	7.82	8.82	9.82
Wcal	28.706	47.780	71.862	100.966	135.080	174.205	218.338	267.480	321.631
Wexp	28.949	48.030	72.141	101.257	135.386	174.520		267.812	321.972
Termca	19800	116000	267600	476100	740300	1060200	1435500	1866200	2352300
Termcor	32800	130200	283000	492700	758100	1079200	1455700	1887600	2374900
Termexp	32600	129200	283800	493800	759600	1080700		1888500	2375200
					($1s^2\ 2p^2$) ^3P *State*				
a	4.21	3.31	2.94	2.74	2.62	2.53	2.46	2.40	2.38
$a\mu$	3.68	4.67	5.67	6.67	7.67	8.67	9.67	10.67	11.67
$2c\mu$	1.75	2.82	3.85	4.86	5.86	6.86	7.86	8.86	9.86
Wcal	28.625	47.613	71.623	100.644	134.673	173.706	217.740	266.785	320.830
Wexp	28.793	47.799	71.820	100.851	134.888	173.931		267.051	321.121
Termcal	10900	97700	241400	440800	695600	1005400	1369800	1789900	2264400
Termcor	15400	103400	248300	448900	704900	1015900	1381500	1802800	2278500
Termexp	15500	104000	248800	449300	705000	1016000		1804800	2281700
$^3P_0-{}^3P_1$ cal	1.11	7.6	27.1	68.2	144	268	462	753	1155
$^3P_0-{}^3P_1$ exp	1.40	8.4	29.4	73.2	156	288			
$^3P_1-{}^3P_2$ cal	2.22	15.4	54.4	136	288	536	924	1506	2310
$^3P_1-{}^3P_2$ exp	2.03	14.0	47.1	125	269	511			
					($1s^2\ 2p^2$) ^1D *State*				
a	4.31	3.38	3.00	2.78	2.65	2.54	2.47	2.41	2.38
$a\mu$	3.68	4.67	5.67	6.67	7.67	8.67	9.67	10.67	11.67
$2c\mu$	1.71	2.77	3.79	4.80	5.81	6.81	7.81	8.81	9.81
Wcal	28.552	47.497	71.462	100.440	134.424	173.413	217.407	266.405	320.407
Wexp	28.686	47.766	71.743	100.727	134.722	173.721		266.742	320.632
Termcal	2900	84900	223800	418400	668300	973300	1333300	1748200	2208000
Termcor	17300	100300	240200	435800	686700	972700	1353700	1768600	2230400
Termexp	3700	100300	240300	435600	686700	993000		1771100	2228100
					($1s^2\ 2p^2$) ^1S *State*				
a	4.47	3.45	3.04	2.82	2.68	2.58	2.50	2.45	2.40
$a\mu$	3.68	4.67	5.67	6.67	7.67	8.67	9.67	10.67	11.67
$2c\mu$	1.65	2.69	3.71	4.72	5.72	6.72	7.72	8.72	9.72
Wcal	28.448	47.323	71.225	100.141	134.064	172.992	216.923	265.853	319.783
Wexp	28.617	47.535	71.409	100.303	134.210	173.121			
Termcal	−8600	65800	197700	385600	628800	927100	1280200	1687600	2149500
Termcor	1400	73800	203700	389600	630800	927100	1278200	1683600	2147500
Termexp	−3900	75000	203600	389100	630500	927200			

FIVE-ELECTRON STATES

Atom	B	C	N	O	F	Ne	Na	Mg
				($1s^2\ 2s^2\ 2p$) ^2P *State*				
a	3.50	3.31	3.19	3.09	3.01	2.95	2.89	2.85
$a\mu$	4.69	5.70	6.72	7.73	8.74	9.74	10.74	11.74
b	3.00	2.97	2.90	2.80	2.69	2.58	2.47	2.38
$b\mu$	4.02	5.11	6.11	7.01	7.81	8.53	9.17	9.75
$2c\mu$	2.41	3.56	4.64	5.69	6.73	7.75	8.76	9.76
2μ	2.68	3.44	4.21	5.00	5.80	6.61	7.43	8.25
Wcal	48.956	74.429	105.415	141.880	183.817	231.269	284.216	342.673
Wexp	49.309	74.866	105.935	142.522	184.618		285.405	344.063
Termcal	63500	196000	385500	625700	921100	1270600	1673800	2132200
Termcor	66900	199000	389100	629900	925900	1276000	1679000	2138800
Termexp	67100	196600	384100	623500	921000		1687000	2152500
$^2P_{1/2}-{}^2P_{3/2}$ cal	12.4	61.1	169	384	754	1325	2147	3288
$^2P_{1/2}-{}^2P_{3/2}$ exp	15.0	64.0	174	387	745		2139	3304

TEN-ELECTRON STATES

Atom	F	Ne	Na	Mg
			($1s^2\ 2s^2\ 2p^6$) ^1S *State*	
a	3.51	3.41	3.31	3.21
$a\mu$	8.75	9.75	10.75	11.75
b	3.00	3.00	3.00	3.00
$b\mu$	7.48	8.62	9.75	10.96
$2c\mu$	4.70	5.60	6.55	7.55
2μ	4.99	5.72	6.51	7.31
Wcal	195.174	252.880	318.640	392.392
Wexp			324.252	398.645

Resulting Wave Functions

The wave functions and energies have been computed for a few of the isoelectronic sequences included in the tables. The best values of the parameters are listed in Table I. The best values of the total atomic energy in atomic units are denoted by W_{cal}, and are compared with the experimental values, W_{exp}, obtained from Bacher and Goudsmit, Edlèn and Söderquist.[4] The term values of the states, the energy differences in wave numbers between the state in question and the lowest state of the same atom with one more electron removed, are also compared with the experimental term values.

Several interesting facts can be obtained from these tables. The quantity $a\mu$ is the effective charge on the $1s$ electron, and from it the screening constant for the other electrons can be obtained. We note that this screening constant is nearly independent of Z and is usually about $0.30(K-1)$, where K is the number of $1s$ electrons present in the state. This is in accordance with Slater's rules.[5] The quantity $2c\mu$ is the effective charge on the $2p$ electron; the corresponding screening constant depends more on Z than does $a\mu$, but it follows Slater's rules approximately. It is to be noticed that $2c\mu$ has a different value for a singlet state than it has for a triplet state. The constants for the $2s$ function do not have as simple meanings, although 2μ can be considered as corresponding to the effective charge on the $2s$ electron in the outer part of its orbit.

By a study of the table, the following rules can be devised for the approximate determination of a, b and c:

$$a=2+\frac{K(L+1)+L'}{Z-(K-1)},\quad b=\frac{K+L}{2}+\frac{2+L+L'}{Z-(K-1)},\qquad c=0.8+0.2L+0.05L\frac{1-L-2L'}{Z-K-L}, \tag{4}$$

where K is the number of $1s$ electrons, L the number of $2s$ and L' the number of $2p$ electrons in the state in question. For very rough calculation of a state, these rules can be used to determine the parameters, and only a single value of the energy need be computed, by interpolation of the tables; the only variation made being that of the scale factor μ. Even when a full variation is carried out, Eqs. (4) are useful in indicating the region in which the minimum lies.

All the states given in Table I, with the exception of the $(1s, 2s)\ ^1S$ state, are the lowest states of a given symmetry, and therefore have energy minima. The $(1s, 2s)\ ^1S$ state is not the lowest of its symmetry, and has no minimum, as is shown in Fig. 1. To determine the energies of such upper states, rules like those of Eqs. (4) must be used. For instance, for the ^1S state, the values of a and b were chosen to be the same as for the ^3S state. When this was done, the values of $a\mu$ and $b\mu$ also came out the same as for the ^3S state, an additional inducement for this choice.

A study of the differences between the calculated and experimental energy values shows that if the outer electron is the only one in its shell, the discrepancy in the term value is less than 2000 wave numbers, but if it is one of several in a shell, the error is of the order of 10,000 wave numbers. This is due to the fact that our wave functions are built up out of separable one-electron functions, an approximation which is less good the closer the electrons are together. However, a study of the table enables one to formulate a rule for correcting the calculated total energy:

$$W_{\text{exp}}\backsimeq W_{\text{cal}}+\Delta,$$

where

$$\begin{aligned}\Delta&=0.059K(K-1)+0.059L(L-1)+AL'(L'-1)+ELL'\\&\quad+(Z-K-L-L')[0.057L(L-1)+BL'(L'-1)+0.001K(L+FL')]\text{ atomic units}\\&=6500K(K-1)+6500L(L-1)+AL'(L'-1)+ELL'\\&\quad+(Z-K-L-L')[6300L(L-1)+BL'(L'-1)+100K(L+FL')]\text{ cm}^{-1}\end{aligned} \tag{5}$$

[4] Bacher and Goudsmit, *Atomic Energy States* (McGraw-Hill); Edlèn, Nova Acta Reg. Soc. Sci. Upsala, Ser. IV, Vol. 9, No. 6; Söderquist, Nova Acta Reg. Soc. Sci. Upsala, Ser. IV, Vol. 9, No. 7; Edlèn, Zeits. f. Physik **89**, 179, 597 (1934).

[5] Slater, Phys. Rev. **36**, 57 (1930).

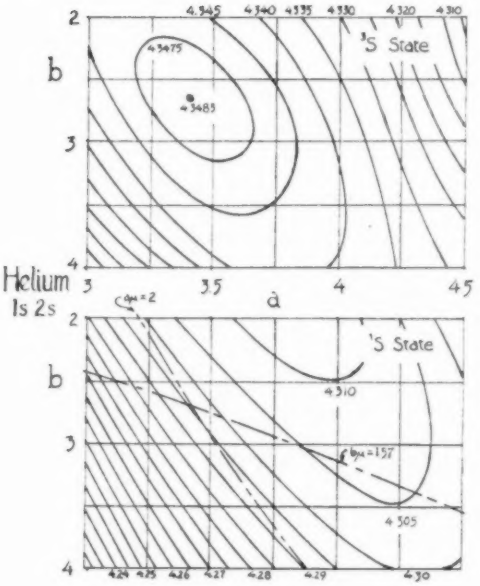

FIG. 1. Energy contours for the configuration $(1s, 2s)$. The triplet state is the lowest of its symmetry, and has a minimum, but the singlet state has no minimum.

where the values of A, B, E and F depend on the configuration of the $2p$ electrons, and have, for the states worked out, the values in Table II.

This expression consists of terms proportional to the number of pairs of electrons in the different shells, and is thus a correction to the interaction and exchange energies, which is the sort of correction nonseparable wave functions would introduce. The total energies $W_{cor}=W_{cal}+\Delta$, differ from the experimental data by only a few thousandths of an atomic unit. The corresponding term values, denoted by Term_{cor}, are given in the table, and differ from the experimental values by only a few hundred wave numbers.[6]

TABLE II.

CONFIGURATION		$(2p)^2$		$(2p)^6$		DOUBLET AND TRIPLET	SINGLET
STATE	^3P	^1D	^1S	^1S			
A (atomic units)	0.020	0.066	0.046	0.155	E (A)	0.011	0.118
A (cm^{-1})	2200	7200	5000	17000	E (cm^{-1})	1200	900
B (atomic units)	0.001	0	−0.014	0.015	F	3	6
B (cm^{-1})	100	0	−1500	1700			

Another way of expressing the above correction is to say that to each one of the interaction and exchange expressions, μV_{nm} and μX_{nm}, entering into the energy expressions for a state, there must be added a correction for nonseparability. Eq. (5) shows that these corrections must be of the form of a constant plus a term linear with Z, or since, in any isoelectronic sequence, μ is linear with Z, they must be a constant plus a term proportional to the scale constant μ. The corrected interaction energy will therefore be $\mu V_{nm}+\mu V_{nm}'+V_{nm}''$ and the corrected exchange energy will be $\mu X_{nm}+\mu X_{nm}'+X_{nm}''$; where V_{nm} and X_{nm} are given in the energy tables,[2] and V_{nm}', V_{nm}'', X_{nm}' and X_{nm}'' are given below. Strictly speaking, the corrections V_{nm}' and X_{nm}' should be included along with the corresponding V_{nm} and X_{nm} before the minimization is carried out, and only the terms X_{nm}'' and V_{nm}'' added later; but the corrections are so small that it is possible to add the proper combination of $(\mu V_{nm}'+V_{nm}'')$ and $(\mu X_{nm}'+X_{nm}'')$ after minimizing, without introducing much error.

Eq. (5) shows that approximate values for these correction terms, in atomic units, are:

$$V_{11}'=0, \quad V_{11}''=-0.118, \quad V_{22}'=-0.236, \quad V_{22}''=+0.164,$$
$$V_{12}'=-0.002, \quad V_{12}''=-0.0005, \quad X_{12}'=0, \quad X_{12}''=+0.0005,$$
$$V_{13}'=-0.002, \quad V_{13}''=-0.003, \quad X_{13}'=0, \quad X_{13}''=+0.001,$$
$$V_{23}'=-0.006, \quad V_{23}''=-0.046, \quad X_{23}'=-0.006, \quad X_{23}''=-0.046,$$
$$V_{44}'=0, \quad V_{44}''=-0.109, \quad (V_{34}'-X_{34}')=-0.026, \quad (V_{34}''-X_{34}'')=-0.002,$$
$$(V_{33}'+2V_{45}')=-0.470, \quad (V_{33}''+2V_{45}'')=+0.026.$$

In the last four cases only linear combinations of the corrections could be worked out from the states which have been calculated. As soon as more states including pairs of $2p$ electrons are computed, the individual values can be obtained.

As an example of the utility of the wave functions, the values of the intramultiplet separations are calculated for those levels having multiplets. They are compared with the experimental values in Table I. Certain approximations

[6] Compare with the method given by Bacher and Goudsmit, Phys. Rev. **46**, 948 (1934). The advantage of the variational method over that given by Bacher and Goudsmit is that a prediction can be made even though no other energy states of the atom are known. Also, of course, once the variational method is carried through, other properties of the atom can be computed.

had to be made in deriving the formulas for these separations. For instance, in the triplet formulas the average value of the quantity $(1/r_{12})^3$ enters, in the term for the spin-spin interaction. Strictly speaking, this average is infinite if separable wave functions are used; to obtain the correct formula one must use the correct, nonseparable functions, which are zero when the two electrons are coincident.[7] The procedure chosen here is the one suggested by Bethe:[8] When electron number two is outside number one, to use, instead of $(1/r_{12})^3$, a constant times $(1/r_2)^3$, the constant being determined by the relative screening of the other electron as indicated by the value of $2\mu c$. In the expression for the spin-orbit interaction, the value of $2\mu c$ is also used, as a measure of the field on the $2p$ electron.

The expressions for the doublet separations which have been used are:

$$(1s^2, 2p) \quad {}^2P_{1/2}-{}^2P_{3/2}=2.911(\mu c)^3(Z-2) \text{ cm}^{-1}, \tag{6}$$

$$(1s^2, 2s^2, 2p) \; {}^2P_{1/2}-{}^2P_{3/2}=5.822(\mu c)^4 \text{ cm}^{-1}.$$

[7] Breit, Phys. Rev. **36**, 383 (1930).

The fundamental expressions for the triplet separations,[7, 8] including spin-spin interaction, for the (sp) configuration, are

$$\begin{aligned} {}^3P_0-{}^3P_1&=ZC-9D, \\ {}^3P_1-{}^3P_2&=2ZC-(18/5)D, \end{aligned} \tag{7}$$

where

$$C=0.9704(\overline{1/r^3}) \quad \text{and} \quad D=0.9704(\overline{1/r_{12}^3}) \text{ cm}^{-1}.$$

For the $(1s, 2p)$ state, we set

$$(\overline{1/r_{12}^3})=(\mu c)^3(Z-2\mu c),$$

and obtain

$$\begin{aligned} {}^3P_0-{}^3P_1&=1.941(\mu c)^3(9\mu c-4Z) \text{ cm}^{-1}, \\ {}^3P_1-{}^3P_2&=0.7763(\mu c)^3(9\mu c-2Z) \text{ cm}^{-1}. \end{aligned} \tag{8}$$

For the $(1s^2, 2s, 2p)$ state we substitute $(Z-2)$ for the Z in Eqs. (8). The spin-spin correction for the $(1s^2, 2p^2)$ state is small and complicated, so we use only the spin-orbit term,

$${}^3P_0-{}^3P_1=1.941(\mu c)^4, \quad {}^3P_1-{}^3P_2=3.882(\mu c)^4, \tag{9}$$

which gives a fairly good check with experiment.

[8] Bethe, *Handbuch der Physik*, Vol. 24, 2nd edition (Springer), p. 380.

DECEMBER 15, 1935 PHYSICAL REVIEW VOLUME 48

The Initiation of Electrical Discharges by Field Emission

JOHN W. FLOWERS, *University of Virginia*

(Received June 13, 1935)

The initiation of highly overvolted discharges produced in effectively ion-free gases by voltage impulses of short duration is shown to be independent of the gas between the electrodes, also of the pressure from one atmosphere down until the vacuum spark stage is reached. In asymmetrical fields values of the field intensity at the cathode required for initiation are the order of 5×10^5 volts/cm, while at the anode the field for initiation is some 20 percent higher. Oscillograms showing the time lags and rates of fall of potentials of such highly overvolted discharges between spheres, and between points and planes have been obtained as well as those of an ordinary discharge for comparison. When the breakdown occurs because of high fields at the cathode, the initiation is readily explained by field emission of electrons. In the case of high fields at the anode it can be said that the initiation is determined by the character of its surface. When the discharge occurs the rate of fall of potential is greater than ordinary discharges in gases. Oscillograms of the wave fronts produced by 60-cycle discharges between magnesium electrodes, and the rate of fall of potential across such discharges have been obtained.

THE time lag of the spark discharge may be defined as the interval between the attainment of normal breakdown potential and the beginning of the rapid fall of potential across the gap. It may in general be divided into two parts.[1, 2] The first part represents the time before

[1] Campbell, Phil. Mag. **38**, 214 (1919).

[2] J. J. Thomson, *Conduction of Electricity Through Gases*, Vol. 2 (1933), pp. 471, 474.

initiation of the spark mechanism, or the time required for the formation of a favorable distribution of ions. This is a statistical time which is influenced by many factors and may be the order of seconds just at the sparking potential.[3, 4] Ultraviolet light of sufficient intensity producing photoelectrons at the cathode removes this part of the lag by providing an initiating agent. The second part is sometimes called a "regular lag" and is the time required to establish the spark mechanism after electrons have been formed in the gap. When ultraviolet light initiates a discharge this lag is a very definite time for any particular sphere gap at the breakdown potential. Overvoltages much reduce not only the total time lag,[5, 6] but each of the parts described above as well, where by overvoltage is meant any applied potential across the spark gap greater than the static breakdown value. Measurements of the time lag will be given in this paper.

Street and Beams[7] have shown that a sphere gap may be overvolted some 16 times when it is inclosed in dry, dust-free, and effectively ion-free gas at atmospheric pressure. Such treatment of the gas essentially delays the initiation of the discharge for it was shown that irradiation of the cathode with ultraviolet light caused breakdown near normal values. The following experiments have been conducted to determine the characteristics of such a discharge and the nature of the initiation.

Experimental Procedure

In order to determine the part played by the cathode, experiments with discharges in asymmetrical fields were carried out.[8, 9] The circuit employed is shown in Fig. 1. The capacity C_1 of about $0.002\mu f$ is slowly charged through R_1 until G_1 breaks down. The circuit constants are of such values that the potential is applied to G_2 and G_3 in less than 10^{-7} sec. This potential is

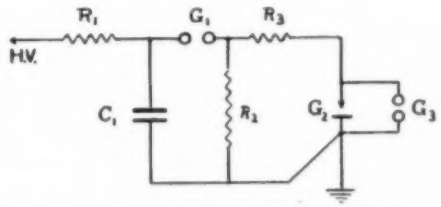

FIG. 1. Circuit for applying potential rapidly to a gap, G_2, to be overvolted and gap, G_3, for measuring potential.

removed by the discharge of G_2 or G_3. G_2 is the gap to be studied and G_3 is a sphere gap used to measure the potential applied to G_2. G_3 was irradiated by the ultraviolet light from an iron arc to reduce its time lag. G_2 was in an enclosure containing gas which had been dried by P_2O_5 and filtered through a bacteriological filter of diatomaceous earth. An auxiliary electrode near G_2 was used to sweep ions from the vicinity of the electrodes. For the point and plane gap this consisted of a ring near the point while, for spheres, the metal case of the container served. Using 2.5 cm brass spheres G_3 could be separated as much as 20 times the separation of G_2 without a discharge in G_2. This gives a breakdown field of 6×10^5 volts/cm. Substituting a point and plane gap for G_2 gave similar results. The discharge with the point positive always occurred at greater separations of G_3 than when negative.

In order to retain more uniform electrode surfaces and determine the effect of different gases, a gap was employed consisting of a wire and concentric cylinder. The cylinder was divided along its length, and a small potential applied between the portions to facilitate removal of ions. The wire was so arranged that it could be heated in vacuum before the gas was admitted. The results obtained by using a platinum wire of radius 0.0036 cm and steel cylinder of internal radius 0.43 cm are shown in Fig. 2. Here the maximum breakdown intensity at the wire surface as measured by G_3 is plotted as a function of the gas pressure for N_2 and He. The curves for air and H_2 fall very near to these. The corresponding field strengths at the surface of the cylinder were only of the order of 5×10^3 volts/cm. It will be observed that the breakdown potential is independent of the pressure from atmospheric down to about 40 cm of Hg. The oscillograph shows (Fig. 4) that this independ-

[3] Tilles, Phys. Rev. **46**, 1015 (1934).
[4] Zuber, Ann. d. Physik **76**, 231 (1925).
[5] Beams, J. Frank. Inst. **206**, 809 (1928).
[6] Rogowski and Tamm, Archiv f. Elektrotechnik **30**, 625 (1928).
[7] Street and Beams, Phys. Rev. **38**, 416 (1931).
[8] Flowers and Beams, Phys. Rev. **46**, 338 (1934).
[9] Flowers, Phys. Rev. **47**, 801 (1935).

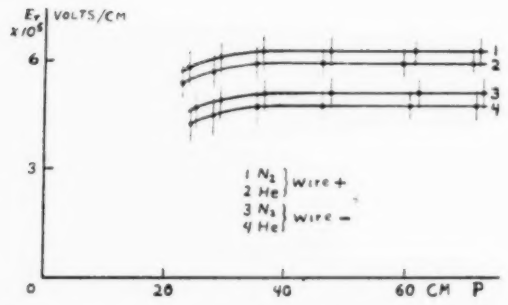

FIG. 2. Overvoltage breakdown intensity-pressure relations between a wire and a concentric cylinder by using circuit in Fig. 1.

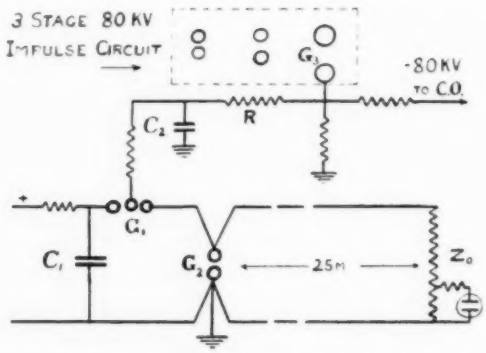

FIG. 3. Circuit for synchronization of the discharge to be studied at G_2 with the oscillograph.

ence continues to low pressure. The static sparking potential is proportional to the pressure and in He is of the order of 1/10 that in N_2 while that in H_2 is about half that in N_2. Thus the very small differences in the breakdown potential observed in Fig. 2 for the different gases indicate that the gas between the electrodes has very little effect on the breakdown potential.

With the wire negative the value of the field at the surface of the wire at breakdown is the order of 5×10^5 volts/cm which is in the region where field emission is observed from metals in high vacua,[10] and is of the order required to produce the vacuum spark.[11, 12] For the discharge in gases this field emission need not be large as a single electron probably suffices to initiate the discharge.[13]

The apparent breakdown at lower field intensities as the pressure is reduced, shown in Fig. 2, is evidently due to the method of measurement or to the construction of G_2 since the oscillograms do not show this decrease.

Oscillographic Measurements

Following these experiments a high voltage oscillograph of the Dufour type was set up. This one employed gas focusing of the electron beam and had deflection plates of about 1 cm calculated capacity. Writing speeds as high as 3×10^8 cm/sec. could be recorded, and all oscillograms shown are continuous on the films. The circuit for timing the discharge, and connecting to the deflection plates of the oscillograph is shown in Fig. 3. The capacity C_1 and the impulse circuit are slowly charged. When the last gap, G_3, of the impulse circuit discharges, high potential is applied to the oscillograph (C.O.), and to the third electrode of G_1 at a rate depending on the value RC_2. G_1 is thus tripped, and C_1 discharges into G_2, the gap to be studied, and the line connecting G_2 to the deflection plates of the oscillograph. The line is terminated by the surge impedance Zo (525 ohms) which also functions as a potential divider. A one-piece electrolytic resistor was found to serve best as surge impedance, potential divider, and critical damping resistance for the deflecting plates. The time constant for the deflection system used was not greater than 10^{-10} sec.

The first two oscillograms (Fig. 4) show the discharge of intensely irradiated zinc spheres of 2 cm diameter in air. The light from G_1 and a 10-ampere iron arc irradiated the cathode G_2 from distances of 10 cm. No. (1) shows the discharge when the applied potential wave just reaches static breakdown voltage. The steeply applied wave permits good measurement of the time lag of the spark. The results of measurements of this and similar oscillograms give about 8×10^{-8} sec.

No. (2) shows the results of reducing the separation of G_2 which tends to overvolt it. The time lag becomes inappreciable (about 10^{-8}) but still sufficiently great to allow an overvoltage of about 10 percent. The gap G_2 is set to discharge statically at 20 kv. The regularity of these oscillograms indicates uniform initiation by photoelectrons.

[10] Millikan and Eyring, Phys. Rev. **27**, 51 (1926).
[11] Hull and Burger, Phys. Rev. **31**, 1121 (1928).
[12] Snoddy, Phys. Rev. **37**, 1678 (1931).
[13] Tiedeman, Physics **1**, 354 (1931).

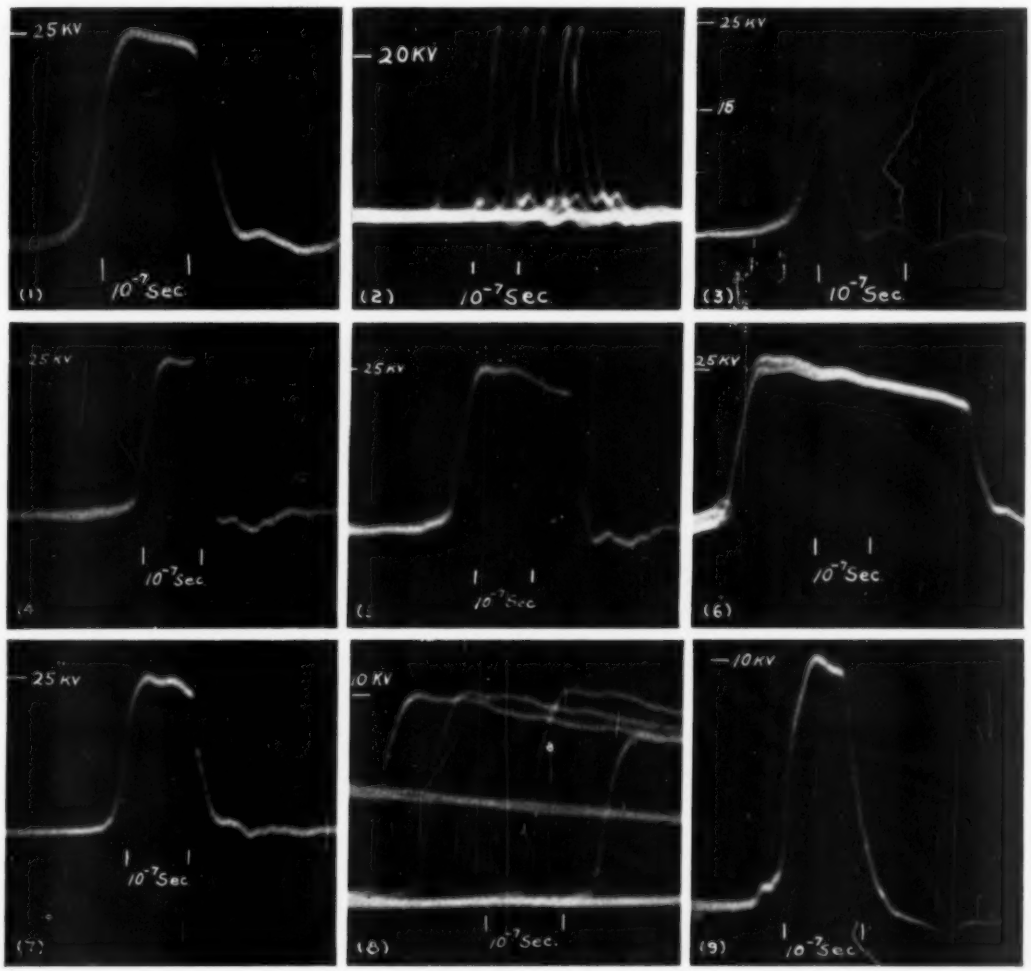

FIG. 4. Oscillograms. (1) Discharge of 2-cm Zn spheres irradiated strongly. Sweep speed 1 mm on film equals 4.5×10^{-9} sec. $d=8$ mm. (2) Same as Fig. 1 at slower sweep speed and gap set to discharge at 20 kv. $d=6$ mm. (3) Highly overvolted 2.5-cm brass spheres. Separation about 0.4 mm. (4) Same as 3. Separation slightly greater. (5) Same as 3. Separation slightly greater. (6) Discharge of negative point to plane, overvolted 100 percent. (7) Highly overvolted negative points. (8) Sixty-cycle wave fronts. (9) Breakdown of sixty-cycle magnesium gap.

In oscillograms (3), (4), and (5) are shown the discharge of the highly overvolted 2.5-cm spheres in dry, relatively ion-free air at atmospheric pressure. The separation of the spheres is approximately 0.4 mm. For separations less than some critical value the discharge always appears as in No. (3). For slightly greater separations a statistical time lag appears as in (4) and (5). Time lags as long as 0.5 microsecond have been observed. In the case of No. (3) the field reaches a value sufficient for considerable field emission so that the time between extraction of electrons is relatively short. This would necessitate a field current of about one electron in 10^{-9} sec. or roughly 2×10^{10} amp. For lesser values of the field the statistical characteristics are observable as in Nos. (4) and (5). If the hypothesis of field emission is correct, the field current here is about one electron in 10^{-7} sec. on the average or about 2×10^{-12} amp. This is in agreement with currents observed in high vacua and their rapid variation with field strength. A discharge such as shown in No. (3) has a minimum time lag and the difficulty of measuring the peak voltage reached by a parallel sphere gap is obvious.

Oscillograms (6) and (7) show the discharge

from negative points in air at atmospheric pressure. The positive discharge appears the same. No. (6) is in room air and overvolted about 100 percent to reduce time lags. The type of time lag shown is extremely erratic, probably because of difficulty of uniform initiation with a point. Even with this overvoltage the rate of fall of potential is less than that for spheres at normal breakdown. No. (7) is a point discharge in dry, ion-free air with about 15 times static breakdown potential applied. This shows the same characteristics as overvolted spheres. In all cases the discharge at high field strengths produces a very rapid fall of potential in the initial stage. For the overvolted spheres the fall to half-value is at least twice as fast as for irradiated spheres. The overvolted points seem to show an earlier diminution in the rate of fall than overvolted spheres.

The relation between pressure and the overvolted discharge potential as measured by the oscillograph is shown in Fig. 5. The breakdown potential is constant from atmospheric pressure down to 8 mm of Hg. Between 8 and 7 mm a rise of about 30 percent occurs. At this pressure it is believed that the electron mean free path becomes of the order of magnitude of the electrode separation, and the electrons removed from the cathode by the field reach the anode without appreciable ionization in the gas. The potential rises higher in the time required to set up the vacuum spark mechanism with attendant electrode temperatures. However, the potential drops at still lower pressures and then rises again. This has been observed repeatedly and may be due to variation of surface conditions with the pressure.

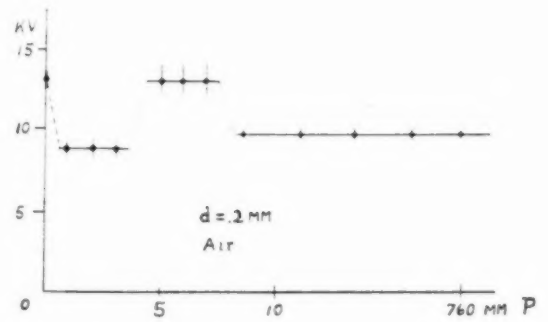

FIG. 5. Overvoltage breakdown potential-pressure relations between 2.5-cm brass spheres as determined by the oscillograph.

DISCUSSION OF RESULTS

The initiation of the highly overvolted discharge is readily explained by the removal of electrons from the cathode by the electrical field when the discharge occurs between spheres or from negative points and wires. The field strengths and field currents have been shown to be of the same order of magnitude as observed in high vacua. The estimation of the field currents depends upon the ability of a single electron to initiate the discharge and the assumption that the fall in potential begins within a negligibly uniform time (time lag) following this event. At the high field strengths and high pressures the fall in potential should begin almost immediately with field emission since even slight overvoltages reduce the time lag of the ordinary spark (oscillogram (2)).

The highly overvolted discharge has been shown to be independent of the pressure over wide ranges. This is to be expected to the extent that the pressure does not change the time lag or the field emission. At some low pressure the gas should cease to be predominant in the discharge mechanism. The characteristics then become those of the vacuum spark and the time after field emission until the potential begins to fall, i.e., the time lag depends upon the electrodes, the amount of energy supplied, and the extent of the field current.

The discharge potential has been shown to be relatively independent of the kind of gas present. It should depend upon the gas only to the extent that different gases change the surface condition and thus field emission. The possible differences observed are thus attributable to different work functions at the surface of the wire.

The conditioning of the electrodes by the passage of several discharges between new or polished electrodes before appreciable overvoltage is attained is a supporting characteristic.

In the case where the point or wire is positive the explanation is not as evident. There are some indications that positive ions may be removed from metal surfaces by electric fields,[14] and the occurrence of such should be sufficient

[14] Beams, Phys. Rev. **41**, 687 (1932).

to initiate the discharge, provided the positive ions can produce sufficient ionization at the existing field strengths. However, at the present such a process is somewhat speculative. It is reasonably certain that in neither the positive nor the negative discharge can the initiation be attributed to chance electrons or ions in the field. Any alternative process must of necessity be new or very complex. For the case of the negative discharge the evidence strongly supports the theory of field emission.

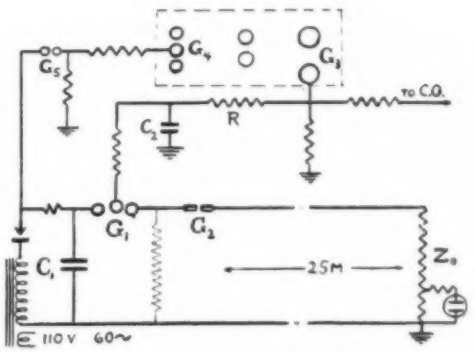

FIG. 6. Circuit for synchronization of the sixty-cycle discharge studied at G_2.

THE 60-CYCLE DISCHARGE

In order to study a discharge under conditions very different from the overvolted one, oscillograms of the 60-cycle magnesium spark have been obtained. A knowledge of the rate of fall of potential across such a discharge and the wave front produced is important from an experimental standpoint. At high resolution speeds of the oscillograph the synchronization of such a discharge presents some difficulty. Fig. 6 shows a successful circuit used. The impulse circuit is slowly charged while C_1 is charged at sixty cycles by the transformer and rectifier. G_1 and G_2 discharge at the same rate and are allowed to run continuously. G_2 is a magnesium gap. The impulse circuit is started by the third electrode in G_4, the first stage of the impulse circuit. This occurs near the peak of the potential cycle applied to C_1. The discharge of G_3 which applies potential to the oscillograph trips the gap G_1 slightly ahead of its regular breakdown time in each cycle and thus times the wave.

Oscillogram (8) shows the wave fronts produced by G_2 discharging into the line. More precisely this is the current-time relation of G_2. The current at any instant is given by V/Zo which gives the maximum of about 20 amperes. Such wave fronts are of interest in many recent experiments. No steep portions are in evidence and for the voltages used the gradients are less than that produced by static breakdown of spheres. No. (9) shows the breakdown of an individual 60-cycle discharge connected across the line as G_2 in Fig. 3. The discharge is damped only by the small resistance of the copper connecting wires and maximum current between breakdowns reaches the order of 500 amperes. Discharging continuously at 60 cycles this current produces considerable heating of the electrodes. This particular oscillogram shows a time lag which is usually absent because of slight over-voltages. A 3.5-megacycle wave for timing purposes is also shown.

Apparently the rapid rate of discharge has only slight effects on the sparking mechanism at these frequencies. Measurements of oscillograms (1) and (9) and many similar ones give a time constant of 3.0×10^{-8} sec. to the 60-cycle discharge and 2.7×10^{-8} sec. to the regular breakdown as shown in oscillogram (1).

This difference for the most part may be due to the shape of the electrodes which were magnesium rods 5 mm in diameter and slightly beveled at the ends.

The sixty-cycle discharge produces a wave front comparable to the ordinary spark discharge and is less steep than sometimes assumed.

In conclusion the author takes pleasure in acknowledging his indebtedness to Dr. J. W. Beams under whose direction this work was accomplished, and also to extend his thanks to Dr. L. B. Snoddy for his valuable advice and interest.

The Surface Ionization of Potassium on Tungsten

M. J. COPLEY AND T. E. PHIPPS, *Department of Chemistry, University of Illinois*

(Received August 5, 1935)

The surface ionization of potassium on tungsten has been investigated by a method which employed a ray of potassium atoms. The use of an atomic ray eliminated photoelectric currents and permitted observations of the degree of ionization to be made up to temperatures as high as 2800°K. Between temperatures of 1350° and 2170°K the graph of the logarithm of the ion-atom ratio *versus* $1/T$ is linear, and when corrected to zero field yields a value of work function for tungsten of 4.51 ±0.01 v. The intercept on the $\log_{10} i_+/i_a$ axis has a value very near to zero instead of the value $\log_{10} 1/2$, expected from theory. This difference between the experimental and the theoretical intercept is interpreted as evidence for a temperature coefficient of the work function. If $\phi=\phi_0+\alpha T$ expresses the temperature dependence of ϕ, α is calculated to have the value 5.6×10^{-5} volt degree^{-1}. It is suggested that the departure from linearity at high temperatures may be accounted for by assuming a temperature dependence in that range of the form $\phi=\phi_0+\alpha T+\beta T^2$.

INTRODUCTION

THE surface ionization of caesium atoms on tungsten and tungsten oxide surfaces partly covered by an adsorbed layer of caesium has been exhaustively investigated by Langmuir[1] and others.[2, 3, 4] Killian[5] has carried out similar investigations upon potassium. The method employed by all the above investigators involved surrounding the ionization unit with the saturated vapor of the alkali metal. Attempts by them to extend the measurements to high temperatures where the surface of the wire would be free of adsorbed alkali metal were not successful because of the onset of large photoelectric currents from collector to wire at about 1500°K.

Recently Morgulis,[6] studying the ionization of sodium on a clean tungsten surface, also used the above method (referred to hereafter as the bulb method). He found in the case of sodium that photoelectric currents did not become serious until a temperature of 1700°K was reached; and by using a magnetron to turn back the photoelectrons, he was able to obtain measurements as high as 2200°K. From the measurement of the positive ion current at different wire temperatures and from vapor pressure data for sodium, Morgulis calculated approximate values for the percentage ionization of sodium on the tungsten surface. His values were in agreement as to order of magnitude with those to be expected from theory.

The authors recently reported[7, 8] upon a preliminary investigation of the surface ionization of potassium on tungsten, in which an atomic ray of potassium was employed. The use of an atomic ray was found to eliminate the photoelectric current, which proved troublesome at high temperatures in the bulb method. The present article describes the continuation of this work under improved experimental conditions, and discusses the agreement of the results with theory.

THEORY

The theory of surface ionization has been discussed by Langmuir,[1] Becker,[4, 9] Fowler,[10] and others. To facilitate the discussion of results, a brief résumé of the theory is given here. For the reaction

$$K(g)=K^+(g)+E^-(g) \qquad (1)$$

the numbers per cm^3 of ions, atoms, and electrons at equilibrium are related by the expression

$$\frac{n_+n_e}{n_a}=\frac{\omega_+\omega_e}{\omega_a}\left[\frac{2\pi m_e kT}{h^2}\right]^{\frac{3}{2}}\exp\left[-\frac{I\epsilon}{kT}\right], \qquad (2)$$

where ω_+, ω_a, ω_e are, respectively, the statistical weights of ions, atoms, and electrons; m_e is the

[1] I. Langmuir, Proc. Roy. Soc. **A107**, 61 (1925).
[2] Ives, Phys. Rev. **21**, 385 (1923).
[3] Meyer, Ann. d. Physik (5) **4**, 357 (1930).
[4] Becker, Phys. Rev. **28**, 341 (1926).
[5] Killian, Phys. Rev. **27**, 578 (1926).
[6] Morgulis, Physik. Zeits. Sowjetunion **5**, 221 (1934).
[7] Copley and Phipps, Phys. Rev. **45**, 344 (1934).
[8] Copley and Phipps, Phys. Rev. **46**, 144 (1934).
[9] Becker, Trans. Am. Electrochem. Soc. **60**, 153 (1929).
[10] Fowler, *Statistical Mechanics* (Cambridge Press, 1929), p. 268.

mass of an electron and I is the ionization potential of potassium. If in Eq. (2) we express n_e by

$$n_e=\omega_e[2\pi m_e kT/h^2]^{\frac{3}{2}} \exp[-\phi\epsilon/kT], \quad (3)$$

where ϕ is the work function at temperature T, and ϵ is the charge on an electron, we obtain

$$n_+/n_a=(\omega_+/\omega_a) \exp[-(I-\phi)\epsilon/kT]. \quad (4)$$

Eq. (4) may be modified by replacing the number of ions per cm^3, n_+, and the number of atoms per cm^3, n_a, by the number of ions, i_+, and number of atoms, i_a, which cross per second in one direction through unit area of an imaginary plane in the equilibrium enclosure. This leads to the equation,

$$i_+/i_a=(\omega_+/\omega_a) \exp[-(I-\phi)\epsilon/kT]. \quad (5)$$

If equilibrium is assumed to be reached by a surface reaction, and no elastic reflection of the particles takes place, then Eq. (5) also gives the ratio of ions to atoms evaporating from the surface. If the possibility of elastic reflection is assumed, then the ratio of ions to atoms evaporating from unit area in unit time will be given by

$$\frac{i_+}{i_a}=\frac{(1-r_+)}{(1-r_a)}\frac{\omega_+}{\omega_a}\exp\left[\frac{-(I-\phi)\epsilon}{kT}\right]. \quad (6)$$

In the present work, a ray of atoms from a source not at the same temperature as the wire is used. If a reflection coefficient for atoms exists, it is possible that it might differ from the one in Eq. (6). However, Taylor and Langmuir[11] have shown that the reflection coefficient of caesium atoms, coming from a source at a low temperature and striking a clean tungsten wire, is zero at wire temperatures as high as 1500°. It seems very likely that the reflection coefficient of potassium atoms on tungsten is also zero. Taylor and Langmuir[11] also discuss the reflection coefficient of positive ions and conclude that, on account of the strong attractive forces between ions and a tungsten surface, it is very likely that r_+ is zero. If these assumptions are justified, then the ratio of ions to atoms coming from the wire should be

$$i_+/i_a=\tfrac{1}{2} \exp[-(I-\phi)\epsilon/kT], \quad (7)$$

where ω_+ is replaced by 1 and ω_a by 2. The degree of ionization is given by

$$(i_+/i_a)/(i_+/i_a+1). \quad (8)$$

The determination of i_a requires a knowledge of the total number of atoms striking the wire. This is determined by coating the wire with an activated layer of oxygen atoms, which raises the work function of tungsten to such a high value that complete ionization is obtained. The value of i_a is then given by

$$i_a=i_{WO}-i_+, \quad (9)$$

where i_{WO} is the total number of atoms striking the wire.

The value of i_+/i_a in Eq. (7) is its value at zero field. Most of the data in this work were obtained with a potential drop of 45 volts between filament and cage. Taylor and Langmuir[11] have shown for caesium on tungsten, and Morgulis[6] for sodium on tungsten, that the positive ion current depends upon the voltage. For this reason, the effect of the voltage on the positive ion current was studied. Morgulis[6] has discussed this voltage effect and has deduced the following relationship between the ion-atom ratio with a field E at the surface of the wire, and its value at zero field,

$$\log_{10}\left(\frac{i_+}{i_a}\right)_E=\log_{10}\left(\frac{i_+}{i_a}\right)_0+\frac{Ex_0\epsilon}{2.303k}\cdot\frac{1}{T}, \quad (10)$$

x_0 is the distance from the surface at which ionization takes place. It is to be noted that the relation between $\log_{10}(i_+/i_a)_E$ and E should be linear, and that the slope of the line obtained should vary inversely with the temperature. Another way of regarding the voltage effect is to consider it as an exactly inverse Schottky effect. In this case there should be a linear relationship between $\log_{10}(i_+/i_a)_E$ and $E^{\frac{1}{2}}$. Both methods have been used in the treatment of the data. It will be shown that by either method the correction to zero field is so slight as to be almost negligible.

Apparatus and Materials

Fig. 1 shows the essential features of the apparatus. The furnace is below; the detector chamber is above. The inner part of the furnace has imbedded in its surface a glass-sheathed

[11] Taylor and Langmuir, Phys. Rev. **44**, 423 (1933).

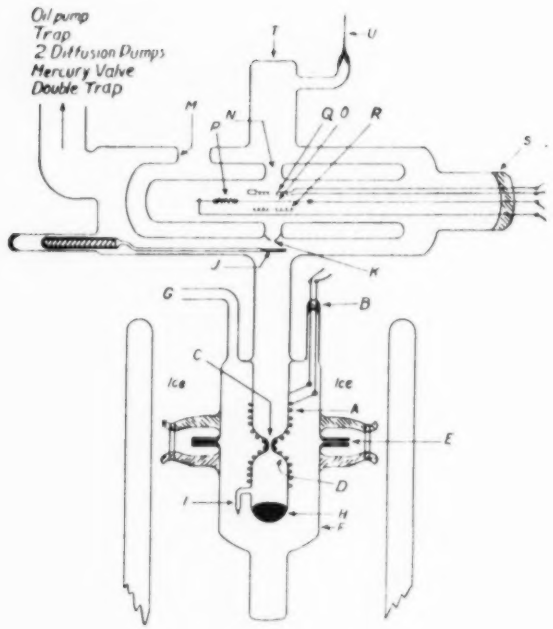

FIG. 1. Diagram of apparatus, detection unit (above) and furnace (below).

10-mil (0.025 cm) tungsten wire *A*, which serves as a heating element. This element is spot-welded to 40-mil (0.1 cm) tungsten wires which lead to the outside through the vacuum seal *B*. The furnace opening *C* is a capillary 0.07 cm in diameter. Below the furnace capillary *C* the inner wall *D* was heavily platinized by a preliminary evaporation process. Without this platinization the ray was observed to fluctuate seriously, due perhaps to the crawling of liquid potassium into the capillary. A ring-sealed vacuum jacket, separable at *E*, encloses the furnace. The inner walls of this jacket *F* are chemically silvered to reduce radiation losses, and a high vacuum is maintained about the furnace through the tube *G*. The outer walls of the jacket and the temporary beeswax-paraffin seal at *E* are kept at ice temperature. The pool of potassium *H* is introduced from a distillation train through *I* before the outer jacket is assembled. A constant current (about 1 ampere) from a storage battery of large capacity serves to maintain an extremely constant ray of potassium over long periods of time.

In the detection unit, above, *J* is a magnetically operated shutter, which serves to interrupt the atomic ray. *K* is a thin-walled circular orifice about 0.07 cm in diameter in the liquid-air cooled insert *M*, which serves to define the atomic ray. The opening *N* in the insert permits direct observation at all times of the wire *O* through the optical window *T*. This facilitates the alignment of the wire with the atomic ray. At the center of the detector unit is the tungsten wire *O*, 5 cm in length and 0.0051 cm in diameter, held taut by a tungsten spiral *P*. Specifications for this spring were taken from Langmuir and Blodgett.[12] Concentric with the wire is a nickel cylinder *Q*, 2 cm in length and 1 cm in diameter, provided with slots about 0.3 cm wide and 0.5 cm long on opposite sides from each other in the ray direction. For outgassing the cylinder and for removing the accumulated potassium from its inner surface during an experiment, a spiral grid *R* is provided. This consists of about 10 turns of tungsten wire 0.03 cm in diameter, which at one end is fastened rigidly to the plate, and at the other is spot-welded to a heavy tungsten lead-out.

U is a thick-walled, very fine capillary which permits the coating of the wire *O* with oxygen by occasional admission of air.

A "GM" galvanometer with a scale located 5 meters away from the galvanometer was used to measure the positive ion current. A phosphor-bronze suspension was used to eliminate zero drift. The sensitivity of the set-up was 1×10^{-10} ampere/mm.

The current for heating the tungsten filament *O* was supplied by storage cells and was regulated by a continuously varying resistance. The current was measured by a carefully calibrated Weston milliammeter. The temperature of the tungsten filament was calculated by the current-temperature-diameter function of Jones and Langmuir.[13] At low temperatures, lead loss corrections were calculated.[14]

The tungsten wire was of high purity and was furnished through the courtesy of Mr. B. Benbow, by the Incandescent Lamp Department of the General Electric Company, Nela Park, Cleveland. The potassium was obtained through the courtesy of Mr. H. N. Gilbert from the

[12] Langmuir and Blodgett, Rev. Sci. Inst. **5**, 321 (1934).
[13] Jones and Langmuir, Gen. Elec. Rev. **30**, 310, 354 (1927).
[14] Langmuir, MacLane and Blodgett, Phys. Rev. **35**, 478 (1930).

Chemical Division of the R. and H. Chemicals Department of the du Pont Company, Niagara Falls, N. Y. It was stated that this metal had not come in contact with oil, and that its only impurity was about one percent of sodium. It was given a fractional distillation for further purification and sealed off in a glass capsule for later use.

Procedure

The apparatus shown in Fig. 1 was sealed to a vacuum line which consisted of the following parts in order: two liquid-air traps, two mercury diffusion pumps in series, a liquid-air trap, and a Hyvac oil pump.

With the lower half of the furnace jacket removed, a distillation train was attached at I. The distillation train held a capsule of potassium and a magnetic hammer for breaking the capsule in the vacuum. The entire apparatus was then surrounded by a furnace and heated to a temperature between 450° and 500°C for a period of several hours; meanwhile the vacuum line was heavily torched as far back as the nearest diffusion pump. Liquid air was put on the trap nearest the diffusion pump on the apparatus side. The grid R was then heated by passing a large current through it to outgas both R and Q. The wire was aged according to the directions of Taylor and Langmuir.[11] After aging the filament, liquid air was placed on the trap nearest the apparatus. The vacuum was tested by noting the constancy of electron emission after flashing the filament to a high temperature to remove any adsorbed gas. Under the best conditions, even without liquid air in the insert M, the electron current did not diminish over a period of several hours. Ordinarily, however, extremely constant emission was not obtained until M was cooled with liquid air.

When the vacuum appeared to be satisfactory, the capsule was broken and approximately 50 percent of the potassium was distilled into the furnace; the distillation train was then sealed off at I. The chemical silvering of the walls, mentioned above, was now carried out and the furnace space was evacuated.

M was then filled with liquid air, the shutter J opened, and the tungsten filament heated to approximately 1500°K. The storage battery current through A was adjusted until a constant galvanometer deflection of approximately 150 mm was obtained. This deflection corresponded to a rate of arrival at the wire of approximately 1×10^{11} atoms sec.$^{-1}$, or to a specific rate of 6×10^{13} atoms cm^{-2} sec.$^{-1}$.

Galvanometer deflections, i_+, were then noted for a series of wire temperatures. At the end of such a series, the wire was brought to a temperature at which a complete activated layer of oxygen would form upon it (1640°K was used throughout this work), and air was admitted cautiously until a maximum galvanometer deflection was obtained. This value, i_{WO}, was taken as equal to the full beam at all of the temperatures of the series. As a check, the wire was then flashed to remove the oxygen layer, and the deflection at 1640° on the clean surface was again observed. The ratio (i_+/i_{WO}) at 1640°K was found to be the same by the two methods. This procedure was repeated at will until the degree of ionization at 1640° was well established. It was found advisable, however, to leave this step until the end of a series of experiments as the vacuum deteriorated somewhat after admission of air. Values of i_a at each temperature were then calculated by Eq. (9), and a value of $\log_{10}(i_+/i_a)$ was determined for each temperature.

The procedure given in the above paragraph is a somewhat idealized one, which was practicable in case the beam remained constant over long periods of time. Actually, in most experiments, small drifts in the beam were observed over the time interval necessary for the taking of a series of i_+ values and the determining of i_{WO} for the series. These drifts in the beam intensity made the following procedure necessary. 1640°K was used as a standard temperature with respect to which fluctuations in the beam intensity could be computed. Deflections were observed at 1640°K both before and after observation at each of the other temperatures; the mean of the two bracketing values at 1640°K was taken as the correct value of i_+ at the time when the bracketed value was taken. In this way the effect of slow drifts in the intensity of the ray was annulled.

At temperatures above 2400°K photoelectric currents were frequently observed. Thus, with the wire at 2400°K, a deflection of a few millimeters might be observed after the shutter was

closed. To minimize this effect, it was found desirable to keep the shutter closed, except during the actual reading of the galvanometer, and to heat out the collector cylinder Q (by heating the grid R) at frequent intervals; this treatment invariably reduced the residual photoelectric current to a very small value, which could be corrected for without introducing a serious uncertainty into the i_+ values.

In observing the effect of voltage upon the ionization, the following procedure was adopted. The i_+ value at a standard voltage (45 volts) and at the standard temperature (1640°K) was employed as the bracketing value. The bracketed value was the deflection at any nonstandard temperature and nonstandard voltage. Since i_{WO} may reasonably be assumed to be independent of voltage, a single determination of it is sufficient for the calculation of i_a values at all voltages and temperatures.

Results

Fig. 2 shows a plot of the data[15] obtained in two different apparatuses, plotted to the axes $\log_{10}(i_+/i_a)$ *versus* $1/T$. Throughout these experiments the collector cylinder Q was negative approximately 45 volts with respect to the negative end of the filament, which corresponded to a field at the surface of the wire of about 3350 volts cm^{-1}. (The correction to zero field is presented later.)

The value of $\log_{10}(i_+/i_a)$ at standard temperature is shown by the solid black circle. This point was calculated by using the mean of seven independent determinations of the degree of ionization, i_+/i_{WO}; namely, 0.800, 0.800, 0.796, 0.790, 0.796, 0.806, and 0.800. The mean of these, 0.7983, was used in calculating the values of $\log_{10}(i_+/i_a)$ at all other temperatures. An example will serve to show the method: i_+ at $T=1887°K$ $(1/T\times10^5=53)$ was 134.4 (in arbitrary units). For the same beam, the mean of the bracketing values at $T=1640°$ was 139.75. Whence, $i_{WO}=139.75\div0.7983=175.06$; $i_a=175.06-134.4=40.66$; $i_+/i_a=134.4\div40.66=3.3054$; $\log_{10}(i_+/i_a=0.5192$. This is one of the six points plotted at $1/T=53$.

[15] Tables of data are omitted at the suggestion of the editor.

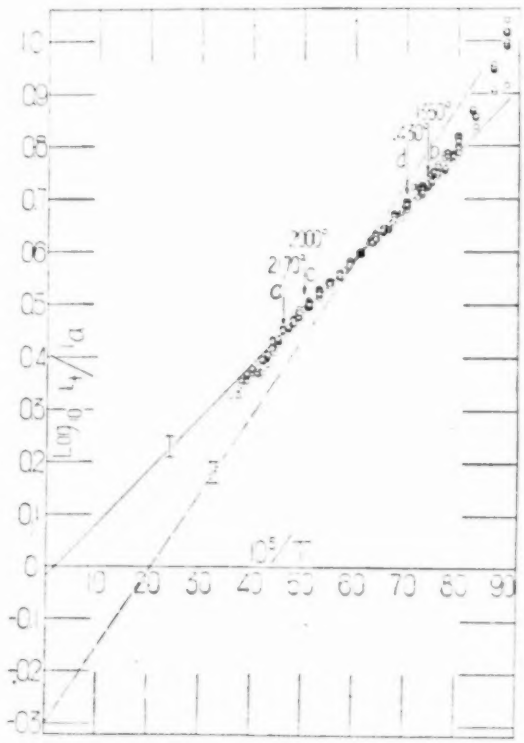

FIG. 2. Plot showing the linear region *ab* represented by line I, and the deviation from linearity above 2170°K and below 1350°K. The solid black circle represents the temperature at which the degree of ionization was determined.

It will be observed that between a and b the points lie on a straight line. The solid line I is the best line through the 105 points which lie between a and b,—as determined by a least-squares method. The equation of this line is

$$\log_{10}(i_+/i_a)_{E\leqq3350}=1007.3/T-0.0173. \quad (11)$$

To the left of a (temperatures above 2170°K), the experimental points lie below I; to the right of b (temperatures below 1350°K) the points lie above I, and the deviation from the mean of the points in a cluster at the same $1/T$ value becomes much greater than in the range ab.

The limits a and b of the linear region were set somewhat arbitrarily. To show the effect upon slope and intercept of choosing narrower limits, the equation of the best straight line through the 71 points which lie between c and d was also determined by the method of least squares. This line (not shown in Fig. 2) had for its equation

$$\log_{10}(i_+/i_a)_{E\leqq3350}=(989.25\pm8.20)/T -0.0055\pm0.005. \quad (12)$$

It thus appears that the intercept of the best line through the narrower region *cd* deviates from zero by an amount which is approximately equal to its probable error. The possibility must therefore be considered that the true value of the intercept is zero, and that the deviation observed is without significance. This point will be discussed later.

Completely satisfactory explanations for the deviations at high and at low temperatures have not as yet been found. That they are not explainable by a defect of apparatus (such, for example, as a lateral shifting of the wire into or out of the beam due to a dissymmetry in the action of the spring) is indicated by the fact that in two preliminary, as well as in the two final apparatuses, deviations were observed at approximately the same $1/T$ values, and always in the same direction. As a direct check upon wire movement, a traveling microscope was focused upon the wire through the optical window, and the wire was observed while its temperature was varied from room temperature to 2800°K. No lateral motion could be detected. However, since a very small motion would be sufficient to explain the deviations observed we do not think that this possibility is entirely excluded in the high temperature region. In future work, it is proposed to remove this uncertainty by replacing the circular orifice at K with a slit which has accurately parallel sides.

The low temperature deviation is thought not to be due to the above cause. It may, however, have been caused by adsorption on the wire of some gas, other than oxygen, which was present in the apparatus. The greater deviations from the mean in that region are accounted for by the fact that i_a becomes small compared with i_+, and that small errors in the determination of i_a are magnified in the quotient.

With regard to the deviation at high temperatures (in the region to the left of *a*, Fig. 1) there appeared to be some evidence of an effect of apparatus upon the course of the curve. Points taken with the second apparatus lay somewhat closer to the line than those taken with the first apparatus. (These points have not, however, been distinguished in the plot.) That the deviations are not due to a photoelectric effect is apparent, since this would tend to give values of

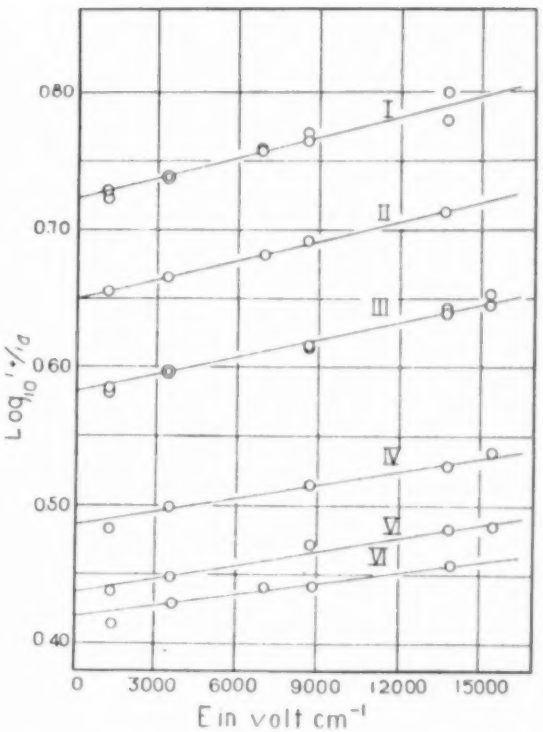

FIG. 3. The effect of field at different temperatures upon ion-atom ratio. I, $T=1337$°K; II, $T=1479$°K; III, $T=1640$°K; IV, $T=1961$°K; V, $T=2174$°K; VI, $T=2381$°K. Values of the ratio,

$$\log_{10}(i_+/i_a)_{E=0}/\log_{10}(i_+/i_a)_{E=3350},$$

for the six temperatures given above are, in order: 0.975, 0.975, 0.977, 0.978, 0.975, 0.977.

$\log i_+/i_a$ above the line. An explanation which suggests itself is that a term in the temperature coefficient of the work function involving a power of T higher than the first becomes significant at temperatures above 2170°K. The same phenomenon has been observed in unpublished measurements which have been made in this laboratory upon the surface ionization of caesium on tungsten.

The difference between the first two resonance levels of potassium and the ground level is small enough so that at the highest temperature in the linear region *ab* (I, Fig. 2) no appreciable change in the ion-atom ratio would result from a correction of the heat capacity and entropy of potassium for internal excitation. However, between 2200° and 2800°K the contribution of internal excitation is no longer negligible, and is in a direction to make the curve to the left of *a* bend upward. Actually the curve bends downward.

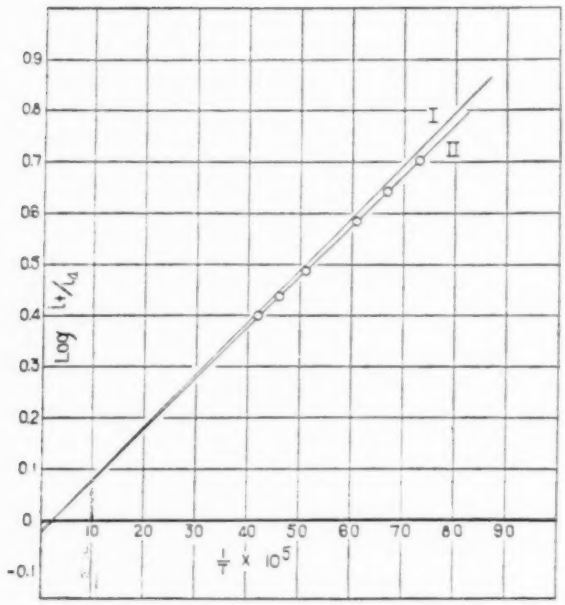

FIG. 4. The correction to zero field (line II) of the data plotted in Fig. 2 (line I).

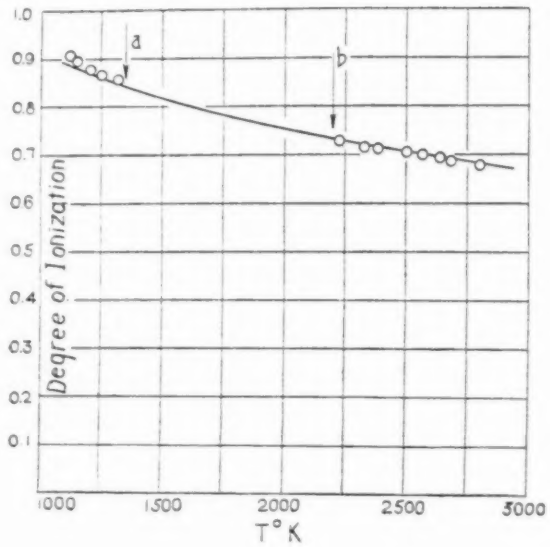

FIG. 5. The degree of ionization of potassium on tungsten at E of 3350 volt cm^{-1}. The heavy line is calculated from Eq. (11).

Since the data in this region were not satisfactorily reproducible, no correction for internal excitation has been made.

Fig. 3 shows a plot of $\log_{10}(i_+/i_a)$ *versus* E, the field at the surface of the wire, for values of the field between zero and 15,000 volts cm^{-1}. It is seen that the relation is linear between 3000 and 15,000 volts cm^{-1}, and that the slopes decrease in the series I to VI as the temperatures increase. The products of T times slope in this series are, respectively: 0.48, 0.51, 0.49, 0.46, 0.53, and 0.50 volt^{-1} cm degree. This constancy of T times slope is in agreement with Eq. (10); however, it is in disagreement with the results of Morgulis,[6] who observed no such constancy for sodium on tungsten.

The circled points in Fig. 4 are calculated in the following manner. Points calculated from Eq. (11) are corrected for voltage by multiplying them by the ratio,

$$\log_{10}(i_+/i_a)_{E=0}/\log_{10}(i_+/i_a)_{E\leqq 3350},$$

obtained from Fig. 3. Line I in Fig. 4 is identical with line I of Fig. 2; that is, it is the best line through the 45-volt values in the *ab* region. The equation of II (Fig. 4) is

$$\log_{10}(i_+/i_a)_{E=0}=(987.24\pm 8.20)/T - 0.0188\pm 0.005. \quad (13)$$

It is evident that the intercept is not appreciably changed by correcting to zero field. The slope is slightly diminished.

If the assumption (to be discussed later) is made that in the *ab* region of Fig. 2 the tungsten surface is clean—that is, free of adsorbed potassium or of electronegative gas—then from (13) and (7) we may write

$$(\phi - I)\epsilon/k = 987.24\times 2.3026, \quad (14)$$

and have upon substituting numerical values

$$\phi - I = 0.196\pm 0.002 \text{ v}. \quad (15)$$

Since I for potassium is 4.318 v, we obtain for ϕ a value of 4.514 ± 0.002 v. The probable error ± 0.002 depends upon the assumption of correctness of temperature in the least squares calculation. If Langmuir's current-diameter-temperature function for tungsten is assumed correct, we estimate that the maximum uncertainty in temperature is $\pm 20°$, which corresponds to an uncertainty of ± 0.005 v in ϕ. Owing to experimental causes, then, the uncertainty in ϕ is of the order ± 0.01 v.

The data plotted in Fig. 3 were also plotted against $E^{\frac{1}{2}}$. There was more deviation from linearity in these plots. The product of T times slope of the best straight lines through the points at the various temperatures showed a greater

trend than the values obtained by the first method. When the intercepts, $\log_{10}(i_+/i_a)_{E^{\frac{1}{2}}=0}$ were plotted against $1/T$, and a work function was calculated from the slope, a value of 4.504 v was obtained. There was no appreciable difference between the intercept obtained by this method and that obtained by the first method.

Fig. 5 shows the degree of ionization of potassium from tungsten as a function of the temperature. The heavy line was constructed by calculating the degrees of ionization from Eq. (11). To the left of a and to the right of b the circled points were calculated from mean values of the experimental clusters at various $1/T$ values in Fig. 1. It is seen, as in Fig. 2, that the experimental points lie high at low temperatures and low in the high temperature range.

Discussion of Results

In the calculation of ϕ by (14) and (15), only the region ab (Fig. 2) was considered; the assumptions were made (1) that the surface is clean at temperatures above 1350°K, and (2) that departures from linearity at high and at low temperatures arise from causes which are not operative or are unimportant in the region ab. It has been suggested to us that in this region a slight amount of potassium is adsorbed on the surface, sufficient to lower the work function by a few hundredths of a volt between the limits 2170 and 1350°K. Such an effect would lead to a curve concave toward the $1/T$ axis in this region. To explain the observed linearity one would have to assume a compensating effect such as the adsorption of an electronegative gas, which would raise the work function.

We have estimated the amount of potassium on a tungsten surface at 1350°K for the rate of arrival used in these experiments. The basis for this calculation was the data of Taylor and Langmuir[11] upon caesium. In making the calculation for potassium we have increased their value for the heat of vaporization of ions by fifteen percent. This estimation led to the conclusion that at 1350°K there was not sufficient potassium adsorbed on the tungsten in our experiment to lower the work function by as much as 0.01 volt. That this estimate is reliable is confirmed by the fact that we observed the positive ion current to decrease rapidly in the neighborhood of 1100°K, in agreement with the temperature at which adsorption becomes important as calculated by the method used above. In view of the above calculation we shall proceed with the discussion under the assumption that the surface was clean above 1350°K.

From the fact that a linear region is found in the plot of Fig. 2, we may conclude that the work function is either temperature independent, or that it has a temperature dependence in the linear region expressible by the relation $\phi=\phi_0+\alpha T$.

Let us consider first the case in which we assume temperature dependence. If we substitute the above value of ϕ into (6), and if we plot $\log_{10}(i_+/i_a)$ *versus* $1/T$, we see that the intercept on the $\log_{10}(i_+/i_a)$ axis is

$$\log_{10}(i_+/i_a)_{1/T=0}=\log_{10}\omega_+/\omega_a+\alpha\epsilon/2.3026k.$$

Substituting numerical values, we obtain for α a value of 5.6×10^{-5} volt degree^{-1}. The value for ϕ calculated from the slope of line II (Fig. 4) is its value at 0°K.

The Richardson line for tungsten is known to be straight in the same region of temperature as that in which the measurements under discussion were taken. Consequently the value of ϕ_0 obtained in this way should agree with the slope of the Richardson line for tungsten. Our value of 4.514 v agrees within experimental error with the value 4.52 v found by Dushman[16] for tungsten. In a recent article, Becker[17] has pointed out that α cannot be evaluated accurately from the intercept of the Richardson line. This comes about because i_e in the theoretical equation for the emission of electrons is the emission per cm^2 of effective surface. The apparent surface of a wire has been estimated to be 25 to 50 percent less than the effective surface. Consequently values of α calculated from the intercept of the Richardson line for tungsten will be too small. It should be noted that this difficulty does not arise in the calculation of α from our experimental results since surface does not appear in the theoretical relationship for the ion-atom ratio.

Dushman[16] obtained a value of 60 amp. cm^{-2} °K^2 for A from his measurements on the emission

[16] Dushman, Rowe, Ewald and Kidner, Phys. Rev. **44**, 345 (1925).
[17] Becker, Rev. Mod. Phys. **7**, 95 (1935).

of tungsten. If we apply a surface correction, this value will be reduced to between 30 and 45. Such a value for A gives a larger value for α than we obtained. In fact to bring the α of thermionic emission measurements into agreement with our value of α, an A sufficiently large to give a value —when corrected for surface—of 60 should have been observed. If we assume our measurements to be correct, then either (a) the experimental value of A obtained by Dushman is too low; or (b) the difference between effective and apparent surface is smaller than hitherto assumed. Measurements[18] made recently in this laboratory of the electron emission of tungsten filaments taken from the same spool as those used in this investigation gave a value of 96 for A, which would indicate a surface correction of more than 50 percent. A value for ϕ_0 of 4.62 v was obtained from these electron emission measurements. This value is 0.1 v higher than that obtained from the slope of line II (Fig. 4). We are at present unable to account for this discrepancy.

Let us consider next the case in which ϕ is assumed to be independent of the temperature. Here the intercept on the $\log_{10}(i_+/i_a)$ axis expected from theory is log (1/2)—that is, -0.301 —instead of the very small value -0.0188 which we obtained. This may be seen graphically in Fig. 2. Line II is the line expected from theory if ϕ is temperature independent. (The solid black circle is the "standard point" through which any experimental line must pass.) It is apparent that the assumption of a temperature independent work function will explain the data only if the ratio $(1-r_+)/(1-r_a)$ nearly cancels the ratio of the statistical weights in (6). As was pointed out in an earlier section, it does not seem likely that the ratio $(1-r_+)/(1-r_a)$ can differ by a sufficient amount from unity to do this.

Future experimental work will be directed toward improving the accuracy of the data in the high temperature range, and toward investigating other metal pairs which have $(\phi-I)$ values of the order of 0.2 to 0.3 v, and which are accordingly suitable for an investigation of this kind. From studies of this sort it should be possible to decide whether the near approach of the intercept on the $\log_{10}(i_+/i_a)$ axis to zero is fortuitous, owing to the existence of a temperature coefficient of tungsten of the order of magnitude required to raise the intercept to nearly zero, or whether (6) requires modification with respect to the omission of the ratio of the statistical weights.[19]

The authors wish to express their thanks to Dr. David H. Thompson and Dr. E. A. K. Culler for suggestions and help in the least squares calculations.

[18] To be published.

[19] Anselm, Compt. rend. acad. sci. U. S. S. R. **3**, 332 (1934).

LETTERS TO THE EDITOR

Prompt publication of brief reports of important discoveries in physics may be secured by addressing them to this department. Closing dates for this department are, for the first issue of the month, the twentieth of the preceding month; for the second issue, the fifth of the month. The Board of Editors does not hold itself responsible for the opinions expressed by the correspondents.

Communications should not in general exceed 600 words in length.

The Variation with Altitude of the Production of Bursts of Cosmic-Ray Ionization

The frequency distribution of large cosmic-ray showers has been found[1] to be represented satisfactorily by a relation of the form $R=A/N^s$, where N is the number of rays in the shower, RdN the rate of occurrence of showers having sizes between N and $N+dN$, and A and s are parameters. Distribution curves, taken from several observers, for showers from lead are shown, in Fig. 1, to be well represented by this relation when the rates of occurrence of the smaller showers, which values are uncertain because of the statistical fluctuations in the ionization, are disregarded. The sizes of the bursts of ionization have been reduced to numbers of rays by somewhat arbitrary assumptions, since sufficient information for the proper reduction was not, in all cases, available. The factors used do not influence the values of s, but cause proportional errors in A. Table I gives values of s and the sources of the data plotted. The value of R for 100-ray showers is of the order of 10^{-5} per hour per cc of lead at sea level for thicknesses of the order of one centimeter.

TABLE I.

CURVE	OBSERVER	REFERENCE	s	REMARKS
1	J. C. Street and R. T. Young	Phys. Rev. **47**, 572 (1935)	3.4	Computed to the basis of 60 ions/cm/ray
2	E. G. Steinke and H. Schindler	Zeits. f. Physik **75**, 115 (1932)	3.1	Assumed 4.8×10^9 ions per ray
3	R. Bennett, G. Brown, and H. A. Rahmel	Phys. Rev. **47**, 435 (1935)	3.1	Mt. Evans data, assumed 2×10^9 ions per ray
4	W. Messerschmidt	G. Hoffmann, Papers & Discussions, Int. Conf. on Physics, London, 1934, I, p. 226	3.1	Assumed 9×10^6 ions/ray
5	C. G. Montgomery and D. D. Montgomery	Phys. Rev. **47**, 429 (1935)	3.3	2×10^9 ions/ray
		mean	3.2	

The assumption of a distribution curve of this form has interesting consequences when applied to measurements of burst production at different elevations. Fig. 2 shows measurements, previously reported,[2] for bursts from lead and magnesium at sea level and at an elevation of 4300 meters. It appears from this that the value of s, although characteristic of the material, is independent of elevation. Although the ratio of the frequencies of occurrence of bursts of a given size at different altitudes is very different for the two substances, the ratio of the sizes of bursts which occur at a given rate at the two elevations is very nearly the same. This is also true for the observations at the

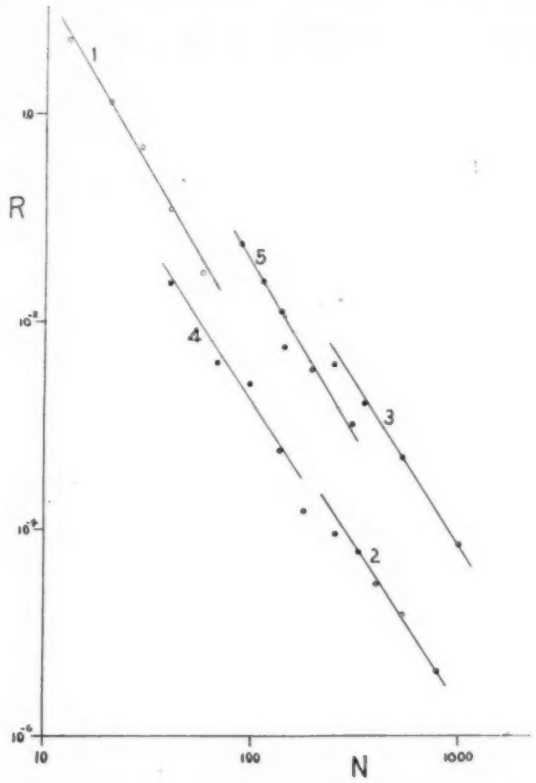

FIG. 1.

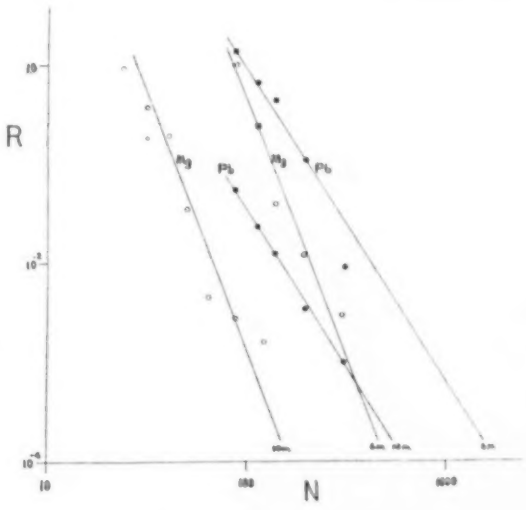

FIG. 2.

intermediate elevations where measurements were made. This suggests that the process which produces a shower of a given size at sea level would occur at the same rate at a high elevation, but would there produce a shower of a larger size, and that this increase is independent of the shower producing material.

If we make this assumption, it can be stated mathematically that the quantity

$$\left[\frac{A(h_1, Z)}{A(h_2, Z)}\right]^{1/s(Z)}$$

is independent of Z, where h_1 and h_2 are two elevations, and Z the atomic number.

This is equivalent to the differential relation

$$\frac{\partial}{\partial Z}\left(\frac{1}{s}\frac{1}{A}\frac{\partial A}{\partial h}\right)=0,$$

whose solution is

$$A=A_0(Z)[F(h)]^{s(Z)}.$$

This immediately suggests the expression postulated by Professor W. F. G. Swann:[3]

$$A=A_0E^{\alpha},$$

where E is the energy of the primary cosmic rays, and A_0 and α are functions of Z only. Since Swann's theory is consistent with the observed variation with altitude for the bursts from lead and magnesium, it appears that the shape of the frequency distribution curve is determined by the exponent α in such a way that s is proportional to α. It is to be noted that the fact that the observed variations with altitude of the frequency of occurrence of bursts from lead and magnesium are different is entirely inconsistent with the hypothesis that bursts are produced by a soft component of the cosmic radiation.

The authors wish to thank Professor Swann for helpful discussions of this matter.

C. G. MONTGOMERY
D. D. MONTGOMERY

Bartol Research Foundation,
Swarthmore, Pennsylvania,
November 22, 1935.

[1] C. G. Montgomery and D. D. Montgomery, Phys. Rev. **48**, 786 (1935).
[2] C. G. Montgomery and D. D. Montgomery, Phys. Rev. **47**, 429 (1935).
[3] W. F. G. Swann, Phys. Rev. **48**, 641 (1935).

Determination of the Saturation Ionization Current from High Speed Electrons in Air

Last year we reported a study[1, 2] of the ionization produced in liquid carbon disulphide by x-rays produced at moderate voltage. Jaffe's[3] theory of columnar ionization furnishes the relationship

$$\frac{I_\infty}{I_x}=\frac{\alpha N}{kudXf(X)}+1,$$

where I_∞/I_x is the fraction of the ions drawn from a column of diameter d by a field X. For high field strengths $f(x)$ approaches 1 so that a plot of $1/I_x$ against $1/X$ gives a straight line which can be extrapolated to $1/X=0$ thus furnishing a calculated value for the ionization current at infinite field. The agreement between values derived from this equation for the energy of ionization per ion pair for CS_2 in the liquid and gaseous state respectively have proved its applicability for x-ray ionization. Subsequently, it has been found that this method for determining saturation current in liquids could be applied well to the ionization produced in CS_2 by gamma-rays.[4]

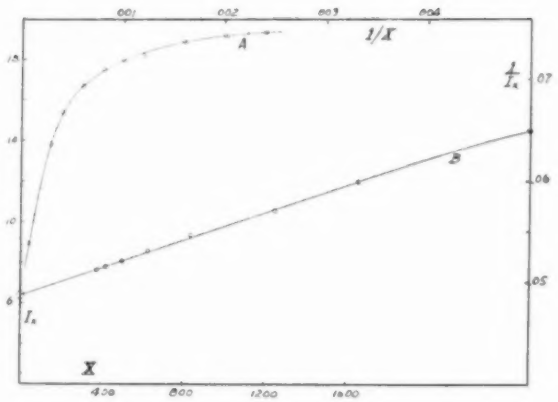

FIG. 1.

The method of plotting has now been extended to determine the ionization produced in air at normal pressure by a heterogeneous beam of electrons having a maximum energy of 150 electron kilovolts. The electron beam produced by a Lenard tube, entered ionization chambers of various forms placed near the tube window (distance 3–10 cm). By using a parallel plate ionization chamber (metal gauze plates 1 cm apart, placed at right angles to the beam), at potentials up to 1300 volts, where the air began to break down by collision ionization, curve A (with coordinates at bottom and left of plot) was obtained for the ionization current as a function of the voltage. Curve B shows the same data plotted reciprocally and extrapolated to $1/X=0$, giving the derived current at infinite field. Air breakdown began when the ratio I_x/I_∞ reached about 0.93.

Jaffe's theory of columnar ionization is presumed to be invalid under the conditions here used, since in air there is an extensive overlapping of the columns and hence strong intercolumnar recombination. It is interesting, therefore, that these empirical results are apparently so similar to those of liquids. The linear relationship between $1/X$ and $1/I_x$ held for values of I_x/I_∞ from about 0.36 to 0.96.

Recent work by Clay and Van Tijn[5] for the ionization produced by gamma-rays in gases under high pressure, gives curves closely similar to those above, but are based on Jaffe's theory of columnar ionization.

LAURISTON S. TAYLOR

National Bureau of Standards,
Washington, D. C.,
November 25, 1935.

[1] F. L. Mohler and L. S. Taylor, Phys. Rev. **45**, 762 (1934).
[2] F. L. Mohler and L. S. Taylor, Bur. Standards J. Research **13**, 659 (1934).
[3] A. Jaffe's, Ann. d. Physik **42**, 303 (1913).
[4] L. S. Taylor and F. L. Mohler, Science **81**, 318 (1935).
[5] J. Clay and M. A. Van Tijn, Physica **2**, 825 (1935).

Fine Structure of $D\alpha$ with Increased Resolution

The fine-structure analysis of the first member of the Balmer series of deuterium, commonly called $D\alpha$, has been reported within the past two years by three sets of investigators in five published papers.[1-5] The general "doublet" structure of the line is readily observable under high dispersion, but the chief minor component resulting from the coincident transitions $2p\,^2P_{1/2}-3s\,^2S_{1/2}$ and $2s\,^2S_{1/2}-3p\,^2P_{1/2}$ has never been resolved from the closely adjacent high frequency main component. The theoretical interval between these components is 0.108 cm^{-1}, and consequently a half-intensity breadth of less than 0.108 cm^{-1} would theoretically be needed to effect a resolution of the components. This would require that the discharge be maintained at about 100°K, and since this is so close to the temperature of liquid-air, it has generally been considered unlikely that the components would ever be resolved with liquid-air cooling.

Recently the fine-structure of $D\alpha$ has been reinvestigated by the authors, using approximately 100 percent deuterium gas kindly given to them by Professor H. C. Urey of Columbia University. The optical equipment was a Zeiss triple-prism spectrograph and a pair of heavily silvered Hilger 7-cm quartz etalon plates, used with a constant 5-mm invar spacer. On several of the plates taken of a low pressure, low current-density discharge the chief minor component was resolved, as is clearly shown in the reproduction of an original microphotometer tracing, Fig. 1.

The measured half-intensity breadth of the high frequency main component is 0.120 cm^{-1}, which indicates clearly that in order to be resolved the minor component must be considerably more than 0.108 cm^{-1} from the main component. Measurements of analyzed curves taken from several plates result in an average interval of 0.134 cm^{-1} between the centers of the components, thus indicating a wide deviation from theory. A possible cause of this deviation is the Stark effect resulting from ionic electric fields in the discharge.

Plates have also been taken by using a 3-mm etalon spacing of the light from a discharge containing equal amounts of hydrogen and deuterium. From the measured interval between the components $2p\,^2P_{3/2}-3d\,^2D_{5/2}$ of the two isotopes a value for e/m has been computed. The new value of the Faraday based on the physical scale of atomic weights,[6] and the atomic weights of hydrogen and deuterium as determined by Bethe[7] from atomic disintegration data have been used in the calculations. The newly

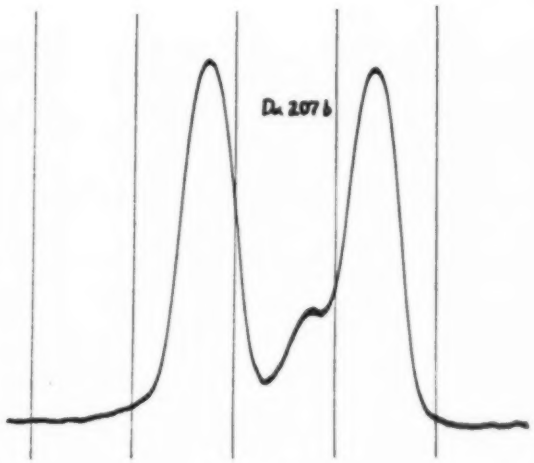

FIG. 1.

obtained value for e/m is $1.7577\pm0.0004\times10^7$ e.m.u./gram.

The value of this constant recently reported by Shane and Spedding[8] using the new value of the Faraday and the old atomic weight values is $1.7579\pm0.0003\times10^7$ e.m.u./gram. However, these authors failed to correct the measured interval between corresponding components of the two isotopes to the interval in vacuum, although they used in their calculations the Rydberg constant for hydrogen reduced to vacuum. The result of this oversight is to make their value 0.0005×10^7 e.m.u./gram too small. However, their e/m value is increased by just 0.0005×10^7 e.m.u./gram when the new atomic weight values determined by Bethe are used. Hence their result with these corrections remains at $1.7579\pm0.0003\times10^7$ e.m.u./gram.

The investigations briefly reported in this letter will be published later in greater detail.

ROBLEY C. WILLIAMS
R. C. GIBBS

Department of Physics,
Cornell University,
November 25, 1935.

[1] Spedding, Shane and Grace, Phys. Rev. **44**, 58 (1933).
[2] Gibbs and Williams, Phys. Rev. **45**, 221 (1934).
[3] Williams and Gibbs, Phys. Rev. **45**, 475 (1934).
[4] Kopferman, Naturwiss. **22**, 218 (1934).
[5] Spedding, Shane and Grace, Phys. Rev. **47**, 38 (1935).
[6] See Shane and Spedding, Phys. Rev. **47**, 36 (1935), for a report of the new Faraday value.
[7] Bethe, Phys. Rev. **47**, 633 (1935).
[8] Shane and Spedding, Phys. Rev. **47**, 33 (1935).

Proceedings of The New England Section of the American Physical Society

MINUTES OF THE PROVIDENCE MEETING, OCTOBER 26, 1935

THE seventh regular meeting of the New England Section was held at Providence, Rhode Island, on Saturday, October 26, at Brown University. The presiding officers for the morning sessions for contributed papers were Professor W. G. Cady, Chairman of the Section, and Professor J. C. Slater. The presiding officer at the Business Meeting and at the afternoon session was Professor Cady. At the Business Meeting, also in the morning, officers were elected for the ensuing year. These officers are:

R. B. Lindsay, *Chairman*
F. A. Saunders, *Vice Chairman*
P. M. Morse, *Secretary-Treasurer*
G. R. Harrison and L. W. McKeehan, *Program Committee*

A vote of thanks was extended to the members of the Physics Department at Brown University for their generous hospitality. After the Business Meeting the Brown Physics Laboratories were open for inspection.

The first part of the afternoon session was a colloquium on "The Teaching of Elementary Physics" led by Professors R. B. Lindsay, Louise McDowell and N. H. Frank. After the three talks, there was considerable general discussion. The second half of the afternoon session was an invited paper by Professor B. E. Warren on "The Structure of Liquids and Glasses."

95 members attended the morning sessions and 125 the afternoon session.

The program of the Section consisted of 15 papers, the abstracts of which are given below.

PHILIP M. MORSE, *Secretary-Treasurer*
New England Section

ABSTRACTS

1. A Vacuum Furnace for the Production of Large Refractory Metal Single Crystals. H. E. FARNSWORTH, *Brown University.*—The arrangement permits a slow progressive cooling of a cylindrical alundum crucible from one tapered end. This is accomplished by slowly decreasing the heating current in a molybdenum heating element wound directly on the crucible in such a manner as to maintain a temperature gradient along the axis. The crucible is supported within a triple radiation shield which is suspended by a single wire in a Pyrex tube which may be evacuated. The temperature is observed by an optical pyrometer. With this arrangement a nickel single crystal $\frac{3}{4}$ inch in diameter and 2 inches in length was formed in a high vacuum.

2. The Heitler-London Repulsive State of H_2. H. M. JAMES, A. SPRAGUE COOLIDGE AND R. D. PRESENT, *Harvard University.*—A variational method has been used in the study of the $1s\sigma 2p\sigma\ ^3\Sigma_u$ state of H_2. Two independent computations with formally different functions gave the same energy for the system, to within 0.03 ev, at a nuclear separation of 1.5 B.R. The functions were compared at some 40 points and were found to have a root-mean-square difference of 2.1 percent; each of these functions should be a good approximation to the correct one. A study of the convergence of the energy to a limit with increasing complexity of the function allows the total energy of the system to be fixed at -21.93 ± 0.02 ev. Computations were also carried out for nuclear separations of 1.6 B.R. and 1.87 B.R. A potential curve passing through the three computed points and approaching the Heitler-London curve for large nuclear separations differs markedly in character from that constructed by Finkelnburg and Weizel to account for the variation with wave-length of the apparent excitation potential of the continuous spectrum of H_2. The method of Finkelnburg and Weizel is briefly analyzed and the reason for the discrepancy is pointed out.

3. Collision Cross Section for Elastic Scattering of Slow Electrons by Diatomic Molecules. J. B. FISK, *Massachusetts Institute of Technology.* (Introduced by P. M. Morse.)—The Ramsauer effect for symmetrical diatomic molecules has been studied on the assumption that the molecular field may be represented by a potential

$$\Phi=\frac{8z^*}{d}\frac{\xi}{\xi^2-\eta^2}\frac{(\xi_0^2-1)-\xi_0(\xi^2-1)}{(\xi_0-1)^2},$$

which leaves the spheroidal wave equation separable. z^* is the effective nuclear charge; ξ_0 a constant giving the shape of the molecule; and d the internuclear distance; ξ and η are the usual spheroidal coordinates. Solutions are obtained making use of the spheroidal functions recently defined by Stratton and Morse[1] and series solutions of the ξ equation. The total cross sections for elastic scattering are calculated for incident electron velocities ranging from 0 to 50 volts in terms of a parameter, $\beta^2=z^*\cdot d\xi_0/4$, defining the molecule. Methods of obtaining z^*, and hence β, are given by utilizing Slater's[2] empirical rules for the "atomic shielding constant." The calculations give good agreement for H_2 and O_2. For N_2 the results are particularly good, giving the proper peak, and also showing a fine structure at $v=3.45\sqrt{V}$ which has hitherto been uncertain in the experiments. As in the explanation of the atomic Ramsauer effect by Allis and Morse[3] a periodicity in the shape of the cross-section curve is observed as the value of β increases.

[1] Stratton and Morse, Proc. Nat. Acad. Sci. **21**, 51, 56 (1935).
[2] Slater, Phys. Rev. **36**, 57 (1930).
[3] Allis and Morse, Zeits. f. Physik **70**, 567 (1931).

4. Mass Ratio of Hydrogen and Deuterium from Band Spectra. WILLIAM W. WATSON, *Yale University.*—Study of the hydrogen isotope effect in diatomic hydride molecules shows that the ratio of the observed B_e constants of the usual rotational energy expressions for the two isotopic molecules is never exactly equal to the ratio of the reduced masses. The size of the several corrections to these constants in order to obtain values close to the "true" B_e values is calculated for some of these hydrides. These calculations demonstrate that the corrections arising from the uncoupling terms due to the interaction of certain electronic levels (Van Vleck, Mulliken) and from the inclusion of the usually neglected interactions between nuclear and electronic motions (Kronig) are by far the most important for most molecules. They also show that, assuming 1.0081 to be the mass of the hydrogen atom, the mass of the deuterium atom has to be greater than the value 2.01423 given in a number of recent articles. A value close to Aston's latest, 2.0148 is indicated.

5. Pressure Effects of Foreign Gases on Spectral Lines. HENRY MARGENAU. *Yale University.*—Experiments show that half-widths and shifts produced in absorption lines by pressures of a foreign gas, are nearly proportional to the pressure of the gas, except at high pressures, where the line is shifted more strongly and the broadening is greater. Customary theories fail to account for these facts. Impact theories, such as that due to Lorentz, predict an increase in half-width *linear* with the pressure, but no shift. Statistical theories predict a shift and a half-width proportional to the square of the pressure, if forces of the van der Waals type are held responsible for the perturbations. The purpose of the present paper is to show how closer investigation removes these discrepancies. The shape of the line may be regarded as the result of an interplay of two causes: (1) The actual distortion of the system of energy levels and the consequent frequency changes which take place during the motion of the molecules; (2) the effective diminution of the coherence length of the wave trains which accompanies these frequency changes. The shape due to cause (1) must be combined with the shape due to cause (2) by means of a "Faltung." If this is done, the experimental facts are explained.

6. The Physical Problem of the Size of the Universe. ARTHUR HAAS, *University of Vienna.*—A system, the mean mass density (ρ) of which is given, cannot exceed a definite volume and a definite mass, because otherwise the gravitational energy to which a negative sign must be given would become larger than the sum of the proper energies of all the objects contained in the system, and hence the resulting energy would become negative. We find for the maximum mass of a homogeneous sphere

$$M_{\max} = \frac{C^3}{6(\pi\rho)^{\frac{1}{2}}}\left(\frac{5}{f}\right)^{\frac{1}{2}}$$

(c, the velocity of light and f, the gravitational constant) or referred to gram and cubic centimeter $M_{\max} \sim 10^{42}/\rho^{\frac{1}{2}}$. To obtain this result, it is superfluous to assume any curvature of space. If we insert for ρ the value which was empirically found for the inner metagalaxies, i.e., 10^{-30}, we obtain as a maximum mass 10^{57} grams. Conversely it follows that the average density of a system of given total mass cannot be above a given maximum value.

7. Specific Resistance of Bismuth Single Crystals. ALFRED B. FOCKE AND JOHN R. HILL, *Brown University.*—The purpose of this investigation is to study the effect of impurities in single crystals. Measurements were made in the temperature range from −185°C to +100°C on samples containing Pb, Sn, Sb and Te. The effects were found to be complicated but the following generalizations may be made. Decreasing temperature results in greater effectiveness of the impurity present except when the impurity concentration is such that a separation of phases occurs at low temperatures. Extremely small amounts (less than 0.03 percent) of all impurities cause a sharp increase in the resistance. The effect of larger amounts depends on the nature of the impurity. Pb and Sn continue to increase the resistance, additional Te forces the resistance to fall to lower values than that of pure Bi; additional Sb causes the initial rise of resistance to fall off and then to be slowly reestablished. More than 0.03 percent Sn and more than 0.3 percent Pb result in a negative temperature coefficient for the resistance parallel to the principal axis. In other cases the coefficient is positive. The results may be explained qualitatively in the light of previous work on the magnetic properties of such crystals and the distribution of impurities within them together with a study of the phase-equilibrium diagrams for the system involved.

8. Investigation of Thermionic Filaments with a Simple Electron Microscope. R. P. JOHNSON AND W. SHOCKLEY, *Massachusetts Institute of Technology.*—The emission properties of a number of small cylindrical filaments have been investigated by means of a simple electron microscope, consisting of a cylindrical glass tube, coaxial with the filament, whose inside wall is coated with fluorescent material and can be maintained at a potential of several thousand volts above the filament by means of a nickel helix anode fitting the wall snugly. An electron image of the emitting surface is formed on the wall, with a lateral magnification of 400 and sufficient resolution to separate points 2° apart on the wire. The emission patterns of drawn wires are characterized by alternate bright and dark stripes (about 50 in a circumference for 0.005 in. tungsten) regularly spaced and continuous down the length of the pattern. These stripes are correlated with die-marks on the wire, visible as grooves under an optical microscope, which are removed by the usual aging. A thoriated tungsten filament after a flash to 2900°K shows at 1200°K a pattern consisting of a large number of small bright spots, many of which reappear in the same places after subsequent flashes. With continued activation at 1800°K to 2200°K, interrupted for observation at 1200°K, these spots are seen to build out into rings around the tube and finally to fill up smoothly the typical striped structure characteristic of the clean filament.

9. Correlation of Emission and Adsorption Properties with Lattice Direction in Single-Crystal Tungsten Wire. W. SHOCKLEY AND R. P. JOHNSON, *Massachusetts Institute of Technology.*—Investigation of single-crystal tungsten

wires by means of the electron microscope arrangement described in the preceding abstract reveals a marked correlation between crystallographic direction in the lattice and the emission and adsorption properties of the surface. Single crystals grown by heat treatment in a drawn wire of pure tungsten, having the 110 direction along the wire axis, give a pattern with a minimum about 20° broad about the 110 direction, and minima about 5° broad in directions 60° from 110. Crystal orientations are determined from Laue pictures of the wire after it has been removed from the tube. When the filament is run at low temperatures in equilibrium with saturated cesium vapor at room temperature the contrast between light and dark regions on the tube wall is much more marked, and the pattern goes through a variety of phases as the filament temperature is changed over the observation range, 700°K to 900°K. In general, directions of minimum emission from clean tungsten are directions of large emission from the cesium-tungsten surface. There is, however, much more "fine structure" in the cesium-tungsten patterns, regions less than 5° apart on the wire circumference differing markedly in electron emission and therefore, presumably, in equilibrium coverage of cesium. In every case the emission pattern exhibits the two reflection planes, 100 and 110, of the tungsten single crystal, and the pattern reproduces itself in each quadrant down to the smallest observable detail. Experiments with potassium-tungsten surfaces and with composite layers give similar results. Preliminary investigations of single-crystal tungsten wires grown by the Pintsch process, which gives crystals of random orientation, indicate the possibility of mapping out emission and adsorption properties over the entire group of lattice directions in tungsten, and in other metals which can be obtained in the form of small single-crystal wire.

10. Collision Induced Radiation. W. M. PRESTON, *Harvard University.*—A new continuous spectrum, associated with the weak forbidden mercury line λ2269.80, has been found in a low pressure mercury discharge with a few centimeters pressure of argon or helium added. The continuum lies on the short wave-length side of the line, has a maximum at 2260A, and falls slowly to 10 percent at 2238A. The ratio of the intensity of the maximum of the continuum to that of the line is proportional to the pressure of the rare gas, and it remains constant when the exciting current is varied. The continuum is attributed to radiation from excited mercury atoms in the metastable $^3P_2$ state perturbed by the close approach of normal rare gas atoms, at which time the thermal energy may be added to the energy of excitation to give a larger quantum. Since the time during which this perturbation is appreciable is much smaller than the time between collisions, while the integrated intensity of the continuum is many times that of the atomic line, we must assume that during a collision the probability of emission is enormously increased. The selection rules which virtually prohibit the transition $^1S_0-{}^3P_2$, giving the mercury line λ2269.80, break down in the perturbing field of a colliding normal rare gas atom, as has been pointed out by Finkelnburg. The molecular states arising from the interaction of a Hg $^3P_2$ atom and a normal rare gas atom have allowed transitions to the ground state, which explains the larger probability of emission.

11. The Intensity of the Continuous Spectrum of Hydrogen. N. D. SMITH, *Harvard University.*—In order to develop a powerful source for use as a background in ultraviolet absorption experiments, the conditions favorable for the most intense production of the continuous spectrum of hydrogen were systematically investigated. With a well-cooled, platinized capillary, flattened to a roughly rectangular cross section, a current density up to 0.125 ma/mm² leaves so many molecules undissociated that the intensity of their continuous spectrum still increases with the current. This source was compared with the carbon arc and found to be superior in intensity below 2995A. Addition of helium produces a shift of the intensity maximum to longer wave-lengths. At the same time the discrete band spectrum of H_2 indicates that the vibration of the excited molecules is practically reduced to zero. It is concluded that the continuous spectrum, emitted in the presence of He, must come from transitions from the lowest vibrational level of the upper state. So any theoretical results are to be checked by this spectrum rather than by that emitted from the ordinary discharge tube in which the distribution in vibrational levels is unknown. The intensity distribution was measured by comparison with the positive crater of the carbon arc, no better ultraviolet standard being available.

12. Observation of the Rotational Structure of Some Ammonia Bands in the Extreme Ultraviolet. A. B. F. DUNCAN, *Brown University* AND G. R. HARRISON, *Massachusetts Institute of Technology.*—Six ammonia bands in the ultraviolet between 1612 and 1490A have been photographed in absorption with the 21-foot normal incidence vacuum spectrograph at the Massachusetts Institute of Technology. The bands have apparently a simple structure and are similar to the infrared bands at 10.3, 10.7μ. Two well-developed branches are present in each band but the present state of the analysis does not permit their positive identification with *P* and *R* branches. The branches toward the ultraviolet form heads. A single narrow line of unusually great intensity near the center of each band may be identified with a *Q* branch.

13. Entladungsstrahlen and the Transparency of Air Below 1200A. ELIZABETH R. LAIRD, *Mount Holyoke College.*—Recent experiments on transmission through thin celluloid films and lithium fluoride make it probable that the portion of Entladungsstrahlen effective in producing ionization in turpentine vapor is of wave-lengths between 1160 and 1200A and also that some radiation of wave-lengths shorter than 900A is transmitted by as much as 3 cm of air and is effective in producing ionization in some constituent of the air. This is in agreement with earlier experiments.

14. Colloquium on the Teaching of Elementary Physics. R. B. LINDSAY, *Brown University,* LOUISE MCDOWELL *Wellesley College,* AND N. H. FRANK, *Massachusetts Institute of Technology.*

15. The Structure of Liquids and Glasses. B. E. WARREN, *Massachusetts Institute of Technology.*

Author Index to Volume 48

References with (A) are to abstracts of papers presented at meetings of the Physical Society. References with (L) are to Letters to the Editor.

Abbott, F. R. and Joseph E. Henderson. Field current emission at small currents—481(A)

Adel, Arthur. Note on the spectra of Jupiter and Saturn—103(L)

Allis, W. P. (see Morse, Philip M.)—412

Almy, G. M. and G. R. Irwin. Mass ratio of the lithium isotopes—104(L)

Anderson, Carl D. (see Neddermeyer, Seth H.)—486(A)

Atkinson, R. d'E. Evidence against He^5—382(L)

Badger, Richard M. Relation between internuclear distances and the force constants of diatomic molecules—284(L)

Ballard, Stanley S. (see Knauss, Harold P.)—796

Bardeen, J. (see Wigner, E.)—84

Barkas, Walter H. (see Kennedy, R. J.)—483(A)

Barker, E. F. (see Bartunek, Paul F.)—516

Barnes, R. Bowling, R. Robert Brattain and Frederick Seitz. On the structure and interpretation of the infrared absorption spectra of crystals—582

Bartberger, C. L. Energy levels of inert-gas configurations—682

Bartunek, Paul F. and E. F. Barker. Infrared absorption spectra of the linear molecules carbonyl sulphide and deuterium cyanide—516

Bauer, S. H. Inhomogeneous fields for mass spectrography—917(L)

Bearden, J. A. Measurement of x-ray wave-lengths by large ruled gratings—385

——— **and H. H. Roseberry.** Cleavage and x-ray planes of calcite crystals—110(L)

——— **and C. H. Shaw.** Shapes and wave-lengths of K series lines of elements Ti 22 to Ge 32—18

Beck, Guido. Remarks on the systematics of isotopes—47

Bernardini, G. and M. Mando. On the stability of $_4Be^8$—468(L)

Beth, Richard A. Direct detection of the angular momentum of light—471(L)

Bethe, H. Nuclear structure and stability—477 (title only)

Bilinsky, S. (see Hughes, A. L.)—155

Birge, Raymond T. Value of the electronic charge—918(L)

Bloch, Felix. Double electron transitions in x-ray spectra—187

——— **and Norris E. Bradbury.** On the mechanism of unimolecular electron capture—689

Boggs, Emily E. and Harold W. Webb. Hyperfine structure of the mercury triplet 6^3P_{012}–7^3S_1 in optical excitation—226

Bohr, N. Can quantum-mechanical description of physical reality be considered complete?—696

Bonner, T. W. (see Brubaker, W. M.)—470(L)

——— **and W. M. Brubaker.** Disintegration of lithium by deuterons—742

——— **and W. M. Brubaker.** Disintegration of nitrogen by slow neutrons—469(L)

Boreman, Robert W. (see Hetzler, Charles William)—656

Boyce, J. C. Spectra of argon in the extreme ultraviolet—396

Boyd, G. A. Computations related to liquid structure by the methods of trial and of Fourier series analysis—473(A)

Bozóky, L. and R. Schmid. Additional first negative oxygen bands—465(L)

——— **and R. Schmid.** Zeeman effect in the first negative oxygen bands—466(L)

Bradbury, Norris E. (see Bloch, Felix)—689

Brattain, R. Robert (see Barnes, R. Bowling)—582

Breazeale, William M. Electro-optical Kerr effect in ammonia, nitrogen and oxygen—237

Breit, G. Rates of nuclear reactions due to bombardment with charged particles—477 (title only)

——— **and E. Wigner.** Note on Majorana's exchange energy—918(L)

——— **and F. L. Yost.** Radiative capture of protons by carbon—203

Brewer, A. Keith. Further evidence for the existence of K^{40}—640(L)

Brickwedde, F. G. (see Scott, R. B.)—483(A)

Bridgman, P. W. Effects of high shearing stress combined with high hydrostatic pressure—825

——— Polymorphism, principally of the elements, up to 50,000 kg/cm²—893

Brown, Joseph G. Local variation of the earth's electric field—484(A)

——— Theory of the local variation of the earth's electric field—487(A)

Brubaker, W. M. (see Bonner, T. W.)—469(L), 742

——— **and T. W. Bonner.** Slow neutrons—470(L)

Burhop, E. H. S. (see Massey, H. S. W.)—468(L)

Burns, Keivin (see Hetzler, Charles William)—656

Cashman, R. J. and W. S. Huxford. Photoelectric properties of pure and gas-contaminated magnesium—475(A), 734

Challacombe, C. N. (see Kruger, P. Gerald)—111(L)

Chao, Siu-Hung. Photographic absorption spectrum of gaseous ammonia—569(L)

Clark, J. C. Measurement of the absolute probability of K-electron ionization of silver by cathode rays—30

Cleaves, Alden P. and Charles W. Edwards. Photography of the third harmonic of hydrogen chloride—850(L)

Collins, George (see Price, W. C.)—714

Compton, K. T. (see Lamar, E. S.)—886

Constant, F. Woodbridge (see Lowance, F. E.)—257

Coolidge, A. Sprague (see James, H. M.)—972(A)

Copeland, Paul L. Secondary emission of electrons from complex targets—96

Copley, M. J. and T. E. Phipps. Surface ionization of potassium on tungsten—960
Cowie, D. B. Geiger-counter characteristics with applied potentials reversed—883
——— (see Swann, W. F. G.)—649
Cram, Winston (see Roebuck, J. R.)—474(A)
Crane, H. R., L. A. Delsasso, W. A. Fowler and C. C. Lauritsen. Cloud chamber studies of the gamma-radiation from lithium bombarded with protons—125
———, **L. A. Delsasso, W. A. Fowler and C. C. Lauritsen.** Gamma-rays from boron bombarded with protons—102(L)
———, **L. A. Delsasso, W. A. Fowler and C. C. Lauritsen.** Gamma-rays from nitrogen bombarded with deuterons—100(L)
———, **L. A. Delsasso, W. A. Fowler and C. C. Lauritsen.** Short-lived β-radioactivity—484(A)
Crawford, F. H. and T. Jorgensen, Jr. Isotope relations in the spectra of LiH and LiD—475(A)
——— **and C. G. Smith.** Low frequency electrodeless ring discharge—477(A)
Crawford, M. F. and Lawrence A. Wills. Hyperfine structure formulae for the configuration p^3s—69
Curtis, Howard J. and Hugo Fricke. Electrical conductance of colloidal solutions at high frequencies—775(L)

Dahl, O. (see Tuve, M. A.)—241, 315
Dahlstrom, R. K., K. V. MacKenzie and Joseph E. Anderson. Total energy distribution for field current electrons—484(A)
Dehlinger, Walter. Statistical distribution curves in the radio tube industry—474(A)
Dellinger, J. H. New radio transmission phenomenon—705(L)
Delsasso, L. A. (see Crane, H. R.)—125, 100(L), 102(L), 484(A)
———, **W. A. Fowler and C. C. Lauritsen.** Protons from the disintegration of lithium by deuterons—848(L)
Delsasso, Leo P. and John H. Munier. Velocity of sound in free air in the frequency range 3.5 to 15 kc as a function of humidity—481(A)
Deming, J. H. (see Jauncey, G. E. M.)—462(L), 577
Deming, Lola S. (see Deming, W. Edwards)—448
Deming, W. Edwards. Solved example illustrating a new property of least squares—486(A)
——— **and Lola S. Deming.** Some physical properties of compressed gases. V. The Joule-Thomson coefficient for nitrogen—448
Dennison, David M. (see Johnson, Manfred)—868
Désirant, Maurice (see Rosen, Boris)—916(L)
Devol, Lee (see Ruark, Arthur E.)—772(L)
Dieke, G. H. $3p^3\Sigma \rightarrow 2s^3\Sigma$ bands of HD and D_2—606
———Triplet $3p$ complex of the hydrogen molecule—610
Doan, Richard L. Increased frequency of cosmic-ray bursts with reduced shielding—470(L)
——— Statistical fluctuations of cosmic-ray ionization in new recording meter—167(L)
Dodd, L. E. Density and surface tension by the capillary elevation method—487(A)
——— Structure of a heavy deposit of solid selenium condensed from the vapor, the liquid being at about 250°C—479(A)
——— (see Goetz, A.)—165(L)
Dolecek, R. L. Discussion of the β-decay theory—13
Duchesne, Jules (see Rosen, Boris)—916(L)
DuMond, Jesse W. M. and J. Paul Youtz. Selective x-ray diffraction from artificially stratified metal films deposited by evaporation—703(L)
Duncan, A. B. F. and G. R. Harrison. Observation of the rotational structure of some bands in the extreme ultraviolet—974(A)
Dunning, J. R. (see Mitchell, D. P.)—774(L)
———, **G. B. Pegram, G. A. Fink and D. P. Mitchell.** Interaction of neutrons with matter—265
———, **G. B. Pegram, G. A. Fink, D. P. Mitchell and E. Segrè.** Velocity of slow neutrons by mechanical velocity selector—704(L)
Duwez, Pol E. Influence of the temperature on the plasticity of crystals—484(A)

Earls, Lester T. Intensities in $^2\Pi$-$^2\Sigma$ transitions in diatomic molecules—423
Eaton, William W. Collisions of alpha-particles with neon nuclei—921
Edwards, Charles W. (see Cleaves, Alden P.)—850(L)
Einstein, A. and N. Rosen. Particle problem in the general theory of relativity—73
Evans, Robley D. Ionization currents produced by radon, RaA and RaC′ in cylindrical ionization chambers—177
——— (see Finney, Gladys D.)—503
——— **and Russel W. Raitt.** Radioactivity of the Earth's crust and its influence on cosmic-ray electroscope observations made near ground level—171

Farnsworth, H. E. Vacuum furnace for the production of large refractory metal single crystals—972(A)
Feenberg, Eugene and Julian K. Knipp. Intranuclear forces—906
Fermi, Enrico. On the recombination of neutrons and protons—570(L)
Fink, G. A. (see Dunning, J. R.)—265, 704(L)
Finney, Gladys D. and Robley D. Evans. Radioactivity of solids determined by alpha-ray counting—503
Fisk, J. B. Collision cross section for elastic scattering of slow electrons by diatomic molecules—972(A)
Fleming, G. M. (see Henderson, Joseph E.)—486(A)
Flowers, John W. Initiation of electrical discharges by field emission—954
Focke, Alfred B. and John R. Hill. Specific resistance of bismuth single crystals—973(A)
Fowler, W. A. (see Crane, H. R.)—125, 100(L), 102(L), 484(A)
——— (see Delsasso, L. A.)—848(L)
Fox, Marvin and I. I. Rabi. On the nuclear moments of lithium, potassium, and sodium—746
Frank, Amelia. Effect of crystalline fields on the magnetic susceptibilities of Sm^{+++} and Eu^{+++}, and the heat capacity of Sm^{+++}—765

Frank, N. H. (see Lindsay, R. B.)—974 (title only)
Frederickson, W. R., M. E. Hogan, Jr. and William W. Watson. Spectra of strontium hydride—602
Fricke, Hugo (see Curtis, Howard J.)—775(L)
Fromer, M. (see Mack, J. E.)—357
Frost, A. A. and O. Oldenberg. Attempt to observe the absorption spectrum of metastable nitrogen molecules—66
Fussler, Karl H. (see Ruark, Arthur)—151

Gardner, M. E. (see White, H. J.)—480(A)
Gaviola, E. and John Strong. Photoelectric effect of aluminum films deposited by the vacuum evaporating process—483(A)
——— **and John Strong.** Spectrum of aluminum vapor distilled by a tungsten coil in vacuum—136
Gibbs, R. C. (see Williams, Robley C.)—971(L)
Gilbert, W. P. Extension of the Rh I-like isoelectronic sequence to the spectrum of Ag III—338
Gilliland, T. R. (see Kirby, S. S.)—849(L)
Gilroy, Helen T. (see Kruger, P. Gerald)—720
Gleason, Paul R. Dark current from barrier-layer photocells—486(A)
Goble, A. T. Four vector problem and its application to energies and intensities in platinum-like spectra—346
Goeppert-Mayer, M. Double beta-disintegration—512
Goetz, A. and L. E. Dodd. About the structure of crystalline bismuth and selenium layers produced by condensation in vacuum—165(L)
Goldsmith, H. H. Relation between the half-lifetimes and the atomic weights of the β-ray emitters—478(A)
Granath, L. P. and R. K. Stranathan. Hyperfine structure and nuclear magnetic moment of caesium I—725
Gray, W. T. Thermal equilibrium of the gas in the d.c. carbon arc—474(A)

Haas, Arthur. Physical problem of the size of the universe—973(A)
Hafstad, L. R. Some current nuclear physics problems in the region below 1000 kilovolts—477 (title only)
——— (see Tuve, M. A.)—106(L), 241, 315
——— **and M. A. Tuve.** Carbon radioactivity and other resonance transmutations by protons—306
Halpern, O. Theorem connecting the energy momentum tensor with the velocity of propagation of waves—431
——— **and G. Heller.** On the Dirac electron in a gravitational field—434
——— **and J. Schwinger.** On the polarization of electrons by double scattering—109(L)
Hammar, G. W. Velocity of light within a massive enclosure—462(L)
Hansen, W. W. (see Webster, D. L.)—486(A)
Hanson, Elmo E. Dissociation of NO and HCl by electron impact—476(A)
——— (see Nier, Alfred O.)—477(A)
Harrington, E. L. and H. H. Penley. Desorptive action of radon—473(A)
——— **and G. A. Wienshall.** Magnitude of the K-absorption discontinuity for tin and for silver—477(A)
Harris, W. (see Hughes, A. L.)—408
Harrison, G. R. (see Duncan, A. B. F.)—974(A)
Haurwitz, Eva S. (see Morse, Philip M.)—948
Haworth, Leland J. Energy distribution of secondary electrons from molybdenum—88
Heaps, C. W. Diffraction of x-rays by liquid Na-K alloy in a magnetic field—491
Hebb, M. H. Λ-type doubling widths in $^3\Pi$ states of molecules intermediate between Hund's cases (a) and (b)—475(A)
Heller, Gabriel. On Dirac's equation in rotating systems—848(L)
——— (see Halpern, O.)—434
Henderson, Joseph E. (see Abbott, F. R.)—481(A)
——— (see Dahlstrom, R. K.)—484(A)
——— **and G. M. Fleming.** Search for temperature changes accompanying field current emission—486(A)
Henderson, M. C. Two radioactive substances from magnesium after deuteron bombardment—855
——— Two radioactivities produced in magnesium by deuteron bombardment and their excitation functions—480(A)
Hendricks, Sterling B. (see Maxwell, Louis R.)—476(A)
Herb, R. G., D. B. Parkinson and D. W. Kerst. Yield of alpha-particles from lithium films bombarded by protons—118
Herzberg, G. and H. Verleger. Two new bands of CO_2 in the photographic infrared—706(L)
Hetzler, Charles William, Robert W. Boreman and Keivin Burns. Spectrum of the zinc arc in vacuum—656
Higgs, Paul M. (see Osborn, F. A.)—480(A)
Hill, Donald M. Principal expansion coefficients of single crystals of mercury—474(A), 620
Hill, Harry. Hyperfine structure in silver—233
Hill, John R. (see Focke, Alfred B.)—973(A)
Hirsh, Frederick R., Jr. Enhancement of x-ray satellites by the Auger effect—776(L)
——— Relative energy of the $L\alpha$ satellites excited by cathode rays in the atomic number range 47 to 52—722
Hogan, M. E., Jr. (see Frederickson, W. R.)—602
Hoge, Harold J. Magnetic anisotropy of crystals of Sn, and of Sn with added Sb, Cd, or Ga—615
Horsley, Lee H. Schematic representation of the anomalous scattering by suitable nuclear fields—1
Howe, J. D. (see Lark-Horovitz, K.)—101(L)
——— (see Yearian, H. J.)—381(L), 475(A)
Hughes, A. L. and S. Bilinsky. Calculation of the elastic scattering of electrons in krypton—155
——— **and W. Harris.** Total scattering of electrons in helium—408
Huntoon, R. D. Inexpensive d.c. amplifier—474(A)
——— Temperatures generated by the passage of high frequency alternating currents through animal tissue with special reference to electro-surgery—478(A)
Huxford, W. S. (see Cashman, R. J.)—475(A), 734

Irwin, G. R. (see Almy, G. M.)—104(L)

James, H. M., A. Sprague Coolidge and R. D. Present. Heitler-London repulsive state of H_2—972(A)
Janes, R. B. Magnetic susceptibilities of salts of the iron group elements—78

Jauncey, G. E. M. and J. H. Deming. Diffuse scattering of x-rays from piezoelectrically oscillating quartz—462(L)
——— **and J. H. Deming.** Extra negative term in the incoherent part of the diffuse scattering of x-rays from neon-like crystals—577
Johnson, E. A. (see Tuve, M. A.)—917(L)
Johnson, Manfred and David M. Dennison. Interaction between vibration and rotation for symmetrical molecules—868
Johnson, R. P. and W. Shockley. Investigation of thermionic filaments with a simple electron microscope—973(A)
——— (see Shockley, W.)—973(A)
Johnson, Thomas H. Progress of the directional survey of cosmic-ray intensities and its application to the analysis of the primary cosmic radiation—287
Jorgensen, T., Jr. (see Crawford, F. H.)—475(A)
Judson, E. B. (see Kirby, S. S.)—849(L)

Kaplan, Joseph. Further study of the Vegard-Kaplan bands—482(A)
——— New afterglow spectrum in nitrogen—800
Kayser, H. "Tabelle der Schwingungszahlen"—Corrections—98
Kemble, Edwin C. Contribution to the theory of the B. W. K. method—549
Kennedy, R. J. and Walter H. Barkas. Search for interaction of matter and radiation as explanation of nebular red-shift—483(A)
Kerst, D. W. (see Herb, R. G.)—118
King, Arthur S. (see King, Robert B.)—485(A)
King, Robert B. and Arthur S. King. Photometry of electric furnace absorption muliplets—485(A)
Kirby, S. S., T. R. Gilliland, E. B. Judson and N. Smith. Ionosphere, sunspots, and magnetic storms—849(L)
Kirkpatrick, D. E. and E. O. Salant. Overtone absorption bands of gaseous HF—945
Kirkpatrick, P. (see Webster, D. L.)—486(A)
Knauss, Harold P. and Stanley S. Ballard. Rotational structure of the Schumann-Runge bands of oxygen in the vacuum region—796
Knipp, Julian K. (see Feenberg, Eugene)—906
Konopinski, E. J. and G. E. Uhlenbeck. On the Fermi theory of β-radioactivity—7
——— **and George E. Uhlenbeck.** Higher order derivatives in the interaction "Ansatz" of the Fermi theory—107(L)
Koontz, Philip G. Beryllium deuteride spectra—707
——— Spectrum of AgD—138
——— **and William W. Watson.** Barium hydride spectra in the infrared—937
Kruger, P. Gerald and C. N. Challacombe. Correction of previous reports concerning the hyperfine structure of Y II lines—111(L)
——— **and Helen T. Gilroy.** Deep terms in the isoelectronic sequence V I to Cu VII—720
——— **and S. G. Weissberg.** Deepest terms in ions of the isoelectronic sequence A I-Mn VIII—659
Krutter, Harry M. Energy bands in copper—664
Kurie, Franz N. D., J. R. Richardson and H. C. Paxton. On the shape of the distribution curves of electrons emitted from artificially produced radioactive substances—167(L)

Ladenburg, R., R. Roberts and M. B. Sampson. Some investigations of neutrons from different sources—467(L)
Laird, Elizabeth R. Entladungsstrahlen and the transparency of air below 1200A—974(A)
Lamar, E. S. (see Morse, Philip M.)—412
——— **and K. T. Compton.** Errata: Potential drop and ionization at mercury arc cathode—777
———, **E. W. Samson and K. T. Compton.** High current ion sources for nuclear investigations—886
Lane, C. T. Size and arrangement of bismuth microcrystals formed from vapor—193
Lang, R. J. Spectrum of Ce IV—481(A)
Langer, R. M. Dynamical theory of gratings—487(A)
Lark-Horovitz, K., H. J. Yearian and J. D. Howe. Origin of the "extra rings" in electron diffraction patterns—101(L)
Latimer, W. M. (see Libby, W. F.)—571
Laun, D. D. Arc spectrum of tungsten—572(L)
Lauritsen, C. C. Gamma-rays and electrons from the transmutation of some light elements—477 (title only)
——— (see Crane, H. R.)—125, 100(L), 102(L), 484(A)
——— (see Delsasso, L. A.)—848(L)
Lawrence, Ernest O., Edwin McMillan and R. L. Thornton. Transmutation functions for some cases of deuteron-induced radioactivity—493
Libby, W. F., M. D. Peterson and W. M. Latimer. Alpha radioactivity of argon formed by radiochlorine—571(L)
Lindsay, R. B., Louise McDowell and N. H. Frank. Colloquium on the teaching of elementary physics—974 (title only)
Lipson, Harry C. and Allan C. G. Mitchell. Quenching of cadmium resonance radiation by foreign gases—625
Livingood, J. J. and A. H. Snell. High voltage Lenard tube and search for radioactivity induced by electron bombardment—485(A)
——— **and Arthur H. Snell.** Search for radioactivity induced by 800-kilovolt electrons—851
Loeb, Leonard B. Energy of formation of negative ions in oxygen—484(A), 684
——— (see Varney, R. N.)—481(A), 484(A), 818
Loomis, F. W. and T. F. Watson. Band spectra of AgO and CuO—280
Loughridge, Donald H. (see Soltau, David L.)—487(A)
——— **and Harold K. Skramstad.** Primary ionization of high speed electrons in nitrogen—485(A)
Lowance, F. E. and F. Woodbridge Constant. Variation with magnetic field and temperature of the thermoelectric properties of ferromagnetics—257
Lyman, Theodore. Transparency of the air between 1100 and 1300A—149

Ma, S. T. (see Wu, Ta-You)—917(L)
Mack, J. E. and M. Fromer. New energy levels in Au II, Hg III, Tl IV, Pb V and Bi VI—357
Mackenzie, K. V. (see Dahlstrom, R. K.)—484(A)
Mando, M. (see Bernardini, G.)—468(L)
Manning, Millard F. Exact solutions of the Schrödinger equation—161

Margenau, Henry. Theory of pressure effects of foreign gases on spectral lines—755, 973(A)
——— (see Pollard, E.)—402
Martin, D. C. Analysis of the spectrum of Se II—938
Massey, H. S. W. and E. H. S. Burhop. Probability of K shell ionization of silver by cathode rays—468(L)
Maxwell, Louis R., V. M. Mosley and Sterling B. Hendricks. Electron diffraction by gas molecules; (I) Structure of phosphorus, (II) Valence angle of oxygen—476(A)
McCorkle, W. H. Effect of a magnetic field upon the polarization of impact radiation—476(A), 532
McDowell, Louise (see Lindsay, R. B.)—974 (title only)
McMillan, Edwin (see Lawrence, Ernest O.)—493
Mitchell, Allan C. G. (see Lipson, Harry C.—625
——— **and Edgar J. Murphy.** Scattering of slow neutrons —653
Mitchell, D. P. (see Dunning, J. R.)—265, 704(L)
———, **J. R. Dunning, E. Segrè and G. B. Pegram.** Absorption and detection of slow neutrons—774(L)
Montgomery, C. G. and D. D. Montgomery. On the showers of rays which produce bursts of cosmic-ray ionization—786
——— **and D. D. Montgomery.** Variation with altitude of the production of bursts of cosmic-ray ionization—969(L)
Montgomery, D. D. (see Montgomery, C. G.)—786, 969(L)
Morgan, J. E. and W. M. Nielsen. Shower production in small thicknesses of lead and other elements—773(L)
Morscher, L. N., Jr. Relative intensities in the principal doublet of thallium under arc and fluorescence excitation—406
Morse, Philip M., W. P. Allis and E. S. Lamar. Velocity distributions for elastically colliding electrons—412
———, **L. A. Young and Eva S. Haurwitz.** Tables for determining atomic wave functions and energies—948
Mosley, V. M. (see Maxwell, Louis R.)—476(A)
Motz, Lloyd and Julian Schwinger. β-radioactivity of neutrons—704(L)
Mouzon, J. C. and N. H. Smith. Ionization of neon and argon by singly charged magnesium ions—420
Munier, John H. (see Delsasso, Leo P.)—481(A)
Murphy, Edgar J. (see Mitchell, Allan C. G.)—653
Mutch, W. W. Fine structure in the K x-ray edge of gallium—569(L)

Neddermeyer, Seth H. and Carl D. Anderson. Absorption of electrons—486(A)
Newson, Henry W. Radioactivity induced in oxygen by deuteron bombardment—790
——— Radioactivity of oxygen, silicon and phosphorus under deuteron bombardment—482(A)
Nielsen, Alvin H. and Harald H. Nielsen. Infrared absorption bands of methane—864
Nielsen, Harald H. (see Nielsen, Alvin H.)—864
——— (see Steward, Wendell B.)—861
Nielsen, W. M. (see Morgan, J. E.)—773(L)
Nier, Alfred O. Evidence for the existence of an isotope of potassium of mass 40—283(L)
——— **and Elmo E. Hanson.** Ionization of hydrogen chloride under electron impact—477(A)
Nye, A. W. Absorption of cosmic radiation in matter—481(A)

Oldenberg, O. (see Frost, A. A.)—66
Olsen, Leonard O. Optical excitation of HgH and CN bands—476(A)
Oppenheimer, J. R. and M. Phillips. Note on the transmutation function for deuterons—500
Osborn, F. A. and Paul M. Higgs. Acoustical absorption as a function of frequency and angle of incidence—480(A)
Osterberg, H. (see Roebuck, J. R.)—450

Parkinson, D. B. (see Herb, R. G.)—118
Paxton, H. C. (see Kurie, Franz N. D.)—167(L)
Pearsall, Anna W. Intensities of satellites of $K\alpha$—133
Pegram, G. E. (see Dunning, J. R.)—265, 704(L)
——— (see Mitchell, D. P.)—774(L)
Penley, H. H. (see Harrington, E. L.)—473(A)
Peterson, M. D. (see Libby, W. F.)—571(L)
Phillips, M. (see Oppenheimer, J. R.)—500
Phipps, T. E. (see Copley, M. J.)—960
Plesset, Milton S. and John A. Wheeler. Inelastic scattering of quanta with production of pairs—302
Plumley, Harold J. (see Siga, Kohei)—105(L)
Pollard, E. and H. Margenau. Collisions of alpha-particles in hydrogen—402
Posin, D. Q. Existence of Townsend's coefficient β in gaseous breakdown at higher pressures—483(A)
——— (see Varney, R. N.)—488(A), 818
Present, R. D. Proton-proton forces in anomalous scattering and in nuclear binding—919(L)
——— Theory of $^3\Sigma^+ - {}^3\Sigma^-$ transitions in band spectra—140
——— (see James, H. M.)—972(A)
Preston, W. M. Collision induced radiation—974(A)
Price, W. C. Rydberg series in I(I)—477(A)
——— **and George Collins.** Far ultraviolet absorption spectrum of oxygen—714

Quarles, L. R. Relation between the electron field emission and the work function of liquid mercury—260

Rabi, I. I. (see Fox, Marvin)—746
——— (see Rosin, Seymour)—373
Raitt, Russell W. (see Evans, Robley D.)—171
Randall, Robert H. and Harold W. Webb. Rate of change of electron temperature in the mercury afterglow—544
Rank, D. H. (see Wood, R. W.)—63
Reynolds, J. A. (see Wahlin, H. B.)—751
Richardson, J. R. (see Kurie, Franz N. D.)—167(L)
Ridenour, Louis N. and Don M. Yost. Absorption of slow neutrons in silver—383(L)
Roberts, R. (see Ladenburg, R.)—467(L)
Roebuck, J. R. and Winston Cram. Multiple-column mercury manometer—474(A)
——— **and H. Osterberg.** Joule-Thomson effect in nitrogen—450
Rojansky, V. Concerning the possibility of a unified interpretation of electrons and protons—108(L)
Rollefson, A. H. (see Rollefson, R.)—779
Rollefson, R. and A. H. Rollefson. Optical dispersion of HCl in the infrared—779

Rose, Morris E. and George E. Uhlenbeck. Formation of electron-positron pairs by internal conversion of γ-radiation—211
Roseberry, H. H. (see Bearden, J. A.)—110(L)
Rosen, Boris, Maurice Désirant and Jules Duchesne. On the predissociation in the sulphur bands—916(L)
Rosen, N. (see Einstein, A.)—73
Rosin, Seymour and I. I. Rabi. Effective collision cross sections of the alkali atoms in various gases—373
Rouse, Arthur G. Scattering of potassium ions by mercury vapor—476(A)
Ruark, Arthur E. Distribution of counts in a counter with constant recovery time—477(A)
——— General theory of radioactive fluctuations—473(A)
——— Is the quantum-mechanical description of physical reality complete?—466(L)
——— **and Lee Devol.** Theory of radioactive fluctuations—772(L)
——— **and Karl H. Fussler.** On the half-lives of potassium, rubidium, neodymium and samarium—151
Rudberg, Erik. Energy distribution of electrons in the photoelectric effect—811
Rudnick, Philip. Computation of spectral intensities for hydrogen—807

Salant, E. O. (see Kirkpatrick, D. E.)—945
Sampson, M. B. (see Ladenburg, R.)—467(L)
Samson, E. W. (see Lamar, E. S.)—886
Sayler, J. N. X-ray ionization chamber materials—472(A)
Schmid, R. (see Bozóky, L.)—465(L), 466(L)
Schneider, E. G. (see Street, J. C.)—463(L)
Schwinger, Julian (see Halpern, O.)—109(L)
——— (see Motz, Lloyd)—704(L)
Scott, F. A. Energy spectrum of the beta-rays of radium E—391
Scott, R. B. and F. G. Brickwedde. Vapor pressure of hydrogen deuteride—483(A)
Segrè, E. (see Dunning, J. R.)—704(L)
——— (see Mitchell, D. P.)—774(L)
Seitz, Frederick (see Barnes, R. Bowling)—582
Serber, Robert. Linear modifications in the Maxwell field equations—49
Shaw, C. H. (see Bearden, J. A.)—18
Shawhan, E. N. Absorption spectrum of tin sulphide—521
——— Band spectrum of Pb_2 in absorption and emission—343
Shearin, Paul E. Infrared absorption spectrum of solid hydrogen chloride—299
Shockley, W. (see Johnson, R. P.)—973(A)
——— **and R. P. Johnson.** Correlation of emission and adsorption properties with lattice direction in single-crystal tungsten wire—973(A)
Siga, Kohei and Harold J. Plumley. Ultraviolet absorption spectrum of hydrogen fluoride—105(L)
Sixtus, K. J. Magnetic reversal nuclei. Part V. Propagation of large Barkhausen discontinuities—425
Skinner, Selby M. Efficiency of the tube counter—438
Skramstad, Harold K. (see Loughridge, Donald H.)—485(A)
Smith, C. G. (see Crawford, F. H.)—477(A)
Smith, Cyril Stanley. Relation between the thermal and electrical conductivities of copper alloys—166(L)
Smith, N. (see Kirby, S. S.)—849(L)
Smith, N. D. Intensity of the continuous spectrum of hydrogen—974(A)
Smith, N. H. (see Mouzon, J. C.)—420
Smith, P. T. (see Tate, John T.)—525
Snell, A. H. (see Livingood, J. J.)—485(A), 851
Soltau, David L. and Donald H. Loughridge. Determination of the variation of carbon content in mild steel by magnetic analysis—487(A)
Spencer, Roy C. Effect of the spectrometer on the width of spectral lines—473(A)
——— Sources of asymmetry in x-ray diffraction grating and refraction measurements—478(A)
Starr, Merle. Study of the Farnsworth cold cathode oscillator—485(A)
Stevenson, A. F. Application of integral equations to eigenvalue problems in quantum mechanics—475(A)
Stevenson, E. C. (see Street, J. C.)—463(L)
——— **and J. C. Street.** Cosmic-ray showers produced by electrons—464(L)
Steward, Wendell B. and Harald H. Nielsen. Infrared absorption spectrum of germane—861
Stewart, G. W. Effect of chlorine ions on x-ray diffraction in aqueous solution—473(A)
Stoddard, K. B. Direct and fluorescence excitation of the K level in thick targets of gold—43
Stranathan, J. D. Dielectric constant of water vapor—538
Stranathan, R. K. (see Granath, L. P.)—725
Street, J. C. (see Stevenson, E. C.)—464(L)
———, **E. G. Schneider and E. C. Stevenson.** Heavy particles from lead—463(L)
Strong, John. Polarization bands—480(A)
——— (see Gaviola, E.)—136, 483(A)
Stuhlman, Otto, Jr. Near ultraviolet band spectra of iodine—381(L)
Sullivan, Roy R. Study of the first spark spectrum of caesium as excited by electron impact—476(A)
Swann, W. F. G. Corpuscular theory of the primary cosmic radiation—641
——— **and D. B. Cowie.** Effect of primary cosmic-ray energy upon burst production—649

Tanaka, Masamichi. After effect of aluminum bombarded by electrons—916(L)
Tate, John T., P. T. Smith and A. L. Vaughan. Mass spectrum analysis of the products of ionization by electron impact in nitrogen, acetylene, nitric oxide, cyanogen and carbon monoxide—525
Taylor, Lauriston S. Determination of the saturation ionization current from high speed electrons in air—970(L)
Thornton, R. L. (see Lawrence, Ernest O.)—493
Tonks, Lewi. Theory of liquid surface rupture by a uniform electric field—562
Trawick, M. W. Spectrum of molybdenum V—223
Tuve, M. A. (see Hafstad, L. R.)—306
———, **O. Dahl and L. R. Hafstad.** Production and focusing of intense positive ion beams—241

——— **and L. R. Hafstad.** Carbon reactions and the corrected mass-scale—106(L)
———, **L. R. Hafstad and O. Dahl.** High voltage technique for nuclear physics studies—315
———, **E. A. Johnson and O. R. Wulf.** New experimental method for study of the upper atmosphere—917(L)

Uehling, E. A. Polarization effects in the positron theory—55
Uhlenbeck, George E. (see Konopinski, E. J.)—7, 107(L)
——— (see Rose, Morris E.)—211

Valasek, Joseph. Influence of chemical combination on x-ray emission spectra—473(A)
Van Vleck, J. H. On the cross section of heavy nuclei for slow neutrons—367
——— Scattering of slow neutrons by heavy atoms—475(A)
Varney, R. N. and L. B. Loeb. Photoionization in gases—481(A), 822
———, **H. J. White, L. B. Loeb and D. Q. Posin.** Role of space charge in the study of the Townsend ionization coefficients and the mechanism of static spark breakdown—488(A), 818
Vaughan, A. L. (see Tate, John T.)—525
Verleger, H. (see Herzberg, G.)—706(L)
Vigness, Irwin. Dilatations in Rochelle salt—198

Wahlin, H. B. and J. A. Reynolds. Positive and negative thermionic emission from molybdenum—751
Wait, G. R. Intermediate ion of the atmosphere—383(L)
Warren, B. E. Structure of liquids and glasses—974 (title only)
Wataghin, G. Remarks on the theory of protons and neutrons—284(L)
Watson, T. F. (see Loomis, F. W.)—280
Watson, W. H. Note on γ-transformation of electromagnetic fields—776(L)
Watson, William W. Mass ratio of hydrogen and deuterium from band spectra—973(A)
——— (see Frederickson, W. R.)—602
——— (see Koontz, Philip G.)—937
——— **and Robert L. Weber.** *E* band system of calcium hydride—732
Webb, Harold W. (see Boggs, Emily E.)—226
——— (see Randall, Robert H.)—544
Weber, Robert L. (see Watson, William W.)—732
Webster, D. L., W. W. Hansen and P. Kirkpatrick. Electron optics of a 3000 kv x-ray tube—486(A)
Weissberg, S. G. (see Kruger, P. Gerald)—659
Wheeler, John A. (see Plesset, Milton S.)—302
White, Harry J. Variation of sparking potential with intense ultraviolet illumination—113, 482(A)
——— (see Varney, R. N.)—488(A), 818
——— **and M. E. Gardner.** a.c. voltage stabilizer unit—480(A)
White, Milton G. Scattering of high energy protons by oxygen nuclei—481(A)
Whitney, L. V. Spectral emissivities of columbium, thorium, rhodium and molybdenum—477(A)
——— Temperature scales of columbium, thorium, rhodium and molybdenum at 0.667μ—458
Wienshall, G. A. (see Harrington, E. L.)—477(A)
Wigner, E. (see Breit, G.)—918(L)
——— **and J. Bardeen.** Theory of the work functions of monovalent metals—84
Williams, Robley C. and R. C. Gibbs. Fine structure of $D\alpha$ with increased resolution—971(L)
Wills, Lawrence A. (see Crawford, M. F.)—69
Wilson, Wm. S. Atomic energy states for excited helium—536
Witmer, Enos E. Magnetic susceptibility of molecular hydrogen—380(L)
Wood, R. W. Anomalous diffraction gratings—482(A), 928
——— Raman spectrum of heavy benzene C_6D_6—488(A)
——— **and D. H. Rank.** Raman spectrum of heavy chloroform—63
Woodbridge, Donald B. Diamagnetism of alkyl acetates—672
Wu, Ta-You and S. T. Ma. Correction. Double excited states of helium—917(L)
Wulf, O. R. (see Tuve, M. A.)—917(L)

Yearian, H. J. Intensity of diffraction of electrons by ZnO—631
——— (see Lark-Horovitz, K.)—101(L)
——— **and J. D. Howe.** Scattering of high speed electrons of varying energy—381(L)
——— **and J. D. Howe.** Scattering intensity of electrons as a function of voltage—475(A)
Yost, Don M. (see Ridenour, Louis N.)—383(L)
Yost, F. L. (see Breit, G.)—203
Young, Lloyd A. Note on the interaction of nuclear particles—913
——— (see Morse, Philip M.)—948
Youtz, J. Paul (see DuMond, Jesse W. M.)—703(L)

Zener, Clarence. Diffuse scattering of x-rays by conduction electrons—573
——— Uncertainty principle as an eigenwert problem—772(L)
Zwicky, F. On Bitter's patterns—111(L)
——— Remarks on the redshift from nebulae—802
——— Where can negative protons be found?—169(L)

Analytic Subject Index to Volume 48

References with (A) are to abstracts of papers presented at meetings of the Physical Society. References with (L) are to Letters to the Editor.

Absorption and reflection of light (see also **Spectra, absorption**)
Transparency of air; 1100 to 1300A, T. Lyman—149
Acoustics
Absorption as function of frequency and angle of incidence, F. A. Osborn, P. M. Higgs—480(A)
Velocity of sound as function of humidity, L. P. Delsasso, J. H. Munier—481(A)
Afterglow
In N_2, J. Kaplan—800
Arcs (see **Discharge of electricity in gases**)
Astrophysics
Interaction of matter and radiation; red-shift, R. J. Kennedy, W. H. Barkas—483(A)
Ionosphere, sunspots, and magnetic storms, S. S. Kirby, T. R. Gilliland, E. B. Judson, N. Smith—849(L)
Red shift; Dirac theory, O. Halpern, G. Heller—434
Redshift from nebulae, F. Zwicky—802
Size of the universe, A. Haas—973(A)
Spectra of Jupiter and Saturn, A. Adel—103(L)
Variation of earth's electric field, J. G. Brown—484(A)
Atomic mass
C reactions and corrected mass-scale, M. A. Tuve, L. R. Hafstad—106(L)
Atomic and molecular beams
Cross sections of alkali atoms in various gases, S. Rosin, I. I. Rabi—373
Atomic and molecular radii (see also **Scattering of electrons, etc.**)
Of alkali atoms in gases, S. Rosin, I. I. Rabi—373
Atomic structure (see **Spectra, atomic**)

Barkhausen effect (see **Magnetic properties**)
Barrier-layer photo-cells
Dark current from cells, P. R. Gleason—486(A)
Biophysics
High frequency currents through animal tissue, R. D. Huntoon—478(A)

Collision phenomena (see also **Scattering of electrons, etc.**)
Calculation of elastic scattering in Kr, A. L. Hughes, S. Bilinsky—155
Cross sections of alkali atoms in various gases, S. Rosin, I. I. Rabi—373
Compton effect (see **X-rays, diffraction, scattering, etc.**)
Constants, physical, standards
E/m from fine structure of Balmer lines, R. C. Williams, R. C. Gibbs—971(L)
Electronic charge, R. T. Birge—918(L)
Cosmic radiation
Absorption of electrons, S. H. Neddermeyer, C. D. Anderson—486(A)
Absorption by various materials, A. W. Nye—481(A)
Burst production; primary energy, W. F. G. Swann, D. B. Cowie—649
Burst production, variation with altitude, C. G. Montgomery, D. D. Montgomery—969(L)
Directional survey, T. H. Johnson—287
Frequency of bursts with shielding, R. L. Doan—470(L)
Heavy particles from Pb, J. C. Street, E. G. Schneider, E. C. Stevenson—463(L)
Negative protons, F. Zwicky—169(L)
Primary radiation; corpuscular theory, W. F. G. Swann—641
Radioactivity influence on cosmic-ray electroscope, R. D. Evans, R. W. Raitt—171
Shower production in small thicknesses of Pb, Al, Cu, Sn, J. E. Morgan, W. M. Nielsen—773(L)
Showers which produce bursts of ionization, C. G. Montgomery, D. D. Montgomery—786
Showers produced by electrons, E. C. Stevenson, J. C. Street—464(L)
Statistical fluctuations, R. L. Doan—167(L)
Tube counters; efficiency, S. M. Skinner—438
Crystalline state
Absorption spectra of crystals, R. B. Barnes, R. R. Brattain, F. Seitz—582
Bi micro-crystals formed from vapor, C. T. Lane—193
C in mild steel, D. L. Soltau, D. H. Loughridge—487(A)
Cleavage and x-ray planes of calcite crystals, J. A. Bearden, H. H. Roseberry—110(L)
Dilatations in Rochelle salt, I. Vigness—198
Emission and adsorption properties of single-crystal W wire, W. Shockley, R. P. Johnson—973(A)
Energy bands in Cu, H. M. Krutter—664
Expansion coefficients of Hg crystals, D. M. Hill—474(A), 620
Magnetic anisotropy of Sn, and of Sn with Sb, Cd, or Ga, H. J. Hoge—615
Polymorphism, up to 50,000 kg/cm², P. W. Bridgman—893
Production of large refractory single crystals, H. E. Farnsworth—972(A)
Resistance of Bi single crystals, A. B. Focke, J. R. Hill—973(A)
Secondary structure, magnetic crystals, F. Zwicky—111(L)
Shearing stress combined with high hydrostatic pressure, P. W. Bridgman—825
Structure of Bi and Se produced by condensation in vacuum, A. Goetz, L. E. Dodd—165(L); L. E. Dodd—479(A)
Temperature and plasticity, P. E. Duwez—484(A)
Thermal and electrical conductivities of Cu alloys, C. S. Smith—166(L)

Dielectric constants
Of H_2O vapor, J. D. Stranathan—538
Diffraction of electrons (see **Electron diffraction**)

Discharge of electricity in gases (see also **Spark discharge**)
Discharges initiated by field emission, J. W. Flowers—954
Electrodeless discharge, low frequency, F. H. Crawford, C. G. Smith—477(A)
Electron temperature in Hg afterglow, R. H. Randall, H. W. Webb—544
Equilibrium of gas in d.c. C arc, W. T. Gray—474(A)
Errata, potential drop and ionization at Hg arc cathode, E. S. Lamar, K. T. Compton—777
Townsend's coefficient β at higher pressures, D. Q. Posin—483(A)
Disintegration of nucleus (see **Neutron, Nucleus, Radioactivity**)
Dissociation
Of NO and HCl by electron impact, E. E. Hanson—476(A)

Efficiency of ionization
Direct and fluorescence excitation of K-level in Au, K. B. Stoddard—43
Of K-electron ionization of Ag by cathode rays, J. C. Clark—30; H. S. W. Massey, E. H. S. Burhop—468(L)
Elasticity
Shearing stress combined with high hydrostatic pressure, P. W. Bridgman—825
Temperature and plasticity of crystals, P. E. Duwez—484(A)
Electrical conductivity and resistance
Of Bi single crystals, A. B. Focke, J. R. Hill—973(A)
Of colloidal solutions at high frequencies, H. J. Curtis, H. Fricke—775(L)
Thermal and electrical conductivities of Cu alloys, C. S. Smith—166(L)
Electromagnetic theory
Detection of angular momentum of light, R. A. Beth—471(L)
Electromagnetic fields, γ-transformation of, W. H. Watson—776(L)
Energy momentum tensor and velocity of waves, O. Halpern—431
Modifications for positron, R. Serber—49
Polarization effects, positron theory, E. A. Uehling—55
Electron affinity
Of O_2, L. B. Loeb—484(A), 684
Unimolecular electron capture; mechanism of, F. Bloch, N. E. Bradbury—689
Electron diffraction (see also **Scattering of electrons, etc.**)
Intensity as function of voltage, H. J. Yearian, J. D. Howe—475(A)
Origin of the "extra rings," K. Lark-Horovitz, H. J. Yearian, J. D. Howe—101(L)
Structure of P_4 valence angle of O_2, L. R. Maxwell, V. M. Mosley, S. B. Hendricks—476(A)
By ZnO, H. J. Yearian—631
Electron lenses; Focusing
Optics of 3000 kv x-ray tube, D. L. Webster, W. W. Hansen, P. Kirkpatrick—486(A)

Electrons (see also **Positive electron**)
Dirac electron in gravitational field, O. Halpern, G Heller—434
Electronic charge, R. T. Birge—918(L)
Polarization by double scattering, O. Halpern, J. Schwinger—109(L)
Unified interpretation of electrons and protons, V. Rojansky—108(L)
Electrons, positive (see **Positive electrons**)
Electrons, scattering of (see **Scattering of electrons, etc.**)
Electrons, secondary
From complex targets, P. L. Copeland—96
From Mo, energy distribution, L. J. Haworth—88
Electro-optical effects (see also **Photoelectric effect and properties; cells**)
Kerr effect in NH_3, N_2 and O_2, W. M. Breazeale—237
Errata
Corrections to H. Kayser's "Tabelle der Schwingungszahlen," H. Kayser—98
Doubly excited states in He, T.-Y. Wu, S. T. Ma—917(L)
Potential drop and ionization at Hg arc cathode, E. S. Lamar, K. T. Compton—777
Errors of measurements
Example of least squares, W. E. Deming—486(A)

Field currents
Energy distribution, R. K. Dahlstrom, K. V. Mackenzie, J. E. Henderson—484(A)
Liquid surface rupture by electric field, L. Tonks—562
At small currents, F. R. Abbott, J. E. Henderson—481(A)
Temperature changes of electrodes, J. E. Henderson, G. M. Fleming—486(A)
Work function of Hg, L. R. Quarles—260

Gamma-rays (see also **Radioactivity**)
Inelastic scattering, production of pairs, M. S. Plesset, J. A. Wheeler—302
Gases (see **Kinetic theory**)
Geophysics
Radioactivity of rocks, G. D. Finney, R. D. Evans—503
Gyromagnetization (see **Magnetic properties**)

Hyperfine structure (see also **Nuclear moments and spin**)
Of Cs I, L. P. Granath, R. K. Stranathan—725
Correction on previous reports on Y II lines, P. G. Kruger, C. N. Challacombe—111(L)
Formulae for configuration p^2s, M. F. Crawford, L. A. Wills—69
Of Hg triplet $6^3P_{012}-7^3S_1$, E. E. Boggs, H. W. Webb—226
Of Ag, H. Hill—233

Induced radioactivity (see **Radioactivity**)
Instruments (see **Methods and instruments**)
Intensities in spectra (see also **Spectra, etc.**)
Doublet of Tl; arc and fluorescence excitation, L. N. Morscher, Jr.—406

In $^3\Pi - {}^2\Sigma$ transitions in diatomic molecules, L. T. Earls—423

Ionization by electrons
High speed electrons in air, L. S. Taylor—970(L)
High speed electrons in N_2, D. H. Loughridge, H. K. Skramstad—485(A)
Of N_2, C_2H_2, NO, C_2N_2 and CO; mass spectrum analysis, J. T. Tate, P. T. Smith, A. L. Vaughan—525

Ionization by positive ions
Ne and A by Mg ions, J. C. Mouzon, N. H. Smith—420

Ionization potentials
Of HCl, A. O. Nier, E. E. Hanson—477(A)
Of N_2, C_2H_2, NO, C_2N_2 and CO, J. T. Tate, P. T. Smith, A. L. Vaughan—525
Of Ag, W. P. Gilbert—338

Ionization by radiation
In various gases, R. N. Varney, L. B. Loeb—481(A), 818

Isotopes
Of Cl, A. O. Nier, E. E. Hanson—477(A)
Evidence against He^6, R. d'E. Atkinson—382(L)
Existence of K^{40}, A. O. Nier—283(L); A. K. Brewer—640(L)
And h.f.s. of Hg triplet, E. E. Boggs, H. W. Webb—226
Mass ratio of H_2 and D_2, W. W. Watson—973(A)
Mass ratio in Li, G. M. Almy, G. R. Irwin—104(L)
Stability of $_4Be^8$, G. Bernardini, M. Mando—468(L)

Joule-Thomson effect
Coefficients for N_2, W. E. Deming, L. S. Deming—448; J. R. Roebuck, H. Osterberg—450

Kerr effect (see **Electro-optical effects**)

Kinetic theory
Joule-Thomson coefficient for N_2, W. E. Deming, L. S. Deming—448; J. R. Roebuck, H. Osterberg—450

Liquids
Liquid surface rupture by electric field, L. Tonks—562
Structure by x-ray methods, G. A. Boyd—473(A)

Magnetic properties
Anisotropy of Sn, and of Sn with Sb, Cd, or Ga, H. J. Hoge—615
On Bitter's patterns, F. Zwicky—111(L)
Diamagnetism of alkyl acetates, D. B. Woodbridge—672
Gyromagnetic effect; Dirac theory, O. Halpern, G. Heller—434
Magnetoresistance in NaK alloy, C. W. Heaps—491
Reversal nuclei; Barkhausen discontinuities, K. J. Sixtus—425
Susceptibilities of salts of Fe group, R. B. Janes—78
Susceptibilities of Sm^{+++} and Eu^{+++}, A. Frank—765
Susceptibility of H_2, E. E. Witmer—380(L)
Thermoelectric properties of ferromagnetics, F. E. Lowance, F. W. Constant—257

Mass defects (see **Isotopes**)

Mass spectrograph (see also **Methods and instruments**)
Inhomogeneous fields for mass spectrography, S. H. Bauer—917(L)

Mechanics, quantum—atomic structure and spectra
Energy levels of inert-gas configurations, C. L. Bartberger—682
Energy states for excited He, W. S. Wilson—536
Intensities for H_2, P. Rudnick—807
Wave functions and energies, tables, P. M. Morse, L. A. Young, E. S. Haurwitz—948

Mechanics, quantum—general
B.W.K. method, E. C. Kemble—549
Description of physical reality, N. Bohr—696; A. E. Ruark—466(L)
Detection of angular momentum of light, R. A. Beth—471(L)
Dirac electron in gravitational field, O. Halpern, G. Heller—434
Dirac's equation in rotating systems, G. Heller—848(L)
Exact solutions of Schrödinger equation, M. F. Manning—161
Formation of electron-positron pairs, M. E. Rose, G. E. Uhlenbeck—211
Integral equations and eigenvalue problems, A. F. Stevenson—475(A)
Magnetic susceptibility of H_2, E. E. Witmer—380(L)
Radiative capture of protons, G. Breit, F. L. Yost—203
Scattering of quanta with production of pairs, M. S. Plesset, J. A. Wheeler—302
Scattering of slow electrons by molecules, J. B. Fisk—972(A)
Uncertainty principle as an eigenwert problem, C. Zener—772(L)
Unimolecular electron capture, F. Bloch, N. E. Bradbury—689

Mechanics, quantum—molecular structure and spectra
Isotope relations in spectra, F. H. Crawford, T. Jorgensen, Jr.—475(A)
Λ-type doubling widths in $^3\Pi$ states, M. H. Hebb—475(A)

Mechanics, quantum—of solid bodies
Energy bands in Cu, H. M. Krutter—664

Metals (see **Crystalline state**)

Meteorology
Intermediate ion of the atmosphere, G. R. Wait—383(L)
Ionosphere, sunspots, and magnetic storms, S. S. Kirby, T. R. Gilliland, E. B. Judson, N. Smith—849(L)
Radio transmission phenomenon, J. H. Dellinger—705(L)
Upper atmosphere, method of study, M. A. Tuve, E. A. Johnson, O. R. Wulf—917(L)
Variation of earth's electric field, J. G. Brown—484(A)

Methods and instruments
α-ray counting, G. D. Finney, R. D. Evans—503
C in mild steel by magnetic analysis, D. L. Soltau, D. H. Loughridge—487(A)
Cold cathode oscillator, M. Starr—485(A)
Continuous source of ultraviolet, N. D. Smith—974(A)
Density and surface tension, L. E. Dodd—487(A)
Desorptive action of Rn, E. L. Harrington, H. H. Penley—473(A)
D.c. amplifier, inexpensive, R. D. Huntoon—474(A)

Electrodeless ring discharge, low frequency, F. H. Crawford, C. G. Smith—477(A)
Example of least squares, W. E. Deming—486(A)
Geiger-counter characteristics with reversed potentials, D. B. Cowie—883
High current ion sources, E. S. Lamar, E. W. Samson, K. T. Compton—886
High pressure technique, P. W. Bridgman—825
High voltage Lenard, J. J. Livingood, A. H. Snell—485(A), 851
High voltage technique, M. A. Tuve, L. R. Hafstad, O. Dahl—315
Inhomogeneous fields for mass-spectrography, S. H. Bauer—917(L)
Ionization chamber materials, J. N. Sayler—472(A)
Ionization in cylindrical chambers, R. D. Evans—177
Multiple-column Hg manometer, J. R. Roebuck, W. Cram—474(A)
Neutron mechanical velocity selector, J. R. Dunning, G. B. Pegram, G. A. Fink, D. P. Mitchell, E. Segrè—704(L)
Positive ion-beams, production and focusing, M. A. Tuve, O. Dahl, L. R. Hafstad—241
Radiation from metastable levels, J. Kaplan—482(A)
Radioactive fluctuations, theory of, A. E. Ruark, L. Devol—772(L)
Single crystals; vacuum furnace for, H. E. Farnsworth—972(A)
Spectrometer and width of spectral lines, R. C. Spencer—473(A)
Temperature scales of Co, Th, Rh, and Mo, L. V. Whitney—458
Theory of local variation, J. G. Brown—487(A)
Tube counters; efficiency, S. M. Skinner—438; A. E. Ruark—477(A)
Upper atmosphere, method of study, M. A. Tuve, E. A. Johnson, O. R. Wulf—917(L)
Voltage stabilizer unit, H. J. White, N. E. Gardner—480(A)

Molecular structure and constants (see also **Spectra, molecular and Raman spectra**)
Internuclear distances and force constants, R. M. Badger—284(L)

Neutrons (see also **Nucleus**)
Absorption and detection, D. P. Mitchell, J. R. Dunning, E. Segrè, G. B. Pegram—774(L)
Absorption in Ag, L. N. Ridenour, D. M. Yost—383(L)
Cross section of nuclei for slow neutrons, J. H. Van Vleck—367, 475(A)
From different sources, R. Ladenburg, R. Roberts, M. B. Sampson—467(L)
Disintegration of N by neutrons, T. W. Bonner, W. M. Brubaker—469(L)
Energy distribution, W. M. Brubaker, T. W. Bonner—470(L)
Interaction with matter, J. R. Dunning, G. B. Pegram, G. A. Fink, D. P. Mitchell—265
Interaction of nuclear particles, L. A. Young—913
Interaction of protons and neutrons, G. Wataghin—284(L)
Majorana's exchange energy, G. Breit, E. Wigner—918(L)
Mechanical velocity selector, J. R. Dunning, G. B. Pegram, G. A. Fink, D. P. Mitchell, E. Segrè—704(L)
Recombination with protons, E. Fermi—570(L)
Scattering in metals, A. C. G. Mitchell, E. J. Murphy—653

Nuclear moments and spin (see also **Hyperfine structure**)
Of Cs, L. P. Granath, R. K. Stranathan—725
Of Li, K and Na, M. Fox, I. I. Rabi—746

Nucleus
α-particles from Li films bombarded by H^1; thick and thin film, R. G. Herb, D. B. Parkinson, D. W. Kerst—118
Creactions and corrected mass-scale, M. A. Tuve, L. R. Hafstad—106(L)
Collisions of α-particles with Ne, W. W. Eaton—921
Cross section for slow neutrons, J. H. Van Vleck—367, 475(A)
Disintegration of Li by deuterons, T. W. Bonner, W. M. Brubaker—742
Disintegration of N by neutrons, T. W. Bonner, W. M. Brubaker—469(L)
Double β-disintegration, M. Goeppert-Mayer—512
Formation of electron-positron pairs, M. E. Rose, G. E. Uhlenbeck—211
γ-radiation from Li, B and N bombarded with H^1, H. R. Crane, L. A. Delsasso, W. A. Fowler, C. C. Lauritsen—125, 100(L), 102(L)
Heavy particles from Pb, J. C. Street, E. G. Schneider, E. C. Stevenson—463(L)
High current ion sources, E. S. Lamar, E. W. Samson, K. T. Compton—886
High voltage technique, M. A. Tuve, L. R. Hafstad, O. Dahl—315
$_1H^1$ from Li by $_1H^2$ bombardment, L. A. Delsasso, W. A. Fowler, C. C. Lauritsen—848(L)
Interaction of neutrons with matter, J. R. Dunning, G. B. Pegram, G. A. Fink, D. P. Mitchell—265
Interaction of nuclear particles, L. A. Young—913
Interaction of protons and neutrons, G. Wataghin—284(L)
Intranuclear forces, E. Feenberg, J. K. Knipp—906; R. D. Present—919(L)
Majorana's exchange energy, G. Breit, E. Wigner—918(L)
Nuclear energy levels, L. H. Horsley—1
Positive ion-beams, production and focusing, M. A. Tuve, O. Dahl, L. R. Hafstad—241
Radiative capture of protons, G. Breit, F. L. Yost—203
Recombinations of neutrons and protons, E. Fermi—570(L)
Resonance-transmutations by H^1, C radioactivity, L. R. Hafstad, M. A. Tuve—306
Stability of $_4Be^8$, G. Bernardini, M. Mando—468(L)
Structure of nuclei, isotopes, G. Beck—47
Transmutation function for deuterons, J. R. Oppenheimer, M. Phillips—500

Optical constants and properties
Dispersion of HCl in the infrared, R. Rollefson, A. H. Rollefson—779
Polarization bands from ruled gratings, J. Strong—480(A); R. W. Wood—482(A), 928
Theory of gratings, R. M. Langer—487(A)
Optical instruments (see **Methods and instruments**)
Oscillators
Cold cathode oscillator, M. Starr—485(A)

Philosophy of physics
Description of physical reality, N. Bohr—696; A. E. Ruark—466(L)
Photoelectric effect and properties; cells
Of Al films, E. Gaviola, J. Strong—483(A)
Energy distribution of electrons, E. Rudberg—811
Formation of electron-positron pairs, M. E. Rose, G. E. Uhlenbeck—211
Of pure and gas contaminated Mg, R. J. Cashman, W. S. Huxford—475(A), 734
Photoionization (see **Ionization by radiation**)
Photometry
Of electric furnace multiplets, R. B. King, A. S. King—485(A)
Photronic cells (see **Barrier-layer photo-cells**)
Piezoelectric effect
Inverse effect in Rochelle salt, I. Vigness—198
Scattering of x-rays from oscillating quartz, G. E. M. Jauncey, J. H. Deming—462(L)
Plasmoidal discharges (see **Discharge of electricity in gases**)
Polarization of radiation
Effect of magnetic field, impact radiation, W. H. McCorkle—476(A), 532
Positive electron
Electromagnetic theory, R. Serber—49; E. A. Uehling—55
Production of, S. H. Neddermeyer, C. D. Anderson—486(A)
Probability of ionization (see **Efficiency of ionization**)

Quenching of radiation
Resonance radiation of Cd, H. C. Lipson, A. C. G. Mitchell—625

Radio
New transmission phenomenon, J. H. Dellinger—705(L)
Statistical distribution curves in tube industry, W. Dehlinger—474(A)
Radioactivity (see also **Neutrons, Nucleus**)
α-radioactivity of A formed by radiochlorine, W. F. Libby, M. D. Peterson, W. M. Latimer—571(L)
β-ray spectrum of Ra E, F. A. Scott—391
C radioactivity, resonance-transmutations by H^1, L. R. Hafstad, M. A. Tuve—306
Desorptive action of Rn, E. L. Harrington, H. H. Penley—473(A)
Distribution of β-rays in induced radioactivity, F. N. D. Kurie, J. R. Richardson, H. C. Paxton—167(L)
Of earth's crust, R. D. Evans, R. W. Raitt—171
Existence of K^{40}, A. O. Nier—283(L); A. K. Brewer—640(L)
Fermi theory of β-radioactivity, E. J. Konopinski, G. E. Uhlenbeck—7, 107(L); R. L. Dolecek—13; L. Motz, J. Schwinger—704(L)
Fluctuation, theory of, A. E. Ruark, 473(A); A. E. Ruark, L. Devol—772(L)
Half-lifetimes and atomic weights of β-ray emitters, H. H. Goldsmith—478(A)
Half-lives of K, Rb, Nd and Sm, A. Ruark, K. H. Fussler—151
Induced by electron bombardment, J. J. Livingood, A. H. Snell—485(A), 851; M. Tanaka—916(L)
Ionization in cylindrical chambers, R. D. Evans—177
Of Mg induced by deuteron bombardment, M. C. Henderson—480(A), 855
In O_2 induced by deuteron bombardment, H. W. Newson—482(A), 790
Short-lived β-radioactivity, H. R. Crane, L. A. Delsasso, W. A. Fowler, C. C. Lauritsen—484(A)
Transmutation function for deuterons, J. R. Oppenheimer, M. Phillips—500
Voltage-yield of deuteron-induced radioactivity, E. O. Lawrence, E. McMillan, R. L. Thornton—493
Raman spectra
Of C_6D_6, R. W. Wood—488(A)
Of heavy chloroform, R. W. Wood, D. H. Rank—63
Relativity
Particle problem in general theory, A. Einstein, N. Rosen—73
Size of the universe, A. Haas—973(A)
Velocity of light within an enclosure, G. W. Hammar—462(L)
Resistance, electrical (see **Electrical conductivity and resistance**)

Scattering of electrons, ions and molecules (see also **Electron diffraction**)
Collision cross sections of alkali atoms in gases, S. Rosin, I. I. Rabi—373
Collisions of α-particles in H, E. Pollard, H. Margenau—402
Collisions of α-particles with Ne, W. W. Eaton—921
Cross section for scattering of electrons by diatomic molecules, J. B. Fisk—972(A)
Elastic scattering in Kr, A. L. Hughes, S. Bilinsky—155
Electrons in He, A. L. Hughes, W. Harris—408
High speed electrons of varying energy, H. J. Yearian, J. D. Howe—381(L)
$_1H^1$ scattered by O, M. G. White—481(A)
K ions scattered by Hg vapor, A. G. Rouse—476(A)
Proton-proton forces in scattering, R. D. Present—919(L)
Scattering of $_1H^1$ by α-particles, L. H. Horsley—1
Velocity distributions of electrons, P. M. Morse, W. P. Allis, E. S. Lamar—412
Scattering of light (see **Raman spectra**)
Secondary electrons (see **Electrons, secondary**)
Solid state (see **Crystalline state**)

Spark discharge
Discharges initiated by field emission, J. W. Flowers—954
Effect of intense ultraviolet illumination, H. J. White—113, 482(A)
Electron field emission, L. R. Quarles—260
Photo-ionization in gases, R. N. Varney, L. B. Loeb—481(A), 822
Space-charge ionization coefficients and mechanism breakdown, R. N. Varney, H. J. White, L. B. Loeb, D. Q. Posin—488(A)
Specific heat
Of Sm^{+++}, A. Frank—765
Spectra, absorption (see also **Absorption and reflection of light**)
Of NH_3, photographic, S.-H. Chao—569(L)
Of NH_3 rotational structure in ultraviolet, A. B. F. Duncan, G. R. Harrison—974(A)
Of carbonyl sulphide and deuterium cyanide, infrared, P. F. Bartunek, E. F. Barker—516
Of crystals, structure and interpretation, R. B. Barnes, R. R. Brattain, F. Seitz—582
Of GeH_4, W. B. Steward, H. H. Nielsen—861
Of HF overtone bands, D. E. Kirkpatrick, E. O. Salant—945
Of HF, ultraviolet, K. Siga, H. J. Plumley—105(L)
Of Pb_2, E. N. Shawhan—343
Of Li_2, G. M. Almy, G. R. Irwin—104(L)
Of metastable N_2; negative result, A. A. Frost, O. Oldenberg—66
Of methane, infrared, A. H. Nielsen, H. H. Nielsen—864
New bands of CO_2; infrared, G. Herzberg, H. Verleger—706(L)
Of O_2, Schumann-Runge bands, H. P. Knauss, S. S. Ballard—796
Of O_2, ultraviolet, W. C. Price, G. Collins—714
Photometry of electric furnace multiplets, R. B. King, A. S. King—485(A)
Of solid HCl, P. E. Shearin—299
Of SnS, E. N. Shawhan—521
Transparency of air below 1200A, E. R. Laird—974(A)
Spectra, atomic
Of A; extreme ultraviolet, J. C. Boyce—396
Of Ce IV, R. J. Lang—481(A)
Energy levels of inert-gas configurations, C. L. Bartberger—682
Energy states for excited He, W. S. Wilson—536; T.-Y. Wu, S. T. Ma—917(L)
Fine structure of $D\alpha$, R. C. Williams, R. C. Gibbs—971(L)
Four vector problem; platinum-like spectra, A. T. Goble—346
Intensities for H_2, P. Rudnick—807
Intensities of Tl doublet, L. N. Morscher, Jr.—406
Of I(I), W. C. Price—477(A)
Isoelectronic sequence A I-Mn VIII, deepest terms, P. G. Kruger, S. G. Weissberg—659
Isoelectronic sequence V I to Cu VII, deep terms, P. G. Kruger, H. T. Gilroy—720
Of Mo V, M. W. Trawick—223
New levels in Au II, Hg III, Tl IV, Pb V and Bi VI, J. E. Mack, M. Fromer—357
Optical excitation of HgH and CN bands, L. O. Olsen—476(A)
Of Se II, D. C. Martin—938
Of Ag III, W. P. Gilbert—338
Spark spectrum of Cs excited by electrons, R. R. Sullivan—476(A)
Of W, D. D. Laun—572(L)
Of Zn arc in vacuum, C. W. Hetzler, R. W. Boreman, K. Burns—656
Spectra, continuous
Associated with Hg line; collision induced, W. M. Preston—974(A)
Intensity of continuous spectrum of H_2, N. D. Smith—974(A)
Spectra, general
Of Al vapor, E. Gaviola, J. Strong—136
Corrections to H. Kayser's "Tabelle der Schwingungszahlen," H. Kayser—98
Pressure effects of foreign gases, H. Margenau—755, 973(A)
Spectra of Jupiter and Saturn, A. Adel—103(L)
Spectra, molecular (see also **Molecular structure and constants**)
Afterglow in N_2, J. Kaplan—800
Of BaH, infrared, P. G. Koontz, W. W. Watson—937
Of BeD, P. G. Koontz—707
Of CaH, W. W. Watson, R. L. Weber—732
First negative O_2 bands, L. Bozóky, R. Schmid—465(L)
Heitler-London repulsive state of H_2, H. M. James, A. S. Coolidge, R. D. Present—972(A)
Of HCl, third harmonic, A. P. Cleaves, C. W. Edwards—850(L)
Of HD and D_2, $3p^3\Sigma \rightarrow 2s^3\Sigma$ bands, G. H. Dieke—606
Of H_2, triplet $3p$ complex, G. H. Dieke—610
Interaction between vibration and rotation, M. Johnston, D. M. Dennison—868
Of I_2, O. Stuhlman, Jr.—381(L)
Isotope relations, F. H. Crawford, T. Jorgensen, Jr.—475(A)
A-type doubling widths in $^3\Pi$ states, H. M. Hebb—475(A)
Of Pb_2, E. N. Shawhan—343
Mass ratio of H^1 and H^2 from band spectra, W. W. Watson—973(A)
Predissociation in S, B. Rosen, M. Désirant, J. Duchesne—916(L)
Radiation from metastable levels, J. Kaplan—482(A)
Of AgD, P. G. Koontz—138
Of AgO and CuO, F. W. Loomis, T. F. Watson—280
Of SrH, W. R. Fredrickson, M. E. Hogan, Jr., W. W. Watson—602
Theory of $^3\Sigma^+ - {}^3\Sigma^-$ transitions, R. D. Present—140
In $^2\Pi - {}^2\Sigma$ transitions, L. T. Earls—423
Spectra, x-ray (see **X-rays, Spectra**)
Spectroscopy, technique, standards
Electrodeless ring discharge, low frequency, F. H. Crawford, C. G. Smith—477(A)
Measurements in far ultraviolet, T. Lyman—149

Surface phenomena
Ionization of K on W, M. J. Copley, T. E. Phipps—960
Surface tension
Density and surface tension, L. E. Dodd—487(A)

Thermal conductivity
And electrical conductivities of Cu alloys, C. S. Smith—166(L)
Thermal expansion
Expansion coefficients of Hg crystals, D. M. Hill—474(A), 620
Thermal radiation
Temperature scales of Co, Th, Rh and Mo, L. V. Whitney—458; 477(A)
Thermionic emission of electrons; Emitting surfaces
And electron field emission, L. R. Quarles—260
Filaments observed with simple electron microscope, R. P. Johnson, W. Shockley—973(A)
From Mo, H. B. Wahlin, J. A. Reynolds—751
Theory of work functions of metals, E. Wigner, J. Bardeen—84
Thermionic emission of positive ions; Emitting surfaces
Filaments observed with simple electron microscope, R. P. Johnson, W. Shockley—973(A)
From Mo, H. B. Wahlin, J. A. Reynolds—751
Thermoelectric effects
Of ferromagnetics, F. E. Lowance, F. W. Constant—257
Thermoluminescence
Test of screen, T. Lyman—149
Transmutation phenomena (see **Neutrons, Nucleus, Radioactivity**

Vapor pressure
Of HD, R. B. Scott, F. G. Brickwedde—483(A)
Viscosity
Of air, electronic charge, R. T. Birge—918(L)

Wave mechanics (see **Mechanics, quantum, etc.**)
Work function (see **Thermionic emission of electrons, etc.; Photoelectric effect, etc.**)

X-rays, absorption
Fine structure in *K* edge of Ga, W. W. Mutch—569(L)
K-absorption for Sn and Ag, E. L. Harrington, G. A. Wienshall—477(A)
X-rays, diffraction, scattering, reflection, refraction and polarization
Asymmetry in diffraction measurements, R. C. Spencer—478(A)
Diffraction by Cl ions, G. W. Stewart—473(A)
Diffraction from stratified metal films, J. W. M. DuMond, J. P. Youtz—703(L)
Diffuse scattering from Ne-like crystals, G. E. M. Jauncey, J. H. Deming—577
Diffuse scattering from oscillating quartz, G. E. M. Jauncey, J. H. Deming—462(L)
Fourier series analysis, G. A. Boyd—473(A)
By liquid Na-K alloy in a magnetic field, C. W. Heaps—491
Scattering of, by conduction electrons, C. Zener—573
X-rays, emission (see also **X-rays, spectra and spectroscopy, etc.**)
Chemical combination, influence of, J. Valasek—473(A)
Direct and fluorescence excitation of *K* level in Au, K. B. Stoddard—43
Double electron transitions, F. Bloch—187
Intensity of satellites of $K\alpha$, A. W. Pearsall—133
Probability of *K*-electron ionization, J. C. Clark—30; H. S. W. Massey, E. H. S. Burhop—468(L)
Relative energy of *L* satellites, F. R. Hirsh, Jr.—722
Satellites enhanced by Auger effect, F. R. Hirsh, Jr.—776(L)
Shapes and wave-lengths, *K* lines, Ti 22 to Ge 32, J. A. Bearden, C. H. Shaw—18
X-rays, spectra and spectroscopy, wave-length measurements (see also **X-rays, emission**)
Cleavage and x-ray planes of calcite crystals, J. A. Bearden, H. H. Roseberry—110(L)
Spectrometer and width of spectral lines, R. C. Spencer—473(A)
Wave-lengths by large ruled gratings, J. A. Bearden—385
X-rays, tubes, apparatus
Ionization chamber materials, J. N. Sayler—472(A)
Optics of 3000 kv x-ray tube, D. L. Webster, W. W. Hansen, P. Kirkpatrick—486(A)

Zeeman effect
In first negative O_2 bands, L. Bozóky, R. Schmid—466(L)

CONTENTS

PHYS. REV. 48 (1935) DECEMBER 15

Collisions of Alpha-Particles with Neon Nuclei . . . WILLIAM W. EATON 921

Anomalous Diffraction Gratings . . . . . R. W. WOOD 928

Barium Hydride Spectra in the Infrared . . . . . PHILIP G. KOONTZ AND WILLIAM W. WATSON 937

Analysis of the Spectrum of Se II . . . . . D. C. MARTIN 938

Overtone Absorption Bands of Gaseous HF . . . . . D. E. KIRKPATRICK AND E. O. SALANT 945

Tables for Determining Atomic Wave Functions and Energies . . . . . PHILIP M. MORSE, L. A. YOUNG AND EVA S. HAURWITZ 948

Initiation of Electrical Discharges by Field Emission . JOHN W. FLOWERS 954

Surface Ionization of Potassium on Tungsten . . . . . M. J. COPLEY AND T. E. PHIPPS 960

Letters to the Editor:

Variation with Altitude of the Production of Bursts of Cosmic-Ray Ionization . . . . . C. G. MONTGOMERY AND D. D. MONTGOMERY 969

Determination of the Saturation Ionization Current from High Speed Electrons in Air . . . . . LAURISTON S. TAYLOR 970

Fine Structure of $D\alpha$ with Increased Resolution . . . . . ROBLEY C. WILLIAMS AND R. C. GIBBS 971

Proceedings of the American Physical Society:

PROVIDENCE MEETING OF THE NEW ENGLAND SECTION, October 26, 1935; Minutes and Abstracts 1–15 972

Author Index to Volume 48 975

Analytic Subject Index to Volume 48 982

LANCASTER PRESS, INC., LANCASTER, PA.